MR07-04

Cruise Report

September, 2007

Edited by

Dr   Takeshi Kawano

Contents

1. Cruise Narrative

2. Underway Measurements

3. Hydrography

4. Floats, Drifters and Moorings

1. Cruise Narrative

1.1 Highlight

Cruise Code :   MR07-04
GHPO Section designation: P01
Chief Scientist :   Takeshi Kawano   kawnaot@jamstec.go.jp
                             Ocean General Circulation Observational Research Program
                   Institute of Observational Research for Global Change
                             Japan Agency for Marine-earth Science and Technology
                             2-15, Natsushima, Yokosuka, Japan 237-0061
                             Fax: +81-46-867-9455

Ship :   R/V MIRAI
Ports of Call :   Sekinehama – Hachinohe – Dutch Harbor

Cruise Date :   July 24, 2007 – September 3, 2007

1.2 Cruise Summary

Cruise Track

 Cruise Track and station locations are shown in Fig.1.1.

Number of Stations

 A total of 88 stations were occupied using a Sea Bird Electronics 36 bottle carousel equipped with 12 liter Niskin X water sample bottles, a SBE911plus equipped with SBE35 deep ocean standards thermometer, SBE43 oxygen sensor, AANDERAA "optode" oxgen sensor and Benthos Inc. Altimeter and RDI Monitor ADCP.

 XCTDs were deployed at 18 stations.

Sampling and measurements

1) Measurements of temperature, salinity, oxygen ,current profile, fluorescence using CTD/O_2 with LADCP.

2) Water sampling and analysis of salinity, oxygen, nutrients, CFC11,12, 113, total alkalinity, DIC, and pH.

3) Water sampling of POM, ^{14}C, ^{13}C, ^{137}Cs, N_2O, CH_4 and DMS.

4) Underway measurements of radon, pCO_2, temperature, salinity, nutrients, surface current, bathymetry and meteorological parameters

Floats, Drifters and Moorings

 Argo floats were deployed at (46°59.46'N, 172°41.04'W), (46°59.34'N, 167°04.38'W), (46°59.69'N, 151°24.37'W), (46°59.35'N, 146°55.35'W) and (46°58.81' N, 145°47.72'W) after the CTD cast at St. 68, 73, 87, 91 and 92, respectively.
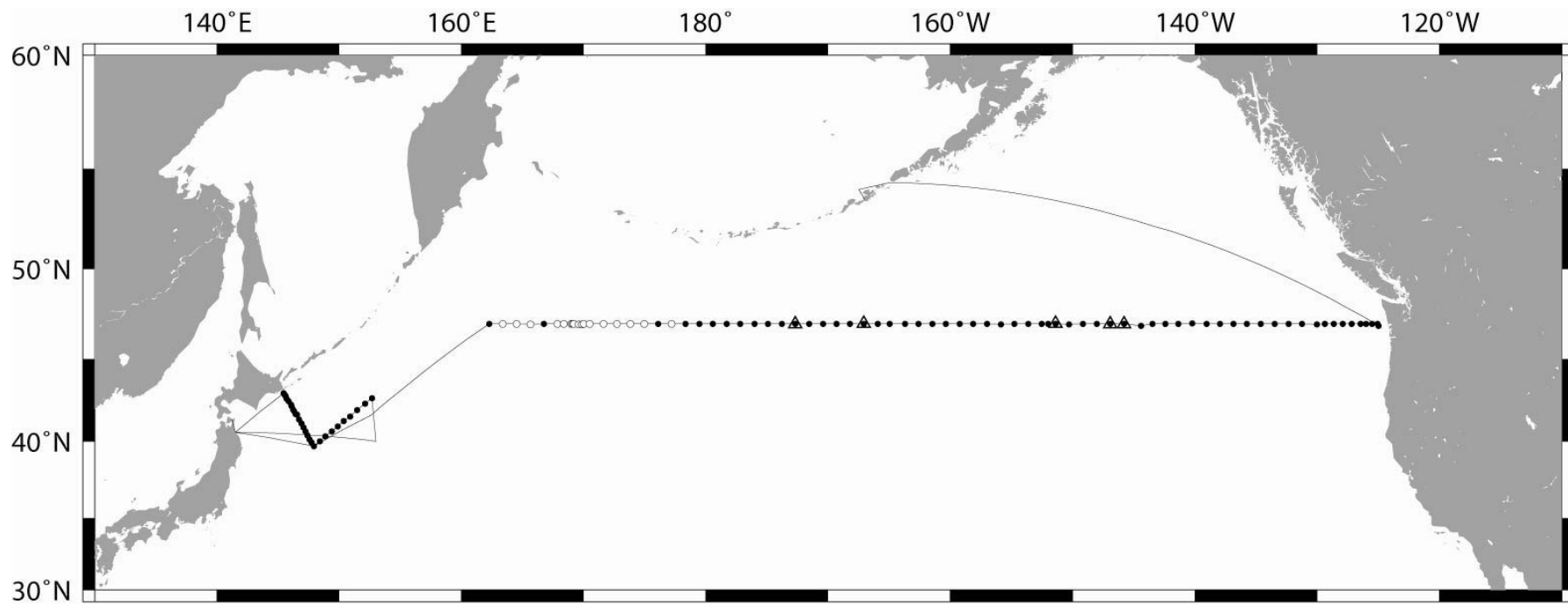
Fig.1.1 Cruise Track

Solid circle (●) and open circle (○) represents CTD station and XCTD station, respectively. Triangle (　) shows a position where ARGO floats were deployed.

1.3 Responsibility

The principal investigators responsible for major parameters are listed in Table.1.1.

1.4 Objective of the Cruise

(1) Objectives

It is well known that the oceans play a central role in determining global climate. However heat and material transports in the ocean and their temporal changes have not yet been sufficiently quantified. Therefore, global climate change is not understood satisfactorily. The purposes of this research are to evaluate heat and material transports such as carbon, nutrients, etc. in the North Pacific and to detect their long term changes and basin-scale biogeochemical changes since the 1990s. This cruise is a reoccupation of the hydrographic section called 'WHP-P1', which was observed by an ocean science group of USA in 1985 as a part of WOCE (World Ocean Circulation Experiment) and by a joint group of Canada and Japan in 1999. Both data-sets are included in the data base of CLIVAR (Climate Variability and Predictability) and Carbon Hydrographic Data Office (http://whpo.ucsd.edu/). We will compare physical and chemical properties along section WHP-P1 with those obtained in 1985 and 1999 to detect and evaluate long term changes of the marine environment in the North Pacific.

Reoccupations of the WOCE hydrographic sections are now in progress by international cooperation in ocean science community, within the framework of CLIVAR, which is as part of World Climate Research Programme (WCRP) and IOCCP (International Ocean Carbon Coordination Project). Our research is planned as a contribution to these international projects supported by WMO, ICSU/SCOR and UNESCO/IOC, and its results and data will be published by 2009 for worldwide use.

The other purposes of this cruise are as follows:

1) to observe surface meteorological and hydrological parameters as a basic data of meteorology and oceanography such as studies on flux exchange, air-sea interaction and so on,

2) to observe sea bottom topography, gravity and magnetic fields along the cruise track to understand the dynamics of ocean plate and accompanying geophysical activities,

3) to observe bio-geochemical parameters to study carbon cycle in the ocean,

4) to observe green house gasses in the atmosphere and the ocean to study their cycle from geochemical aspect.

(2) Data Policy

Obtained data will be quality controlled and opened through GHPO and JAMSTEC within two years .

1.5 List of Cruise Participants

Cruise participants for each leg are listed in Table 1.2a, b and c.

1.6 Major Problems

(1) Stations not occupied

Both propellers got entangled in a fishing net at the station 29. Therefore we were forced to return to the port, Hachinohe, to cut remove the fishing net. We spent 10 days for the trouble and it made us giving up our observation in the western part of the P1 line, from station 29 to station 60. We restarted

the observation at the dateline, station P61.

At stations 40, 45, 58 and 60, we made a CTD cast specially designed for DMS, Nitrous oxide (N_2O), Methane (CH_4), Carbonyl sulfide (COS), and related substances.

From stations 41 to 59 (except 45 and 58), we deploy XCTD (1,000m) instead of CTD cast.

(2) Misfiring and mistrip

The carousel water sampler misfired at station 23 (bottle #15).

(3) CTD sensor replacement

We encountered to several problems (drift, shift, noise) of CTD sensors and replaced them after the following stations:

Sta. 10:　primary conductivity sensor

Sta. 29:　secondary temperature sensor

Sta. 44:　primary temperature sensor

Table 1.1 List of principal investigator and person in charge on the ship

Chief Scientist :   Takeshi Kawano

Chief Technologist :   Satoshi Ozawa

Item	Principal Investigator	Person in Charge on the Ship
Hydrography		
CTDO	Hiroshi Uchida	Satoshi Ozawa
LADCP	Shinya Kouketsu	Shinya Kouketsu
BTL Salinity	Takeshi Kawano	Naoko Takahashi
BTL Oxygen	Yuichiro Kumamoto	Kimiko Nishijima
Nutrients	Michio Aoyama	Ayumi Takeuchi
DIC	Akihiko Murata	Yoshiko Ishikawa, Yasuhiro Arii
Alkalinity	Akihiko Murata	Fuyuki Shibata, Minoru Kamata
pH	Akihiko Murata	Fuyuki Shibata, Minoru Kamata
CFCs	Kenichi Sasaki	Kenichi Sasaki
^{14}C	Yuichiro Kumamoto	Yuichiro Kumamoto
Radionuclides	Michio Aoyama	Junji Matsushita
N_2O & CH_4	Naohiro Yoshida	Osamu Yoshida
XCTD	Hiroshi Uchida	Satoshi Okumura
Underway		
ADCP	Shinya Kouketsu	Satoshi Okumura
Bathymetry,	Takeshi Matsumoto	Satoshi Okumura
Gravity	Takeshi Matsumoto	Satoshi Okumura
Geomagnetic Measurement	Takeshi Matsumoto	Satoshi Okumura
Meteorology	Kunio Yoneyama	Satoshi Okumura
Thermo-Salinograph	Yuichiro Kumamoto	Keisuke Wataki
DMS	Ippei Nagao	Ippei Nagao
Aerosol and Fog water	Mitsuo Uematsu	Yoko Iwamoto
Stable Isotopes in rain	Kimpei Ichiyanagi	Satoshi Okumura
Laser Radar	Nobuo Sugimoto	Satoshi Okumura
pCO_2	Akihiko Murata	Yoshiko Ishikawa, Yasuhiro Arii
Radon Flux	Shigeki Tasaka	Shigeki Tasaka
Organic & inorganic carbon	Yukiko Kuroki	Masao Uchida
Floats, Drifters		
Argo float	Toshio Suga	Tomoyuki Takamori

Table 1.2 List of Cruise Participants

Name	Responsibility	Affiliation
Yasuhiro Arii	Carbon Items	MWJ
Miyo Ikeda	Dissolved Oxygen / Water Sampling	MWJ
Yoshiko Ishikawa	Carbon Items	MWJ
Yoko Iwamoto	Aerosol and Fog water	ORI
Minoru Kamata	Carbon Items	MWJ
Kenichi Katayama	CTD / Water Sampling	MWJ
Kaori Kawana	Aerosol and Fog water	ORI
Kohei Kawano	CH_4 and N_2O / Water Sampling	Tokyo Inst. Tech.
Takeshi Kawano	Chief Scientist / Salinity	IORGC/JAMSTEC
Kei Kojima	Water Sampling	MWJ
Chihiro Komatsu	Water Sampling	MWJ
Shinya Kouketsu	LADCP/ADCP / Water Sampling	IORGC/JAMSTEC
Yuichiro Kumamoto	DO / Thermosalinograph / $\Delta^{14}C$	IORGC/JAMSTEC
Yukiko Kuroki	Organic and Inorganic Carbon	University of Tsukuba
Takashi Makino	Water Sampling	MWJ
Junji Matsushita	Radionuclides / Water Sampling	MWJ
Shunsuke Miyabe	Nutrients	MWJ
Tomohiro Miyabukuro	CH_4 and N_2O / Water Sampling	Tokyo Inst. Tech.
Dai Motomura	Water Sampling	MWJ
Maki Mukai	Water Sampling	MWJ
Akihiko Murata	Carbon Items/ Water sampling	IORGC/JAMSTEC
Ippei Nagao	DMS	Nagoya University
Kimiko Nishijima	Dissolved Oxygen / Water Sampling	MWJ
Satoshi Okumura	Meteorology / Geophysics	GODI
Shinya Okumura	Meteorology / Geophysics	GODI
Ryo Oyama	Meteorology / Geophysics	GODI
Satoshi Ozawa	Chief Technologist /CTD / Water Sampling	MWJ
Katsunori Sagishima	CFCs	MWJ
Kenichi Sasaki	CFCs	MIO/JAMSTEC
Takayoshi Seike	Nutrients	MWJ
Fuyuki Shibata	Carbon Items	MWJ
Yuichi Sonoyama	CFCs	MWJ
Kazuto Suzuki	Water Sampling	MWJ
Naoko Takahashi	Salinity / Water Sampling	MWJ
Tomoyuki Takamori	CTD / Water Sampling	MWJ
Ayumi Takeuchi	Nutrients	MWJ
Tatsuya Tanaka	Salinity / Water Sampling	MWJ
Shigeki Tasaka	Radon	Gifu University
Shoko Tatamisashi	CFCs	MWJ
Hiroshi Uchida	CTD / LADCP / Warter Sampling	IORGC/JAMSTEC
Hirokatsu Uno	CTD / Water Sampling	MWJ
Keisuke Wataki	Dissolved Oxygen / Water Sampling	MWJ
Osamu Yoshida	CH_4 and N_2O / Water Sampling	Rakuno Gakuen University

GODI	Global Ocean Development Inc.
IORGC	Institute of Observational Research for Global Change
JAMSTEC	Japan Agency for Marine-earth Sceinece and Technology
MIO	Mutsu Institute of Oceanography
MWJ	Marine Works Japan Ltd.
ORI	Ocean Research Institute, The University of Tokyo
Tokyo Inst. Tech.	Tokyo Institute of Technology

2 Underway Measurements

2.1 Meteorological observation

2.1.1 Surface Meteorological Observation

(1) Personnel
Kunio Yoneyama   *(JAMSTEC) Principal Investigator / Not on-board*
Satoshi Okumura   *(Global Ocean Development Inc., GODI)*
Shinya Okumura   *(GODI)*
Ryo Ohyama   *(GODI)*

(2)Objectives

The surface meteorological parameters are observed as a basic dataset of the meteorology. These parameters bring us the information about the temporal variation of the meteorological condition surrounding the ship.

(3) Methods

The surface meteorological parameters were observed throughout the MR07-04 cruise. During this cruise, we used two systems for the observation.

     i. MIRAI Surface Meteorological observation (SMET) system
     ii. Shipboard Oceanographic and Atmospheric Radiation (SOAR) system

        i. MIRAI Surface Meteorological observation (SMET) system
     Instruments of SMET system are listed in Table.2.1.1-1 and measured parameters are listed in Table.2.1.1-2. Data were collected and processed by KOAC-7800 weather data processor made by Koshin-Denki, Japan. The data set consists of 6-second averaged data.

        ii.Shipboard Oceanographic and Atmospheric Radiation (SOAR) system
     SOAR system designed by BNL (Brookhaven National Laboratory, USA) consists of major three parts.
a) Portable Radiation Package (PRP) designed by BNL – short and long wave downward radiation.
b) Zeno Meteorological (Zeno/Met) system designed by BNL – wind, air temperature, relative humidity, pressure, and rainfall measurement.
c) Scientific Computer System (SCS) designed by NOAA (National Oceanic and Atmospheric Administration, USA) – centralized data acquisition and logging of all data sets.
     SCS recorded PRP data every 6 seconds, Zeno/Met data every 10 seconds. Instruments and their locations are listed in Table.2.1.1-3 and measured parameters are listed in Table.2.1.1-4.

We have checked the following sensors, before and after the cruise for the quality control as post processing.

     i. Young Rain gauge (SMET and SOAR)

Inspect of the linearity of output value from the rain gauge sensor to change input value by adding fixed quantity of test water.

ii. Barometer

(SMET and SOAR)Comparison with the portable barometer value, PTB220CASE, VAISALA.

iii. Thermometer (air temperature and relative humidity) (SMET and SOAR)

Comparison with the portable thermometer value, HMP41/45, VAISALA.

(4) Preliminary results

Figures.2.1.1-1 to Figures.2.1.1-3 shows the time series of the following parameters;

Wind (SOAR)

Air temperature (SMET)

Relative humidity (SMET)

Precipitation (SOAR, Capacitive rain gauge)

Short/long wave radiation (SMET)

Pressure (SMET)

Sea surface temperature (SMET)

Significant wave height (SMET)

(5) Data archives

These meteorological data will be submitted to the Marine-Earth Data and Information Department (MEDID) of JAMSTEC just after the cruise. Corrected data sets will be available from K. Yoneyama of JAMSTEC.

(6) Remarks

i. FRSR sensor has been removed from Jul. 27 to the end of this cruise for sensor trouble.

ii. From 22:01 Jul. 28 to 08:16 Jul. 29, PSP and PIR data of SOAR system are not available due to the maintenance.

iii. SST(Sea Surface Temperature) data are available in the following periods.

25 Jul. 2007 09:00UTC - 8 Aug. 2007 01:02UTC

10 Aug. 2007 00:00UTC - 01 Sep. 2007 18:00UTC

iv. Three sensors of SOAR system, anemometer, capacitive rain gauge and optical rain gauge, were put 50 - 70 cm higher than their original positions to avoid interference with other equipment during this cruise. Temporary positions are shown in table.2.1.1-3.

Table.2.1.1-1 Instruments and installations of MIRAI Surface Meteorological observation system

Sensors	Type	Manufacturer	Location (altitude from surface)
Anemometer	KE-500	Koshin Denki, Japan	foremast (24 m)
Tair/RH	HMP45A	Vaisala, Finland	
with 43408 Gill aspirated radiation shield R.M. Young, USA			compass deck (21 m)
			starboard side and port side
Thermometer: SST	RFN1-0	Koshin Denki, Japan	4th deck (-1m, inlet -5m)
Barometer	AP370	Koshin Denki, Japan	captain deck (13 m)
			weather observation room
Rain gauge	50202	R. M. Young, USA	compass deck (19 m)
Optical rain gauge	ORG-815DR	Osi, USA	compass deck (19 m)
Radiometer (short wave)	MS-801	Eiko Seiki, Japan	radar mast (28 m)
Radiometer (long wave)	MS-202	Eiko Seiki, Japan	radar mast (28 m)
Wave height meter	MW-2	Tsurumi-seiki, Japan	bow (10 m)

Table.2.1.1-2 Parameters of MIRAI Surface Meteorological observation system

	Parameter	Units	Remarks
1	Latitude	degree	
2	Longitude	degree	
3	Ship's speed	knot	Mirai log, DS-30 Furuno
4	Ship's heading	degree	Mirai gyro, TG-6000, Tokimec
5	Relative wind speed	m/s	6sec./10min. averaged
6	Relative wind direction	degree	6sec./10min. averaged
7	True wind speed	m/s	6sec./10min. averaged
8	True wind direction	degree	6sec./10min. averaged
9	Barometric pressure	hPa	adjusted to sea surface level 6sec. averaged
10	Air temperature (starboard side)	degC	6sec. averaged
11	Air temperature (port side)	degC	6sec. averaged
12	Dewpoint temperature (starboard side)	degC	6sec. averaged
13	Dewpoint temperature (port side)	degC	6sec. averaged
14	Relative humidity (starboard side)	%	6sec. averaged
15	Relative humidity (port side)	%	6sec. averaged
16	Sea surface temperature	degC	6sec. averaged
17	Rain rate (optical rain gauge)	mm/hr	hourly accumulation
18	Rain rate (capacitive rain gauge)	mm/hr	hourly accumulation
19	Down welling shortwave radiation	W/m2	6sec. averaged
20	Down welling infra-red radiation	W/m2	6sec. averaged
21	Significant wave height (bow)	m	hourly
22	Significant wave height (aft)	m	hourly
23	Significant wave period (bow)	second	hourly
24	Significant wave period (aft)	second	hourly

Table.2.1.1-3 Instrument and installation locations of SOAR system

Sensors(Zeno/Met)	Type	Manufacturer	Location (altitude from surface)
Anemometer	05106	R.M. Young, USA	foremast (25 m)
Tair/RH	HMP45A	Vaisala, Finland	
with 43408 Gill aspirated radiation shield		R.M. Young, USA	foremast (23 m)
Barometer	61201	R.M. Young, USA	
with 61002 Gill pressure port		R.M. Young, USA	foremast (22 m)
Rain gauge	50202	R. M. Young, USA	foremast (24 m)
Optical rain gauge	ORG-815DA	Osi, USA	foremast (24 m)

Sensors (PRP)	Type	Manufacturer	Location (altitude from surface)
Radiometer (short wave)	PSP	Epply Labs, USA	foremast (24 m)
Radiometer (long wave)	PIR	Epply Labs, USA	foremast (24m)
Fast rotating shadowband radiometer		Yankee, USA	foremast (24 m)

Table.2.1.1-4 Parameters of SOAR system

|	Parameter	Units	Remarks
1	Latitude	degree	
2	Longitude	degree	
3	SOG	knot	
4	COG	degree	
5	Relative wind speed	m/s	
6	Relative wind direction	degree	
7	Barometric pressure	hPa	
8	Air temperature	degC	
9	Relative humidity	%	
10	Rain rate (optical rain gauge)	mm/hr	
11	Precipitation (capacitive rain gauge)	mm	reset at 50 mm
12	Down welling shortwave radiation	W/m2	
13	Down welling infra-red radiation	W/m2	
14	Defuse irradiance	W/m2	
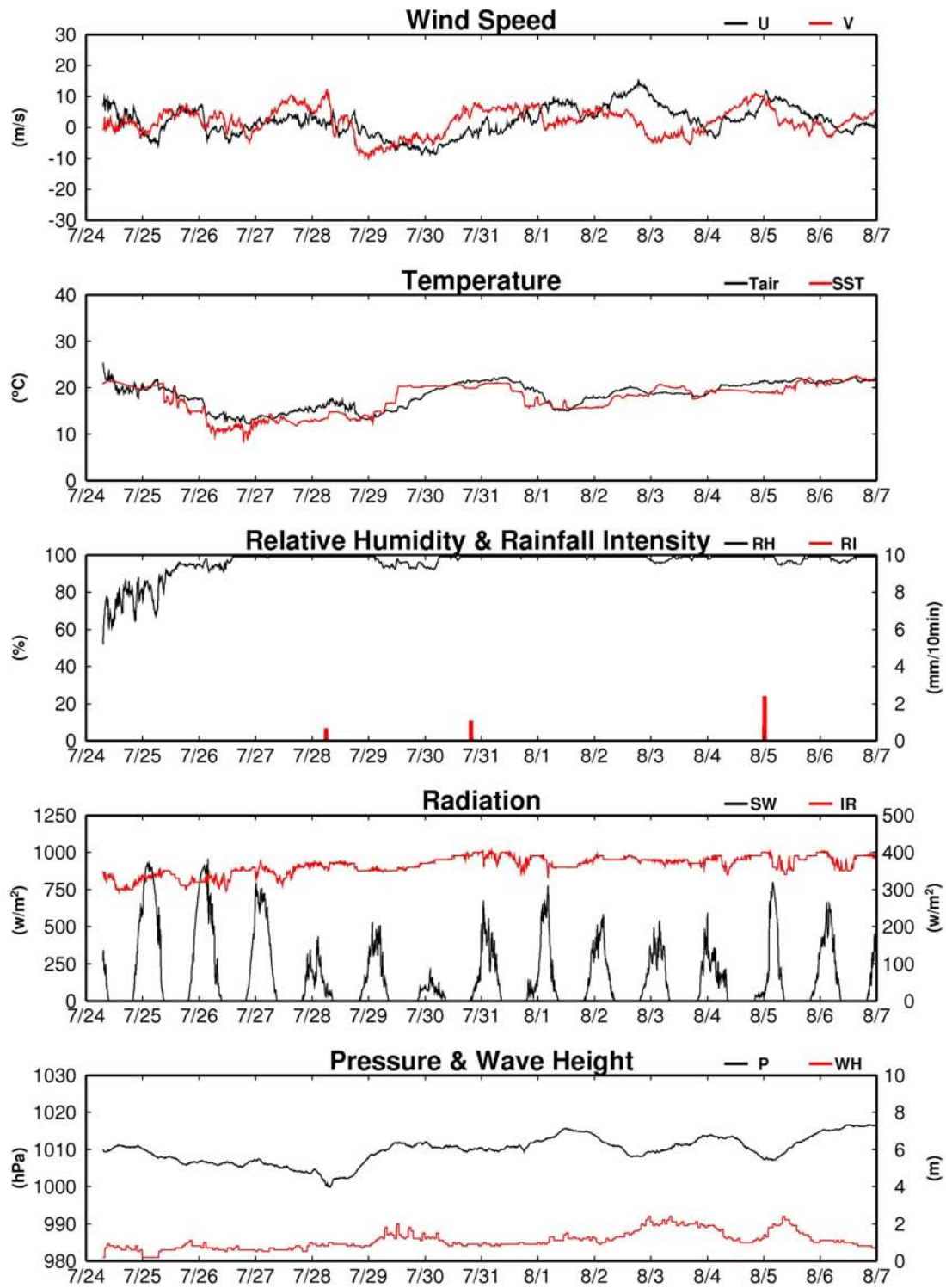
Fig.2.1.1-1 Time series of surface meteorological parameters during the MR07-04 cruise
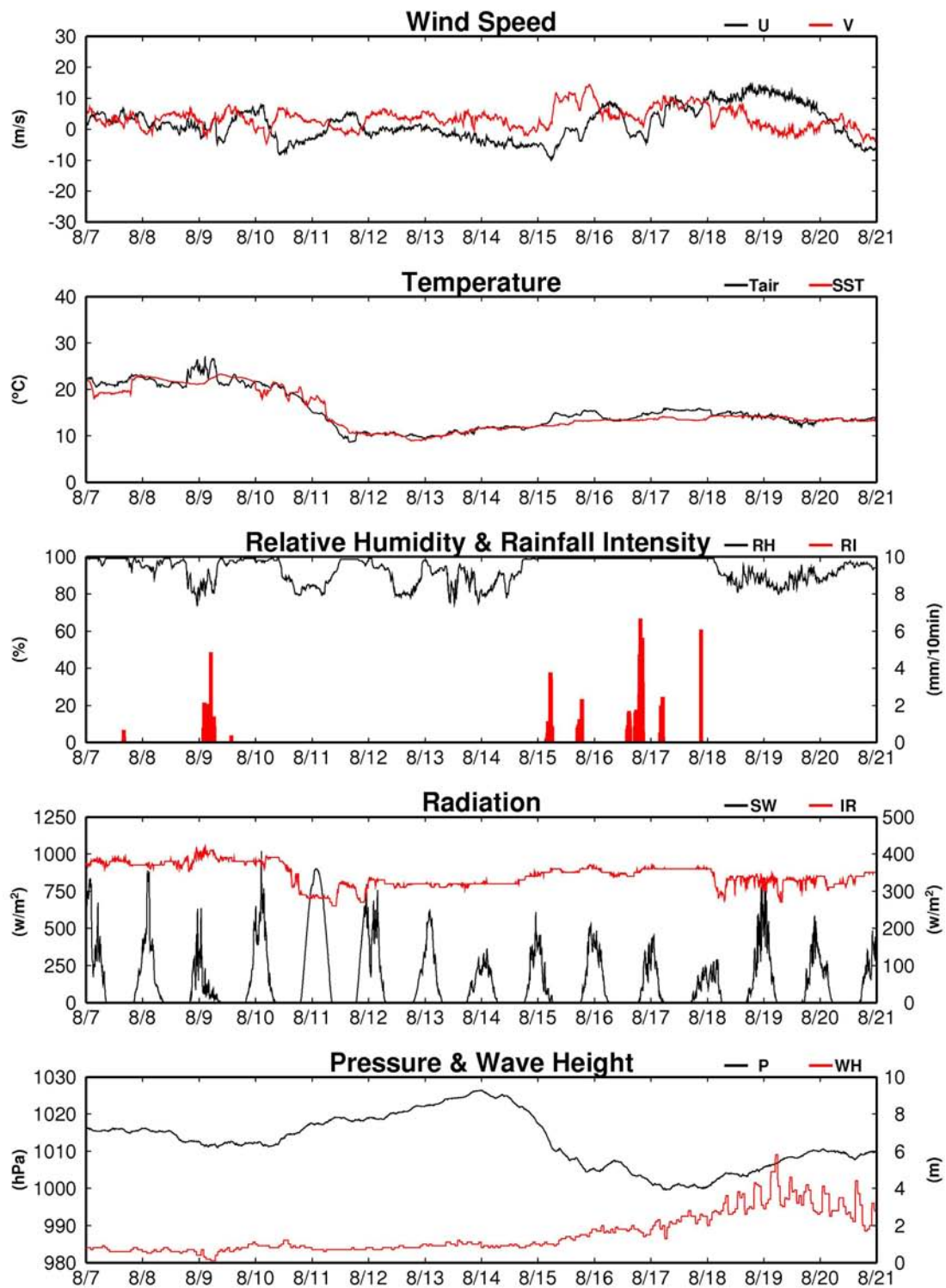
Fig.2.1.1-2 Time series of surface meteorological parameters during the MR07-04 cruise
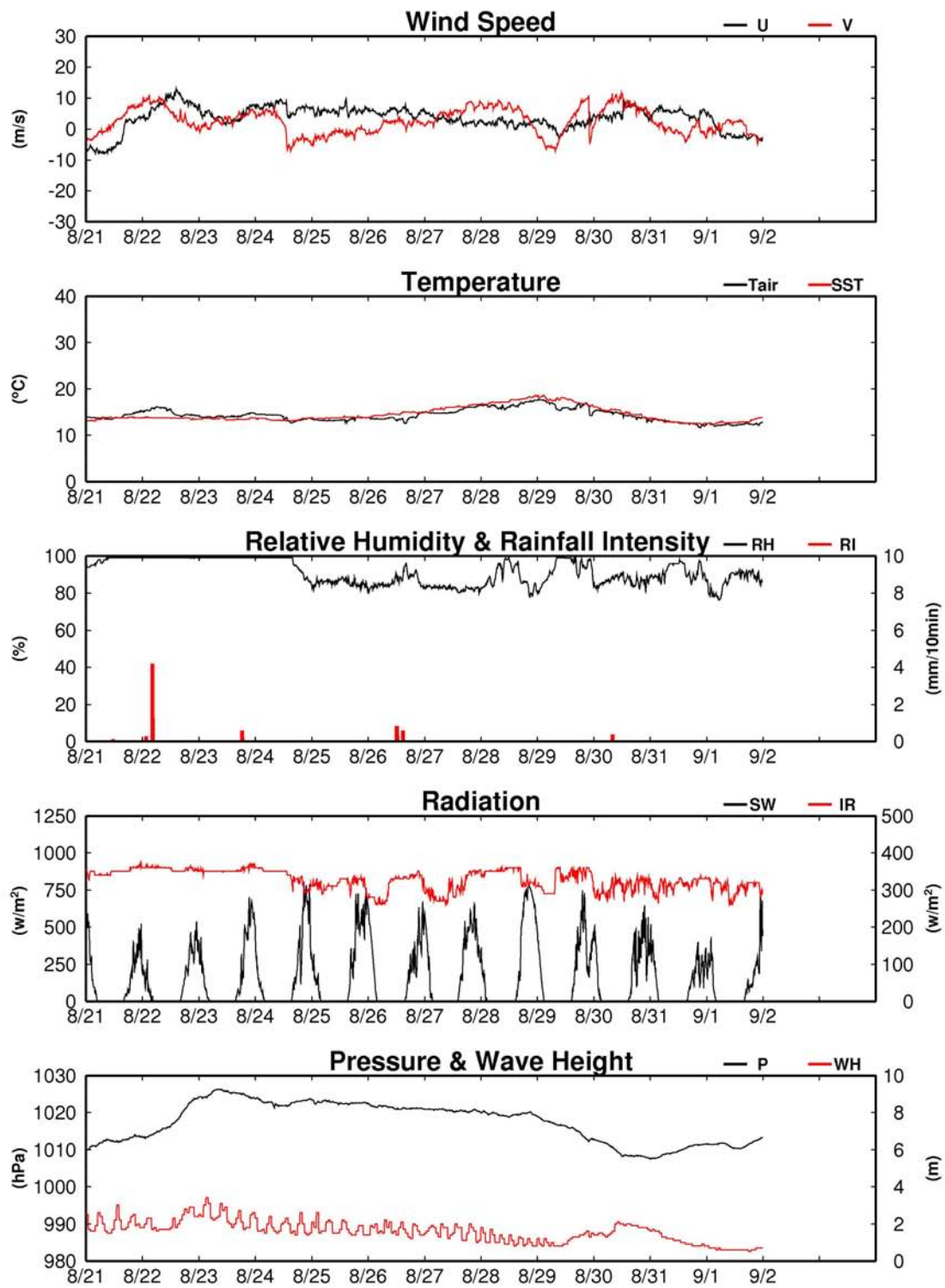
Fig.2.1.1-3 Time series of surface meteorological parameters during the MR07-04 cruise

2.1.2 Ceilometer Observation

(1) Personnel

Kunio Yoneyama   *(JAMSTEC) Principal Investigator / Not on-board*
Satoshi Okumura   *(Global Ocean Development Inc., GODI)*
Shinya Okumura   *(GODI)*
Ryo Ohyama   *(GODI)*

(2) Objectives

The information of cloud base height and the liquid water amount around cloud base is important to understand the process on formation of the cloud. As one of the methods to measure them, the ceilometer observation was carried out.

(3) Methods

We measured cloud base height and backscatter profile using ceilometer (CT-25K, VAISALA, Finland) throughout the MR07-04 cruise. Major parameters to be measured are
i. cloud base height in meters, ii. backscatter profiles, and iii. estimated cloud amount in octas.

Specifications of the system are as follows.

Laser source:	Indium Gallium Arsenide Diode
Transmitting wavelength:	905±5 mm at 25 degC
Transmitting average power:	8.9 mW
Repetition rate:	5.57 kHz
Detector:	Silicon avalanche photodiode (APD)
Responsibility at 905 nm:	65 A/W
Measurement range:	0 ~ 7.5 km
Resolution:	50 ft in full range
Sampling rate:	60 sec
Sky Condition:	0, 1, 3, 5, 7, 8 octas (9: Vertical Visibility)
	(0: Sky Clear, 1:Few, 3:Scattered, 5-7: Broken, 8: Overcast)

On the archive dataset, cloud base height and backscatter profile are recorded with the resolution of 30 m (100 ft).

(4) Preliminary results

Figure.2.1.2 shows the time series of the first, second and third lowest cloud base height during the cruise.

(5) Data archives

Ceilometer data obtained during this cruise will be submitted to and archived by the Marine-Earth Data and Information Department (MEDID) of JAMSTEC.
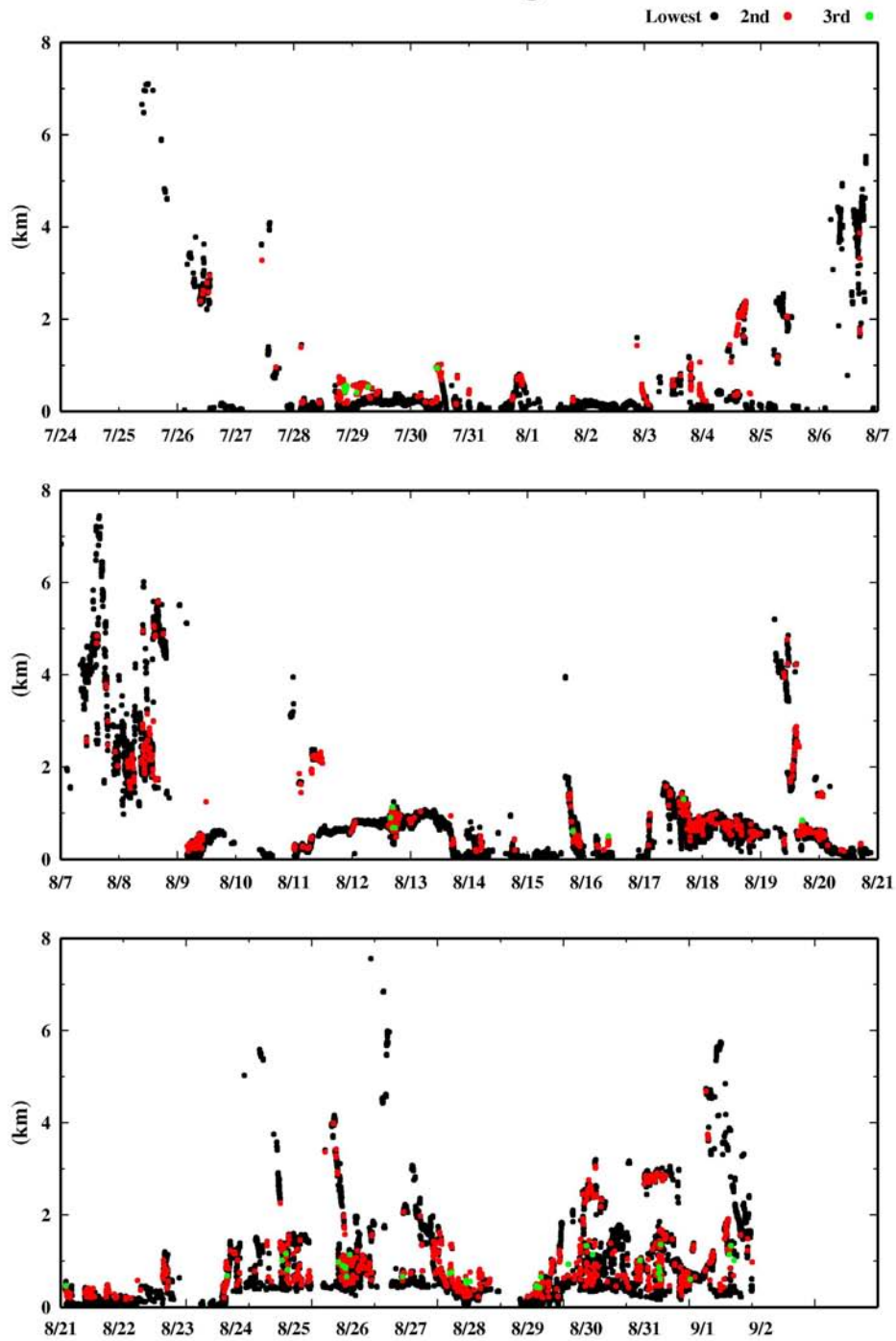
Cloud Height

Fig.2.1.2 1st (black) 2nd (red) and 3rd (green) lowest cloud base height.

2.1.3 Surface Atmospheric Turbulent Flux Measurement

(1) Personnel

Kunio Yoneyama	*(JAMSTEC) Principal Investigator / Not-onboard*
Osamu Tsukamoto	*(Okayama University) Not-onboard*
Satoshi Okumura	*(Global Ocean Development Inc.)*
Shinya Okumura	*(Global Ocean Development Inc.)*
Ryo Ohyama	*(Global Ocean Development Inc.)*

(2) Objective

To better understand the air-sea interaction, accurate measurements of surface heat and fresh water budgets are necessary as well as momentum exchange through the sea surface. In addition, the evaluation of surface flux of carbon dioxide is also indispensable for the study of global warming. Sea surface turbulent fluxes of momentum, sensible heat, latent heat, and carbon dioxide were measured by using the eddy correlation method that is thought to be most accurate and free from assumptions. These surface heat flux data are combined with radiation fluxes and water temperature profiles to derive the surface energy budget.

(3) Methods

The surface turbulent flux measurement system (Fig. 2.1.3-1) consists of turbulence instruments (Kaijo Co., Ltd.) and ship motion sensors (Kanto Aircraft Instrument Co., Ltd.). The turbulence sensors include a three-dimensional sonic anemometer-thermometer (Kaijo, DA-600) and an infrared hygrometer (LICOR, LI-7500). The sonic anemometer measures three-dimensional wind components relative to the ship. The ship motion sensors include a two-axis inclinometer (Applied Geomechanics, MD-900-T), a three-axis accelerometer (Applied Signal Inc., QA-700-020), and a three-axis rate gyro (Systron Donner, QRS-0050-100). LI7500 is a CO_2/H_2O turbulence sensor that measures turbulent signals of carbon dioxide and water vapor simultaneously.

These signals are sampled at 10 Hz by a PC-based data logging system (Labview, National Instruments Co., Ltd.). By obtaining the ship speed and heading information through the Mirai network system it yields the absolute wind components relative to the ground. Combining wind data with the turbulence data, turbulent fluxes and statistics are calculated in a real-time basis. These data are also saved in digital files every 0.1 second for raw data and every 1 minute for statistic data.

(4) Preliminary results

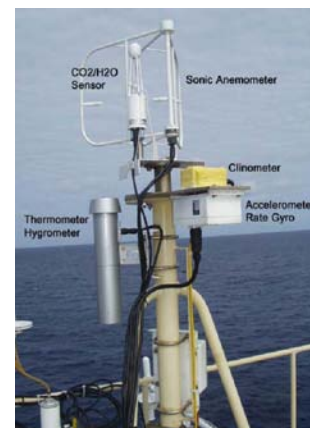Data will be processed after the cruise at Okayama University.

Fig. 2.1.3-1 Turbulent flux measurement system on the top deck of the foremast.

(5) Data Archive

All data are archived at Okayama University, and will be open to public after quality checks and corrections by K. Yoneyama and O. Tsukamoto. Corrected data will be submitted to JAMSTEC Marine-Earth Data and Information Department.

2.1.4 Lidar observations of clouds and aerosols

(1) Personnel

Nobuo Sugimoto   (National Institute for Environmental Studies, not on board)
Ichiro Matsui   (National Institute for Environmental Studies, not on board)
Atsushi Shimizu   (National Institute for Environmental Studies, not on board),
lidar operation was supported by GODI.

(2) Objectives

Objectives of the observations in this cruise is to study distribution and optical characteristics of ice/water clouds and marine aerosols using a two-wavelength   lidar.

(3) Measured parameters
- Vertical profiles of backscattering coefficient at 532 nm
- Vertical profiles of backscattering coefficient at 1064 nm
- Depolarization ratio at 532 nm

(4) Method

Vertical profiles of aerosols and clouds were measured with a two-wavelength lidar. The lidar employs a Nd:YAG laser as a light source which generates the fundamental output at 1064 nm and the second harmonic at 532 nm. Transmitted laser energy is typically 30 mJ per pulse at both of 1064 and 532 nm. The pulse repetition rate is 10 Hz. The receiver telescope has a diameter of 20 cm. The receiver has three detection channels to receive the lidar signals at 1064 nm and the   parallel and perpendicular polarization components at 532 nm. An analog-mode avalanche photo diode (APD) is used as a detector for 1064 nm, and photomultiplier tubes (PMTs) are used for 532 nm. The detected signals are recorded with a transient recorder and stored on a hard disk with a computer. The lidar system was installed in the radiosonde container on the compass deck. The container has a glass window on the roof, and the lidar was operated continuously regardless of weather.   Every 15 minutes vertical profiles of four channels (532 parallel, 532 perpendicular, 1064, 532 near range) are recorded.

(5) Results

Lidar raw data have not been collected by NIES because this is unattended subject. So we show here only sample vertical profiles of backscattering intensity which was automatically generated   onboard and   transferred to NIES by e-mail. Figure 1 shows an atmospheric structure revealed by lidar on   July 25, 2007. There was a cloud layer around 8 km. High depolarization ratio (perpendicular to parallel at 532 nm) indicates this layer is consist of non-spherical ice particles. Below the cloud, some structure of aerosol layers was evident. Aerosol mixing layer was located blow 2.5km, but weak aerosol signal was extended up to 4 km. Similar profiles are obtained every 15 minutes, and three dimensional structure of atmospheric scatterers (clouds and aerosols) are revealed in whole troposphere.
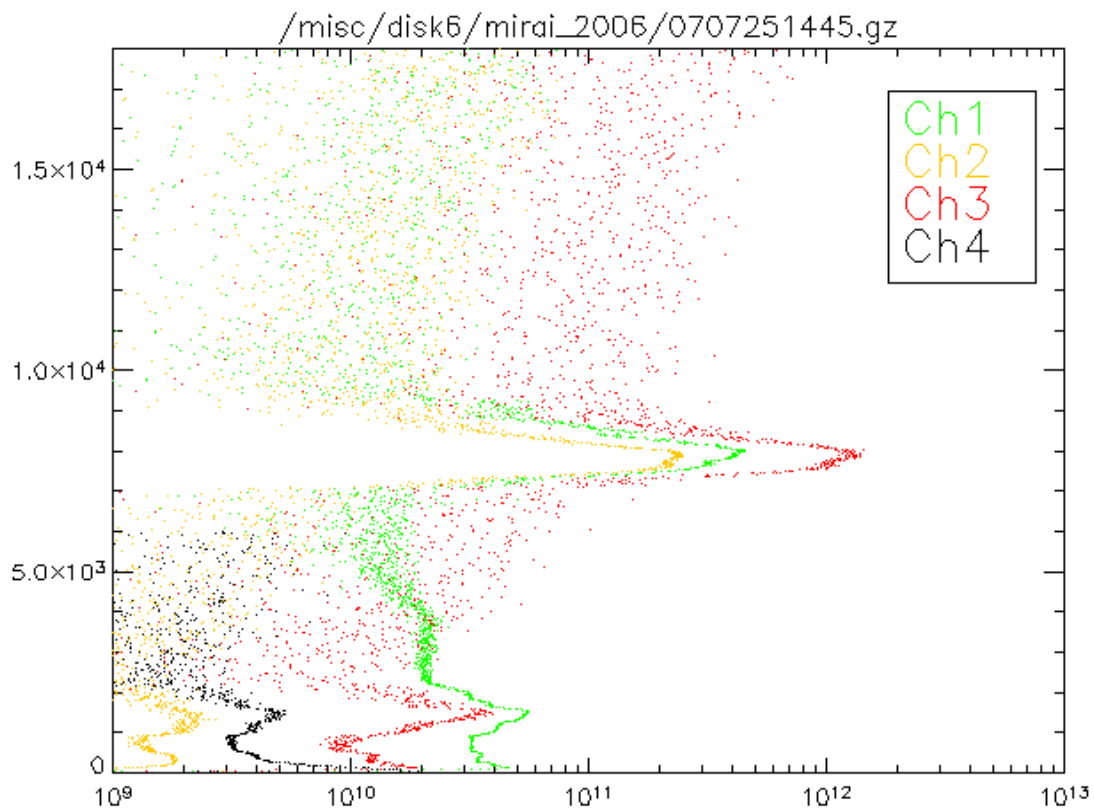
Figure 1: Vertical profiles of backscattering intensity at 532 nm parallel (green), 532 nm perpendicular (yellow), 1064 nm (red) at UTC1445 on July 25, 2007. Black indicates signal from near field telescope (532nm).

(6) Data archive
- raw data
    lidar signal at 532 nm
    lidar signal at 1064 nm
    depolarization ratio at 532 nm
    temporal resolution 10 sec/ vertical resolution 6 m
    data period : July 24, 2007 – August 31, 2007
- processed data
    cloud base height, apparent cloud top height
    phase of clouds (ice/water)
    cloud fraction
    boundary layer height (aerosol layer upper boundary height)
    backscatter coefficient of aerosols
    particle depolarization ratio of aerosols

2.1.5 Rain Sampling for Stable Isotopes

(1) Personnel

Kimpei Ichiyanagi (JAMSTEC) (Not on board)

(2) Objective

To determine the spatial distribution of isotopic composition of rainfall on the Ocean

(3) Method

Rainfall samples are collected in 6cc glass bottle with plastic cap. Isotopic compositions for hydrogen and oxygen in rainfall are determined by the Isotope Ratio Mass Spectrometry (IRMS).

(4) Preliminary results

During this cruise, we collected 18 samples in total. Table 1 lists the date and location of rainfall samples. Analysis will be done after the cruise.

(5) Data archive

Original samples will be analyzed by IORGC. Inventory and analyzed digital data will be submitted to JAMSTEC Data Management Office.

Table 1   Dates and locations to show when and where rain water were sampled.

Sample No.	Date (UTC)	Location (lat/lon)	Rain (mm)
001	06:14, July 28	41-42.79N, 146-26.00E	0.6
002	13:12, July 30	40-01.35N, 148-24.15E	0.8
003	20:55, July 30	40-19.59N, 148-51.83E	0.3
004	05:14, August 5	40-13.66N, 152-49.84E	4.7
005	01:55, August 10	40-30.65N, 147-57.60E	2.1
006	05:23, August 15	47-00.06N, 179-25.88W	1.8
007	11:44, August 15	47-00.13N, 178-17.78W	5.6
008	20:33, August 15	47-00.31N, 177-04.46W	1.8
009	16:22, August 16	47-00.00N, 173-47.36W	0.6
010	20:59, August 16	46-59.78N, 172-42.69W	12.6
011	06:38, August 17	47-00.69N, 171-33.43W	6.4
012	16:16, August 17	46-59.66N, 170-05.54W	3.2
013	03:41, August 18	46-59.90N, 168-12.43W	1.0
014	03:15, August 22	46-59.53N, 152-32.42W	0.6
015	06:34, August 22	46-59.03N, 152-20.66W	1.2
016	20:33, August 23	47-00.35N, 148-01.88W	0.2
017	14:34, August 24	46-54.04N, 144-26.04W	0.2
018	17:26, August 26	46-59.98N, 135-43.88W	0.2

2.2 Navigation and Bathymetry

2.2.1 Navigation

(1) Personnel
Satoshi Okumura (Global Ocean Development Inc.)
Shinya Okumura (GODI)
Ryo Ohyama (GODI)

(2) System description
Ship's position and velocity were provided by Radio Navigation System on R/V Mirai. This system integrates GPS position, log speed, gyro compass heading and other basic data for navigation, and calculated speed/course over ground on HP workstation. Radio navigation System also distributed ship's standard time synchronized to GPS time server via Network Time Protocol. These data were logged on the network server as "SOJ" data every 60 seconds.

Sensors for navigation data are listed below;
i) GPS receiver: Trimble DS-4000 with two GPS antennas located on navigation deck, starboard and port side, manually switched as to GPS receiving state and offset to radar-mast position, datum point.
ii) Dopplar log: Furuno DS-300, which use three acoustic beam for current measurement under the hull.
iii) Gyrocompass: Tokimec TG-6000, sperry type mechanical gyrocompass.
iv) GPS time server: Datum Tymserv 2100, NTP server synchronizing to GPS satellite every 1 second.

2.2.2 Swath Bathymetry

(1) Personnel
Takeshi Matsumoto (University of the Ryukyus)   Principal Investigator (Not on-board)
Satoshi Okumura (Global Ocean Development Inc.)
Shinya Okumura (GODI)
Ryo Ohyama (GODI)

(2) Introduction
R/V MIRAI is equipped with a Multi Narrow Beam Echo Sounding system (MNBES), SEABEAM 2112.004 (SeaBeam Instruments Inc.).

The main objective of MNBES survey is collecting continuous bathymetry data along ship's track to make a contribution to geological and geophysical investigations and global datasets.

(3) Data Acquisition
The system was operated in this cruise from Sekinehama, Japan on 24 July 2007 to fulfillment point of observation, on 1st September 2007. To get accurate sound velocity of water column for ray-path correction of acoustic multibeam, we used Surface Sound Velocimeter (SSV) data at the surface (6.2m) sound velocity, and the others depth sound velocity calculated temperature and salinity profiles from CTD and XCTD data by the equation in Mackenzie (1981) during the cruise. And also, we applied these calculated sound velocity profiles to each raw data in place, recalculated swath bathymetry data. Table

2.2.2-1 listed system configuration and performance of SEABEAM 2112.004 system.

Table 2.2.2-1 System configuration and performance

SEABEAM 2112.004 (12kHz system)

Frequency:	12 kHz
Transmit beam width:	2 degree
Transmit power:	20 kW
Transmit pulse length:	3 to 20 msec.
Depth range:	100 to 11,000 m
Beam spacing:	1 degree athwart ship
Swath width:	150 degree (max)
	120 degree to 4,500 m
	100 degree to 6,000 m
	90 degree to 11,000 m
Depth accuracy:	Within < 0.5% of depth or +/-1m, whichever is greater, over the entire swath. (Nadir beam has greater accuracy; typically within < 0.2% of depth or +/-1m, whichever is greater)

(4) Preliminary Results

The results will be published after primary processing.

(5)Data Archives

Bathymetric data obtained during this will be submitted to the Marine-Earth Data and Information Department　MEDID　of JAMSTEC.

2.2.3 Sea Surface Gravity

(1) Personnel

Takeshi Matsumoto (University of the Ryukyus)　Principal Investigator (Not on-board)
Satoshi Okumura (Global Ocean Development Inc.)
Shinya Okumura (GODI)
Ryo Ohyama (GODI)

(2) Introduction

The distribution of local gravity is an important parameter in geophysics and geodesy. We collected gravity data at the sea surface during the MR07-04 cruise from Sekinehama, Japan on 24th July 2007 to fulfillment point of observation, on 1st September 2007.

(3) Parameters

Relative Gravity [CU: Counter Unit]
[mGal] = (coef1: 0.9946) * [CU]

(4) Data Acquisition

We have measured relative gravity using LaCoste and Romberg air-sea gravity meter S-116 (Micro-g LaCoste, LLC) during this cruise. To convert the relative gravity to absolute one, we measured gravity using portable gravity meter (Scintrex gravity meter CG-3M and CG-5) at Sekinehama Port.

(5) Preliminary Results

Absolute gravity shown in Table 2.2.3-1

Table 2.2.3-1

No.Date	U.T.C.	Port	Absolute Gravity [mGal]	Sea Level [cm]	Draft [cm]	Gravity at L&R *[2] Sensor *[1] [mGal]	Gravity [mGal]
---- Jul/23	06:16	Sekinehama	980371.94	261	15	980372.78	12711.24
---- Oct/5	??:??	Sekinehama	980371.85	???	??	???????.??	?????.??

----

*[1]: Gravity at Sensor = Absolute Gravity + Sea Level*0.3086/100 + (Draft-530)/100*0.0431
*[2]: LaCoste and Romberg air-sea gravity meter S-116

(6) Data Archives

These data obtained in this cruise will be submitted to the Marine-Earth Data and Information Department　MEDID　of JAMSTEC.

2.2.4 On-board geomagnetic measurement

(1) Personnel

Takeshi Matsumoto (University of the Ryukyus)　Principal Investigator (Not on-board)
Satoshi Okumura (Global Ocean Development Inc.)
Shinya Okumura (GODI)
Ryo Ohyama (GODI)

(2) Introduction

Measurement of magnetic force on the sea is required for the geophysical investigations of marine magnetic anomaly caused by magnetization in upper crustal structure. We measured geomagnetic field using a three-component magnetometer during the MR07-04 cruise from Sekinehama, Japan on 24 July 2007 to fulfillment point of observation, on 1st September 2007.

(3) Parameters

Three-component magnetic force [nT]
Ship's attitude [1/100 deg]

(4) Method of Data Acquisition

A sensor of three-component fluxgate magnetometer is set on the top of foremast. Sampling is controlled by 1pps (pulse per second) standard clock of GPS signals. Navigation information, 8 Hz three-component of magnetic force, and VRU (Vertical Reference Unit) data are recorded every one second.

For calibration of the ship's magnetic effect, we made a "figure-eight" turn (a pair of clockwise and anti-clockwise rotation). This calibration carried out as below.

22 Aug 2007, 06:49 to 07:17 about at 46-59N, 152-31W

(5) Preliminary Results

The results will be published after primary processing.

(6) Data Archives

These data obtained in this cruise will be submitted to the Marine-Earth Data and Information Department　MEDID　of JAMSTEC.

2.3 Acoustic Doppler Current Profiler

(1) Personnel

Shinya Kouketsu (JAMSTEC)

Satoshi Okumura (GODI)

Shinya Okumura (GODI)

Ryo Ohyama (GODI)

(2) Instruments and method

The instrument used was an RDI 76.8kHz unit, hull-mounted on the centerline and approximately 23m aft of the bow at the water line. The firmware version was 5.59 and the data acquisition software was the RDI VMDAS Version. 1.4. The Operation was made from the Sekine port to the last CTD station. The instrument was used in the water-tracking mode during the most of operations, recording each ping raw data in 8m x 100bins from about 23m to 815m in deep. Typical sampling interval was 3.5 seconds. Bottom track mode was added in the easternmost shallow water region. GPS gave the navigation data. Two kinds of compass data were recorded. One was the ship's gyrocompass, which is connected the ADCP system directory, were stored with the ADCP data. Current field based on the gyrocompass was used to check the operation and the performance on board. Another compass used was the Inertial Navigation Unit (INU), DRU-H, Honeywell Inc. Its accuracy is 1.0mile (about 0.056 degree) and had already set on zero bias before the beginning of the cruise. The INU compass data were collected and stored through VMDAS, and were combined with the ADCP data after the cruise.

(3) Performance of the ADCP data

The performance of the ADCP instrument was almost good: on streaming, profiles usually reached to about 600m. Profiles were rather bad on CTD station. The profiles were sometimes obtained from 200m to 500m. In these cases the ADCP signal was weak typically at about 350m in deep. It is probably due to the babbles from the bow-thruster.

(4) Data processing

We processed ADCP data as described below. ADCP-coordinate velocities were converted to the earth-coordinate velocities using the ship heading from the INU. The earth-coordinate currents were obtained by subtracting ship velocities from the earth-coordinate velocities. Corrections of the misalignment and scale factors were made using the bottom track data obtained during this cruise. The misalignment angle calculated was 0.4 degree and the scale factor was 0.976. Criteria for the correlation less than 64 and error velocity more than 10 mm/s are removed here. Therefore the error is estimated at 10 mm/s. Cruise-averaged beam correlation and echo intensity are shown in Fig 2.3.1. Although the echo intensities rapidly became weak till the 20th bin, the correlations were more than 64 in the upper 60bins (about 500m). So the velocities were often obtained from the sea surface to the depth of about 500m in

this cruise.

The flow at the depth of about 50m measured the shipboard ADCP along the ship course is shown in the Fig. 2.3.2. The data when the ship was moving are used to plot.
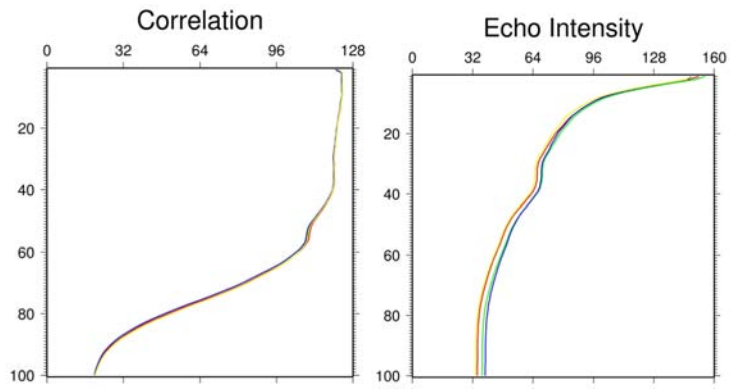

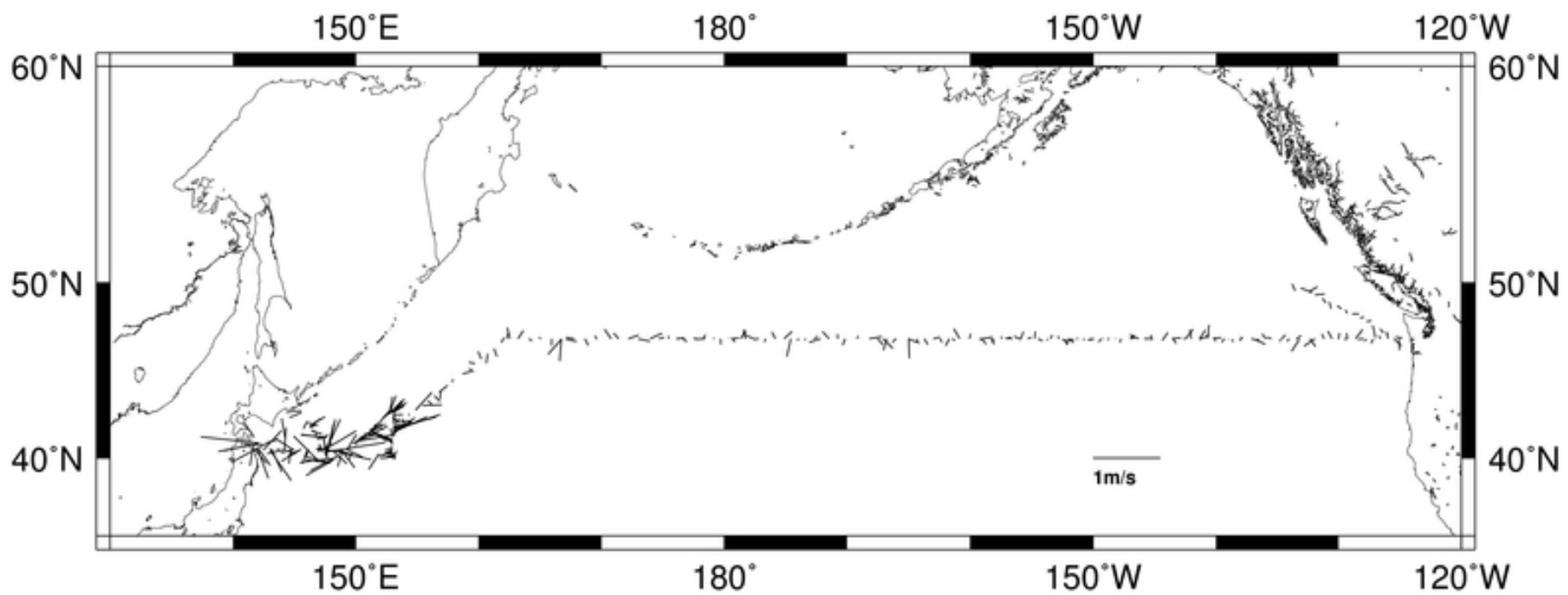Fig. 2.3.1 Correlations and echo intensities for each beam averaged over this cruise.

Fig. 2.3.2 Adcp velocity at the depth of about 50m.

2.4 Thermo-salinograph and related measurements

September 03, 2007

(1) Personnel

Yuichiro KUMAMOTO [1], *Kimiko NISHIJIMA* [2], *Keisuke WATAKI* [2], and *Miyo Ikeda* [2]

    1) Japan Agency for Marine Earth Science and Technology

    2) Marine Works Japan Co. Ltd

(2) Objective

Our purpose is to measure salinity, temperature, dissolved oxygen, and fluorescence in near-sea surface water during MR07-04 cruise.

(3) Methods

The Continuous Sea Surface Water Monitoring System (Nippon Kaiyo Co. Ltd.), including the thermo-salinograph, has five sensors and automatically measures salinity, temperature, dissolved oxygen, and fluorescence in near-sea surface water every one minute.   This system is located in the sea surface monitoring laboratory on R/V MIRAI and connected to shipboard LAN system. Measured data, time, and location of the ship were displayed on a monitor and then stored in a data management PC (IBM NetVista 6826-CBJ).

The near-surface water was continuously pumped up to the laboratory from about 4 m water depth and flowed into the system through a vinyl-chloride pipe.   The flow rate of the surface seawater was controlled by several valves and adjusted to be 12 L/min except for a fluorometer (about 0.5 L/min). The flow rate was measured by two flow meters.

Specifications of the each sensor in this system are listed below.

    a) Temperature and salinity sensors

        SEACAT THERMOSALINOGRAPH

Model:	SBE-21, SEA-BIRD ELECTRONICS, INC.
Serial number:	2641(7/25 ~ 7/31), 3126(7/31 ~ 9/1)
Measurement range:	Temperature −5 to +35°C, Salinity 0 to 6.5 S m^{-1}
Accuracy:	Temperature 0.01°C 6month^{-1}, Salinity 0.001 S m^{-1} month^{-1}
Resolution:	Temperatures 0.001°C, Salinity0.0001 S m^{-1}

    b) Bottom of ship thermometer

Model:	SBE 3S, SEA-BIRD ELECTRONICS, INC.
Serial number:	2175
Measurement range:	−5 to +35°C
Resolution:	±0.001°C
Stability:	0.002°C year^{-1}

    c) Dissolved oxygen sensor

Model:	2127A, HACH ULTRA ANALYTICS JAPAN, INC.
Serial number:	47477
Measurement range:	0 to 14 ppm
Accuracy:	±1% at 5°C of correction range
Stability:	1% month^{-1}

d) Fluorometer

     Model: 10-AU-005, TURNER DESIGNS

     Serial number: 5562 FRXX

     Detection limit: 5 ppt or less for chlorophyll-a

     Stability: 0.5% month^{-1} of full scale

e) Flow meter

     Model: EMARG2W, Aichi Watch Electronics LTD.

     Serial number: 8672

     Measurement range: 0 to 30 l min^{-1}

     Accuracy: ±1%

     Stability: ±1% day^{-1}

(4) Measurements

Periods of measurement, maintenance, and problems during MR07-04 are listed in Table 2.4.1.

Table 2.4.1 Events list of the thermo-salinograph during MR07-04

Date [UTC]	Time [UTC]	Event	Remarks
25-July-07	09:37	All the measurements started.	Departure Sekinehama
31-July-07	20:49	All the measurements stopped. Checked SBE21(S/N2641)	
31-July-07	21:49	All the measurements started. Exchanged SBE21(S/N2641 −> S/N3126)	
02-Aug.-07	23:15 23:16	Failure of data storage for location.	
08-Aug.-07	01:01	All the measurements stopped.	Arrival Hachinohe
10-Aug.-07	00:16	All the measurements started.	Departure Hachinohe
01-Sep.-07	17:55	All the measurements stopped.	Arrival Dutch Harbor

(5) Calibrations
i. Comparison with bottle data

We collected the surface seawater samples for salinity sensor calibration. The seawater were collected approximately twice a day from the outlet equipped in the middle of water line of the system using a 250ml brown grass bottle with plastic inner stopper and screw cap. The sample bottles were stored in the sea surface monitoring laboratory. The samples were measured using the Guildline 8400B at the end of the legs after all the measurements of the hydrocast bottle samples. The results are shown in Table 2.4.2.

Table 2.4.2 Comparison of the sensor salinity with the bottle salinity during MR07-04

Date [UTC]	Time [UTC]	Sensor salinity [PSS-78]	Bottle salinity [PSS-78]
25-Jul-07	11:45	33.5532	33.5435
25-Jul-07	22:50	33.1134	33.1092
26-Jul-07	7:50	33.0332	32.9148
26-Jul-07	18:35	32.8070	32.7676
27-Jul-07	6:57	32.7934	32.7528
27-Jul-07	18:26	32.6836	32.6956
28-Jul-07	6:25	32.7105	32.7144
28-Jul-07	17:42	32.7118	32.7226
29-Jul-07	6:17	32.7539	32.8174
29-Jul-07	18:17	34.3895	34.3785
30-Jul-07	6:15	34.3704	34.3733
30-Jul-07	18:49	34.4994	34.4946
31-Jul-07	6:58	34.4920	34.4889
31-Jul-07	19:15	33.0052	32.9972
01-Aug-07	7:01	33.2326	33.2204
01-Aug-07	17:05	33.0865	33.0802
02-Aug-07	3:43	33.0909	33.0860
02-Aug-07	14:40	33.7921	33.7798
03-Aug-07	11:06	34.5137	34.5066
03-Aug-07	21:09	33.7968	33.8032
04-Aug-07	8:43	34.1606	34.1553
04-Aug-07	23:16	33.8481	33.8440
05-Aug-07	7:25	33.9156	33.9139
05-Aug-07	22:56	33.5227	33.5537
06-Aug-07	8:29	33.7495	33.7120
06-Aug-07	22:49	34.4521	34.4463
07-Aug-07	8:34	33.6041	33.5854
10-Aug-07	3:29	32.6756	32.6924
10-Aug-07	15:38	33.0687	33.0622
11-Aug-07	2:43	33.9769	33.9437
11-Aug-07	7:34	32.8430	32.8564
11-Aug-07	21:08	32.9301	32.9136
12-Aug-07	10:23	32.7841	32.8029
12-Aug-07	20:49	32.8503	32.8436
13-Aug-07	10:17	32.7411	32.7608
13-Aug-07	22:10	32.8015	32.8139
14-Aug-07	12:08	32.7989	32.7947

Table 2.4.2 (continued)			
Date [UTC]	Time [UTC]	Sensor salinity [PSS-78]	Bottle salinity [PSS-78]
14-Aug-07	21:53	32.7283	32.7244
15-Aug-07	9:26	32.6862	32.6819
15-Aug-07	21:48	32.5401	32.5288
16-Aug-07	9:45	32.6165	32.6103
16-Aug-07	21:05	32.7305	32.7317
17-Aug-07	8:58	32.6261	32.6201
17-Aug-07	20:13	32.5481	32.5443
18-Aug-07	8:55	32.6200	32.6132
18-Aug-07	21:57	32.7182	32.7068
19-Aug-07	7:47	32.6417	32.6403
19-Aug-07	20:06	32.6488	32.6454
20-Aug-07	8:42	32.8259	32.7851
20-Aug-07	19:06	32.6516	32.6507
21-Aug-07	8:05	32.6803	32.6594
21-Aug-07	20:49	32.6733	32.6492
22-Aug-07	8:51	32.5771	32.5925
22-Aug-07	21:01	32.5729	32.5669
23-Aug-07	7:05	32.5377	32.5289
23-Aug-07	19:37	32.4434	32.4448
24-Aug-07	7:13	32.4713	32.3907
24-Aug-07	19:29	32.3720	32.3577
25-Aug-07	6:47	32.3190	32.3614
25-Aug-07	21:10	32.4736	32.4163
26-Aug-07	7:39	32.4100	32.4496
26-Aug-07	17:20	32.4774	32.4267
27-Aug-07	5:59	32.4447	32.4419
27-Aug-07	17:02	32.3672	32.3549
28-Aug-07	6:43	32.3364	32.2963
28-Aug-07	18:37	32.0321	32.1002*
29-Aug-07	6:10	31.8860	31.5810*
29-Aug-07	16:56	31.8923	32.3276*
30-Aug-07	7:34	32.2969	32.0908*

* Difference between the sensor salinity and the bottle one is large.

ii. Sensor calibrations

The sensors for temperature and salinity were calibrated before the cruise.   After the cruise the sensors will be calibrated again in order to evaluate drifts of measurements during the cruise.   The results of the calibrations will be available via JAMSTEC MIRAI DATA Web, http://www.jamstec.go.jp/mirai/2007/.

(6) Date archive

Quality controlled data of temperature, salinity, dissolved oxygen, and fluorescence will be available via the JAMSTEC MIRAI DATA Web as shown above.

2.5. pCO_2

(1) Personnel

Akihiko Murata (JAMSTEC)
Yoshiko Ishikawa (MWJ)
Yasuhiro Arii (MWJ)

(2) Objective

Concentrations of CO_2 in the atmosphere are now increasing at a rate of 1.5 ppmv y^{-1} owing to human activities such as burning of fossil fuels, deforestation, and cement production. It is an urgent task to estimate as accurately as possible the absorption capacity of the oceans against the increased atmospheric CO_2, and to clarify the mechanism of the CO_2 absorption, because the magnitude of the anticipated global warming depends on the levels of CO_2 in the atmosphere, and because the ocean currently absorbs 1/3 of the 6 Gt of carbon emitted into the atmosphere each year by human activities.

In this cruise, we are aimed at quantifying how much anthropogenic CO_2 are absorbed in the surface ocean in the North Pacific. For the purpose, we measured pCO_2 (partial pressure of CO_2) in the atmosphere and surface seawater along the WHP P1 line at 47°N.

(3) Apparatus

Concentrations of CO_2 in the atmosphere and the sea surface are measured continuously during the cruise using an automated system with a non-dispersive infrared (NDIR) analyzer (BINOS^{TM}). The automated system is operated by one and a half hour cycle. In one cycle, standard gasses, marine air and an air in a headspace of an equilibrator are analyzed subsequently. The concentrations of the standard gas are 289.75, 349.02, 393.75 and 439.73 ppmv. The standard gases will be recalibrated after the cruise.

The marine air taken from the bow is introduced into the NDIR by passing through a mass flow controller which controlls the air flow rate at about 0.5 L/min, a cooling unit, a perma-pure dryer (GL Sciences Inc.) and a desiccant holder containing $Mg(ClO_4)_2$.

A fixed volume of the marine air taken from the bow is equilibrated with a stream of seawater that flowed at a rate of 5-6L/min in the equilibrator. The air in the equilibrator is circulated with a pump at 0.7-0.8L/min in a closed loop passing through two cooling units, a perma-pure dryer (GL Science Inc.) and a desiccant holder containing $Mg(ClO_4)_2$.

(4) Results

Concentrations of CO_2 (xCO_2) of marine air and surface seawater are shown in Fig. 2.5.1. From this figure, it is found that the ocean acted generally as a sink for atmospheric CO_2 during the cruise.
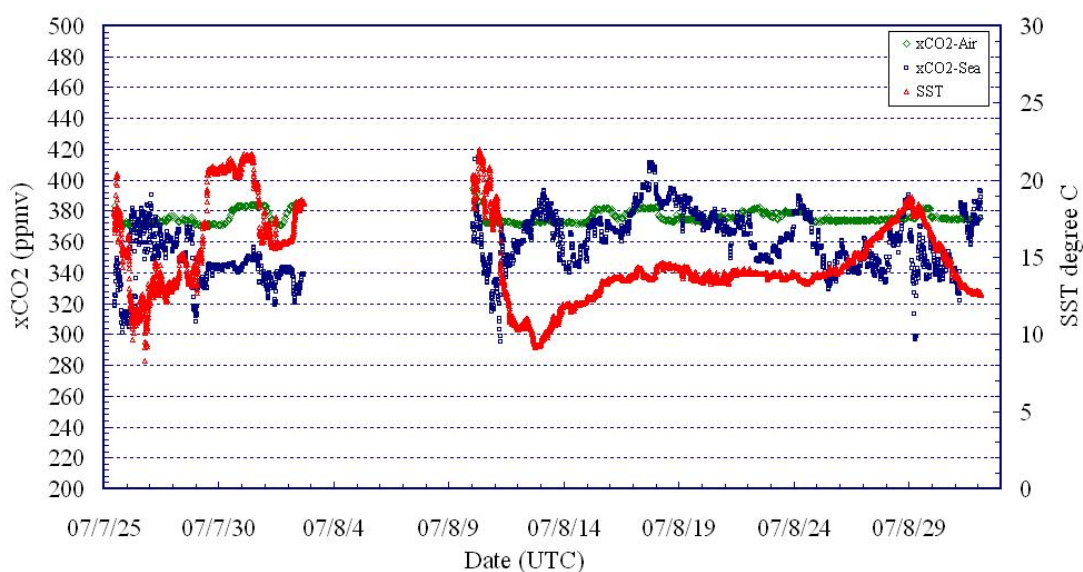
Fig. 2.5.1. Concentrations of CO_2 (xCO_2) in atmosphere (green) and surface seawater (blue), and SST (red).

2.6 Ocean Radon Flux across Air-Sea Interface

(1) Personnel

Shigeki Tasaka (Gifu Univ.)

Corresponding author. E-mail: tasaka@gifu-u.ac.jp

(2)Objectives

The concentrations of [222]Rn in near-surface seawater and atmosphere were continuously observed in order to measure the ocean radon flux across the air-sea interface. And twenty near-surface seawater samplings were carried out for the [226]Ra concentration measurements. The radon flux was estimated from the measurements of radon concentrations, wind speed and sea surface temperature by using the model of Wanninkhof(1992) for gas transfer velocity.

(3)Instrument and Method

i. Instrument

Radon observation system consisted of two high sensitivity radon detectors, degasification units for radon gas dissolved in seawater, radon free air producing module and radon data collection system. The method of radon detection is electrostatic collection of daughter nuclei of [222]Rn, and -spectrometry using PIN photodiode. The volume of radon detector vessel is 70liter. In order to keep the background at low level, the inside of the vessel is electro-polished. The background level of two radon detectors was measured among a month before this cruise. The result of background run is 10.2([214]Po count/day) giving detection limit of 0.01(Bq/m^3). This radon detector was developed for continuous monitoring of low level radon concentration in the Super-Kamiokande experiment (Takeuchi et al 1999).

ii. Method

The sample atmosphere air was taken from the fore mast with air sampling platform at the

height of 12.5m from sea level into the sea surface water monitoring laboratory, R/V MIRAI.   Sampling air was used as the source of the radon free air and atmosphere air sample. Radon free air producing module was consisted of charcoal(active carbon granular), cooling device and desiccant $Mg(ClO_4)_2$. Seawater was pumped up from sea surface at depth 4.5m, which is successively flowed into the top of degasification units with flow rate 2.7liter/min and radon free air was supplied to the bottom of one with flow rate 1.7liter/min. Radon free air after passing the degasification units was continuously introduced into one of the radon detector after electronic-dehumidifier with dew-point temperature 0.1(deg C). Sample of atmospheric air was directly introduced into other radon detector after electronic-dehumidifier with flow rate 5liter/min.

   Real observation data of   -rays energy spectrum from two radon detectors were processed to measure radon concentration of atmospheric air and seawater by note-PC, 10minutes interval. PC was working to measure and analysis, and Web Server. Radon concentration and flow rate, temperature, dew-point of sample air and seawater were browsed and watched in the local area networks.

(4) Preliminary Results
i. Radon Concentration in Atmosphere air
         Hourly average of atmospheric radon concentration was measured from July-25 to August-31, 2007. Fig.2.6.1 shows atmospheric radon concentration in Cruise MR07-04. Maximum radon concentration was recorded to be 12(Bq/m^3) at Hachinohe port on July-25 and August-9, 2007. The radon concentration was gradually decreasing after August-9, 2007, and became   to be 0.29(Bq/m^3) after crossing the meridian of 180° in latitude 47° N. Minimum value was observed to be 0.03 (Bq/m^3) on August-4, August-24 and August-29, 2007, when the clean air mass came into the navigation area from the southern sea of Pacific Ocean by reference of the back trajectory analysis results. Observation data will be compared with the global atmospheric transport model.
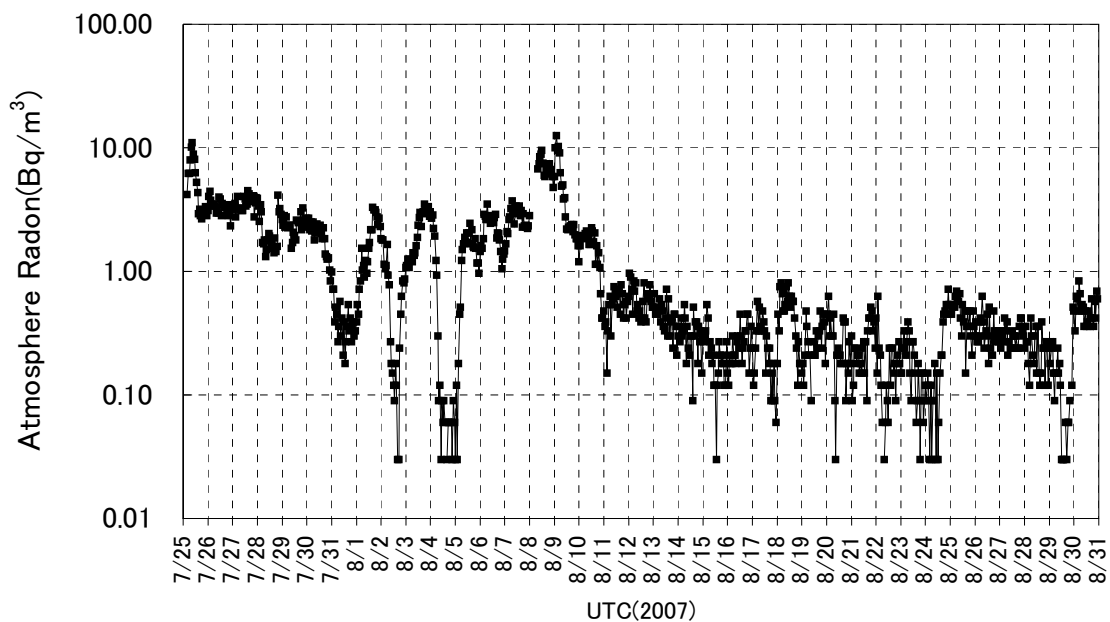

Fig.2.6.1 Atmospheric Radon Concentration in Cruise MR07-04 from July-25 to August-30, 2007.

ii. Radon Concentration in seawater
         Seawater radon measurements of RUN#0   RUN#22 were carried out from August-2 to

August-30, 2007, in the North Pacific, longitude of 146° E to 127° W. Total live time was 385hr in all run. Flow rate of radon free air was decreasing after 18hr from start of run, because of the loss pressure in the charcoal element. We also re-started new run after changing new charcoal and desiccant $Mg(ClO_4)_2$. Seawater radon concentration Cw was estimated by use of blows form,

$$Cw=C(1+)Fa/Fw \quad (1)$$

where C is radon concentration measured by high sensitivity radon detector, Fa and Fw is the flow rate of radon free air and sample seawater, respectively. Coefficient is the radon solubility depend on sample seawater temperature. Fig.2.6.2 shows the hourly average of seawater radon concentration in the cruise MR07-04. Table 2.6.1 shows RUN#, RUN time, navigation sea area, the average of wind speed(m/s) and Standard Deviation, seawater radon concentration(Bq/m^3) and SD, atmosphere radon concentration(Bq/m^3) and SD, in RUN#0 RUN#22, respectively.
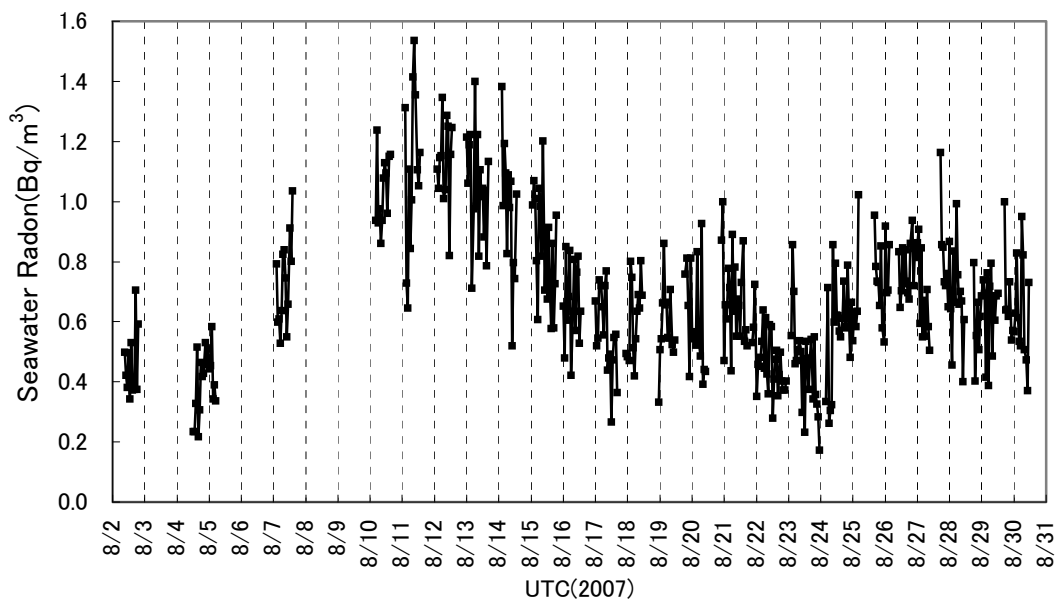

Fig.2.6.2 Seawater Radon Concentration in Cruise MR07-04 from August-2 to August-30, 2007.

In this cruise, low pressure zone pass through periodically in North Pacific. The sea surface was rough due to strong wind more than 10(m/s) on RUN #0, #1, #10, #11, #12 and #15. In these RUN, seawater radon concentration was showed less than 0.5 (Bq/m^3). And correlation coefficient between wind speed and seawater radon concentration was estimated to be –0.64.

Table 2.6.1 RUN#, RUN time, navigation sea area, the average of wind speed(m/s) and standard deviation, seawater radon concentration(Bq/m³) and SD, atmosphere radon concentration(Bq/m³) and SD, of RUN#0 to RUN#22 in Cruise MR07-04 from August-2 to August-30, 2007.

#	RUN time	navigation area	wind speed	SD	seawater Rn	SD	atmosphereRn	SD
0	08/02 09:00-08/02 19:00	(42-35.38N,153-03.13E)-(42-02.10N,153-04.11E)	11.6	1.1	0.46	0.11	0.17	0.12
1	08/04 12:00-08/05 05:00	(40-01.49N,153-03.71E)-(40-13.75N,152-51.78E)	10.0	2.0	0.40	0.11	0.12	0.14
2	08/07 02:00-08/07 14:00	(40-24.84N,146-50.74E)-(40-27.44N,145-20.72E)	5.8	1.2	0.73	0.15	2.94	0.52
3	08/10 01:40-08/10 16:02	(40-30.65N,147-54.22E)-(41-50.33N,152-25.98E)	5.6	2.6	1.03	0.12	1.93	0.19
4	08/11 00:05-08/11 14:05	(42-53.80N,154-53.75E)-(45-06.40N,158-47.65E)	2.6	0.6	1.11	0.27	0.51	0.18
5	08/12 00:22-08/12 14:10	(46-52.09N,162-01.23E)-(46-59.51N,165-26.13E)	4.7	0.9	1.13	0.14	0.60	0.19
6	08/12 22:50-08/13 19:15	(46-59.47N,169-31.00E)-(47-00.22N,174-29.09E)	3.5	0.8	1.05	0.18	0.47	0.12
7	08/14 00:42-08/14 14:04	(47-00.02N,176-05.97E)-(47-00.36N,178-18.35E)	5.5	0.9	0.98	0.23	0.32	0.10
8	08/14 23:05-08/15 20:00	(47-00.48N,179-37.51E)-(47-00.35N,177-11.68W)	9.5	1.7	0.85	0.18	0.23	0.12
9	08/15 23:03-08/16 15:04	(47-00.75N,176-08.74W)-(47-00.05N,173-47.80W)	8.3	1.6	0.66	0.14	0.24	0.08
10	08/16 22:50-08/17 18:11	(46-59.72N,172-42.23W)-(47-00.11N,169-21.25W)	10.4	1.4	0.56	0.14	0.31	0.13
11	08/17 21:56-08/18 12:08	(46-59.64N,169-20.12W)-(46-59.27N,167-04.61W)	11.5	0.8	0.61	0.13	0.53	0.24
12	08/18 21:00-08/19 12:10	(47-00.55N,165-17.44W)-(47-00.28N,162-51.53W)	11.8	1.0	0.58	0.13	0.21	0.12
13	08/19 16:53-08/20 11:10	(46-59.48N,162-33.11W)-(46-59.37N,159-15.56W)	4.9	2.0	0.61	0.17	0.38	0.12
14	08/20 20:57-08/21 18:00	(47-00.31N,158-03.38W)-(46-59.73N,154-33.50W)	7.3	1.1	0.68	0.15	0.21	0.08
15	08/21 20:12-08/22 23:00	(47-00.18N,153-40.07W)-(47-00.15N,151-24.97W)	10.3	1.4	0.47	0.11	0.20	0.14
16	08/23 01:38-08/24 01:06	(46-59.77N,151-21.22W)-(47-00.04N,146-55.57W)	5.4	1.9	0.46	0.15	0.18	0.10
17	08/24 03:25-08/25 08:04	(46-59.65N,146-55.65W)-(46-59.64N,141-24.47W)	8.0	1.3	0.60	0.17	0.30	0.22
18	08/25 15:45-08/26 05:04	(47-01.55N,140-13.58W)-(46-59.47N,137-57.84W)	6.0	0.5	0.76	0.13	0.35	0.09
19	08/26 08:20-08/27 10:02	(46-59.52N,137-10.13W)-(47-00.02N,132-22.01W)	5.8	1.1	0.74	0.12	0.32	0.08
20	08/27 16:01-08/28 14:17	(47-00.41N,131-13.96W)-(46-59.64N,127-11.93W)	8.0	0.5	0.74	0.17	0.29	0.09
21	08/28 17:30-08/29 14:01	(47-00.36N,126-28.82W)-(47-40.97N,127-01.83W)	3.8	1.7	0.63	0.13	0.18	0.07
22	08/29 16:01-08/30 13:01	(47-55.31N,127-41.00W)-(50-10.18N,134-33.12W)	8.2	1.9	0.65	0.16	0.38	0.25

iii. Ocean Radon Flux Across Air-Sea Interface

Estimations for ocean radon flux was the used model of Wanninkhoh(1992) for gas transfer velocity containing a quadratic dependence on wind speed. The flux of soluble radon gas across the air-sea interface can be expressed as

$$F=k(Cw- \quad Ca) \qquad (2)$$

where k is the gas transfer velocity, Cw is seawater radon concentration and Ca is atmosphere radon concentration near the air-sea interface, and   is the Ostwald solubility coefficient. The k is a function of the interfacial turbulence, the kinematic viscosity of the seawater μ, and the diffusion coefficient of gas, D. The dependence of k on the last two terms is expressed as the Schmidt number $Sc=\mu /D$. k is proportional $Sc^{-0.5}$ for an interface with waves. For steady winds, relationship between gas transfer and wind speed is taken to be following form by Wanninkhoh,

$$k=0.31u^2(Sc/660)^{-0.5} \qquad (3)$$

where 660 is the Schmidt number of CO_2 in seawater at 20   and u is wind speed. In the Wanninkhoh paper, radon Schmidt number

$$Sc=A- Bt+Ct^2- Dt^3 \qquad (4)$$

where A=3412.8, B=224.3, C=6.7954, D=0.083, and t is sea surface temperature (deg C).   And radon solubility coefficient

$$=9.12(273+t)/273(17+t) \qquad (5)$$

  Ocean radon flux across air-sea interface was obtained by substitution of observation results Ca, Cw, u, t for the form (2), (3), (4), (5).

   Fig.2.6.3 shows the hourly average of ocean radon flux in RUN#0 RUN#22. Large radon flux more than 0.05(mBq/m²/s) was obtained on July-20, August-4, August-15 to August-19 and August-22, 2007,

with the strong wind more than 10(m/s). Total averaged ocean radon flux was measured to be 0.02(mBq/m^2/s) with averaged wind speed 7.4(m/s) in this cruise.
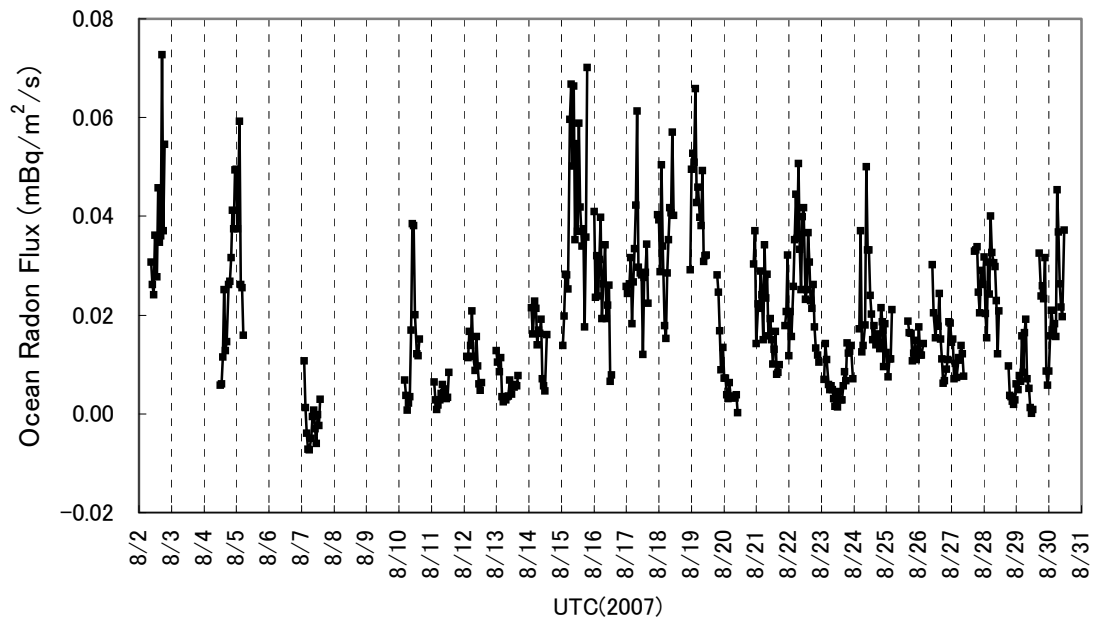

Fig.2.6.3 Ocean Radon Flux in Cruise MR07-04 from August-2 to August-30, 2007.

S.D.Schery and S.Huang predicted an annually average of the global ocean radon flux by using a radon flux model of wind speed and temperature dependence of form(3), and assuming sea surface radon concentration proportional to sea surface ^{226}Ra concentration. They calculated an annually average global radon flux of 0.038(mBq/m^2/s). They predicted the annually averaged radon flux of 0.015(mBq/m^2/s) for latitude bands between 40° and 60° N in this cruise. Our experimental result of radon flux 0.02(mBq/m^2/s) in summer season was consistent with their prediction values, but was smaller than values that have been assumed for the ocean source term in global model predictions of atmospheric radon.

(5) Further data quality check

These preliminary results will be checked the uncertainty of the calibrated factor of radon concentration and the difference of detection efficiency between two high sensitivity radon detector. ^{226}Ra concentration of seawater samples   will be measured by low background   - spectrometry method, and ^{222}Rn and ^{226}Ra concentration in the surface seawater will be compared with each others.

References

Rik Wanninkhof : Relationship Between Wind Speed and Gas Exchange Over the Ocean, Journal of Geophysical research, Vol. 97, 7373-7382, 1992.
Y. Takeuchi, K.Okumura, T.Kajita, S.Tasaka, H.Hori, M.Nemoto, H.Okazawa : Development of high sensitivity radon detectors, Nuclear Instruments and Methods in Physics Research, A421, 334-341, 1999.
S.D.Schery and S.Hung : An estimate of the global distribution of radon emissions from the ocean, Geophysical research Letters, Vol. 31, L1910, 2004.

2.7 Measurements of DMS in seawater and atmosphere

September 2, 2007

(1) Personnel

Ippei Nagao (Nagoya University)

(2) Objectives

My objectives in MR07-04 cruise were to understand the spatial and temporal variations in dimethylsulfide (DMS) and its precursor dimethylsulfoniopropionate (DMSP) over the North Pacific along the P01 line, and to set up the measurement system of fluorine induced chemiluminescence technique for direct measurement of turbulent DMS flux from ocean to atmosphere.

(3) Instruments and Methods

i. Measurements of DMS and DMSP by GC/FPD system

Atmospheric DMS concentration

Continuous measurement of the atmospheric DMS concentration was carried out at almost every 2 hours. Sample air was introduced through 15 m long Teflon-tube (OD: 10mm, and ID: 8 mm) from the compass deck to the Environmental Research Laboratory of R/V Mirai with the flow rate at 30~36 L/min by sampling pump (Iwaki Co. Ltd.). This sample air was separated in the manifold to introduce the analysis system with the flow rate at 150 ml min^{-1}. The sample air was then concentrated on the concentration tube (60/80 mesh Tenax-GR, GL Science Co. Ltd.) at -75 by liquid CO_2 after removing water vapor by perma pure dryer (MD-070-48F, GL Science Co. Ltd.). Then pre-concentration tube was heated at +200 within 1.5 min, and DMS trapped on Tenax-GR was introduced to Gas Chromatography equipped with a flame photometric detector (GC-14B, Shimadzu Co. Ltd.) by the ultra high pure N_2 gas. Analysis column of this system was - ' oxydipropionitrile glass column (ZO-1, Shimadzu Co. Ltd.). The carrier gas was 99.9999% quality nitrogen. Temperature in the column oven was set to be 60 C. Calibration of this system was performed by DMS standard gas (5.16 ppmv, N_2 base, Nagoya-Kosan Co. Ltd.). By standard gas dilutor (Thermo Electron Co. Ltd. Model-88), three or four levels of DMS concentration were analyzed to calibrate this system. The detection limit (DL) was estimated to be 8 pptv in 5 liter of STP. The precision was ± 10%.
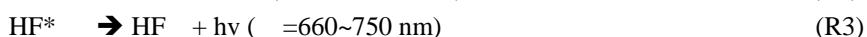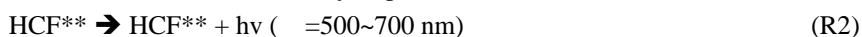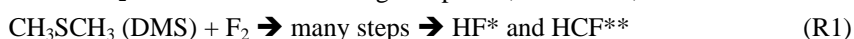
Seawater DMS and DMSP concentrations

100mL of seawater samples were taken from the Niskin bottles at five depths (10m, 50m, 100m, 150m, and 200m) to the brown glass bottles. After overflow of seawater, the sample bottle was immediately sealed with butyl gum cap with care to exclude air bubbles. Then these samples were stored in the refrigerator. Analysis of DMS was performed on board within a day by a purge and trap system. A 30 ml of seawater sample was introduced into a degasification vessel by syringe through GF/F filter. Then sample water was sparged for 10 min by ultra high pure N_2 gas (99.9999%, Nagoya-Kosan Co. Ltd.). The flow rate was about 120 ml min^{-1}. The extracted gas was then concentrated on the concentration tube (60/80 mesh Tenax-GR, GL Science Co. Ltd.). Then the determination of DMS was carried out by the same procedures as those for air samples. Reproducibility of this system was about ± 8.5%, and the detection limit was about 0.05nM in 30 ml water sample.

Dissolved DMSP (DMSPd) was determined as DMS by the cold alkali treatment method. After removal of volatiles from filtered water by purging, the sample was transferred to a 30 mL glass vial. Then 100 mg of NaOH was added to set the pH to ~13. The sample was left to react at room temperature for a day to achieve the full transformation of DMSP into DMS. The newly formed DMS was purged from the solution and measured as described above. For particulate DMSP (DMSPp), the GF/F filter

(Whatman Co. Ltd.   25mm) used during the sample filtration to the purge flask was replaced into a 30 mL glass vial, filled with MillQ water, and allowed to react for a day with 100 mg NaOH. The entire volume was taken with a syringe to follow the purging procedure.

ii. Atmospheric DMS measurement by fluorine induced chemiluminescence

High speed sensor for DMS based on its fast chemiluminescence reaction with molecular fluorine (F_2) was developed following the document by Hills et al [1998]. Intense chemiluminescence occurred upon reaction of F_2 with a sulfur-containing compound, as follows;

$$CH_3SCH_3 \text{ (DMS)} + F_2 \rightarrow \text{many steps} \rightarrow HF^* \text{ and } HCF^{**} \qquad (R1)$$
$$HCF^{**} \rightarrow HCF^{**} + h\nu \ (\quad =500\text{\textasciitilde}700 \text{ nm}) \qquad (R2)$$
$$HF^* \quad \rightarrow HF \ + h\nu \ (\quad =660\text{\textasciitilde}750 \text{ nm}) \qquad (R3)$$

Emission in the wavelength range 450~650 nm was monitored via photon counting with a photomultiplier tube (R2228P, Hamamatsu Photonics, Co. Ltd.). Residence time of the sample air in the reaction cell was very short (much less than 0.1 sec). Assuming that reaction (R1) was a pseudo 1st order reaction, reaction (R1) was expected to almost complete within the residence time of sample air in the cell (0.012sec). Product gases were evacuated from the reaction cell and then scrubbed of F_2 and HF via a two-stage chemical trap, which first converts excess F_2 to CF_4 on activated carbon and then HF to H_2O on Ascarite II. This system was installed in the ship store (1) of R/V Mirai. Sample air was introduced from the top of the foremast through a Teflon-tube (10mm o. d. and c.a. 40m of length), and the sample air after analysis was exhausted outside. Signals of this reaction were recorded in personal computer, and then analyzed to calculate the DMS concentration by DMS standard gas (1.0 ppmv).

(4) Preliminary Results

Figure 2.7.1 shows the temporal variation in the atmospheric DMS concentration measured by GC/FPD system during this cruise. A large variation of DMS concentration ranged from DL to 3000 pptv was observed. For instance, high concentration was observed from JD226 to JD229 and from JD233 to JD235, while low concentration was observed from JD209 to JD225. Maximum concentration (c.a. 3200 pptv) was observed on JD234. Since the DMS in the surface seawater is the source of the atmospheric DMS over ocean, the temporal variation in the seawater DMS concentrations at several depths measured during this cruise were shown in Figure 2.7.2. As shown in Figure 2.7.2, the period of high DMS concentration in the atmosphere roughly corresponded to those when the seawater DMS concentration at the depth of 10 m was high. High concentration of the seawater DMS (tentative definition of high DMS concentration in this report was > 10nM) was observed in the area of between 175 W and 135 W (Figure 2.7.3). Further analysis to explain the high DMS concentration both in the seawater and atmosphere will be required by including phytoplankton abundance, wind speed, stratification of the lower atmosphere and the abundance of species which oxidize DMS in the atmosphere.

Figure 2.7.4 shows the scatter plot of the atmospheric DMS concentration measured by GC/FPD system and the signal output of F_2-induced chemiluminescence technique for determination of the atmospheric DMS concentration. Fairly good positive correlation was obtained from 11 run, although the slope and intercept of the regression equation were apart from 1.0 and 0.0, respectively. Further improvements should be required. For instance, other interference gases such as volatile organic compounds (VOCs) other than DMS should be identified, and their influence should be reduced in future.
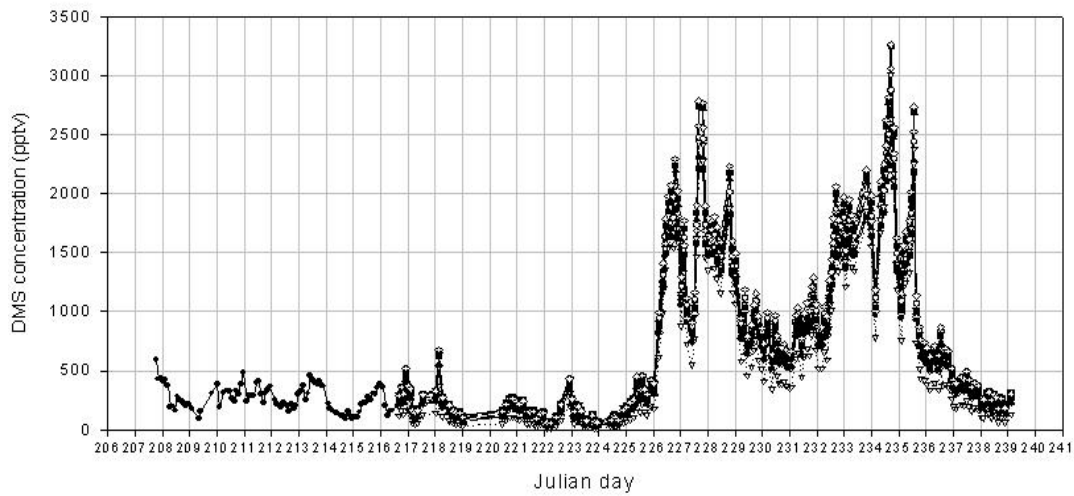
Figure 2.7.1 Temporal variation in the atmospheric DMS concentration measured during MR07-04 cruise. The DMS concentration was dependent on the calibration curves. Several symbols in this figure indicate this dependency.
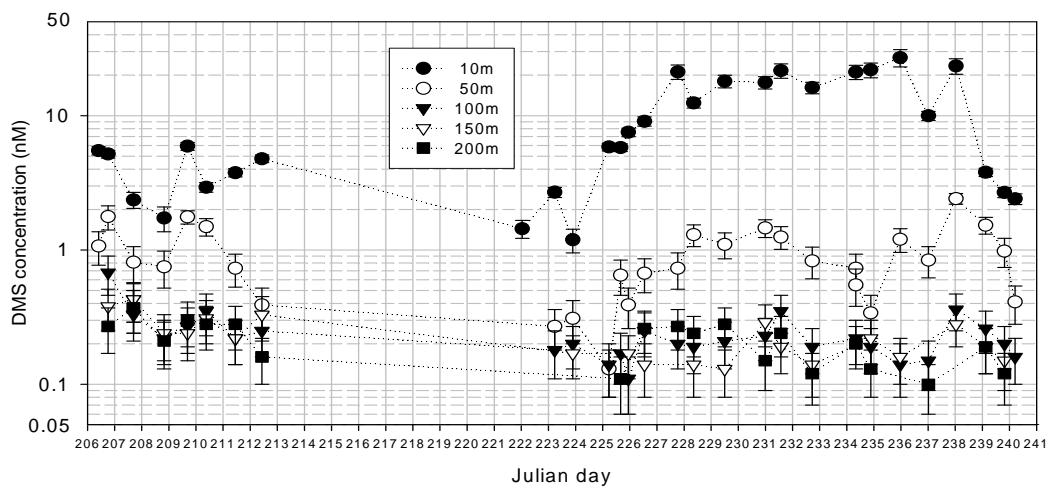

Figure 2.7.2 Temporal variations in the seawater DMS concentrations at 5 depths (10m, 50m, 100m, 150m, and 200m) measured during MR07-04 cruise. The DMS concentration was dependent on the calibration curves, and error bars in this figure indicate this dependency.
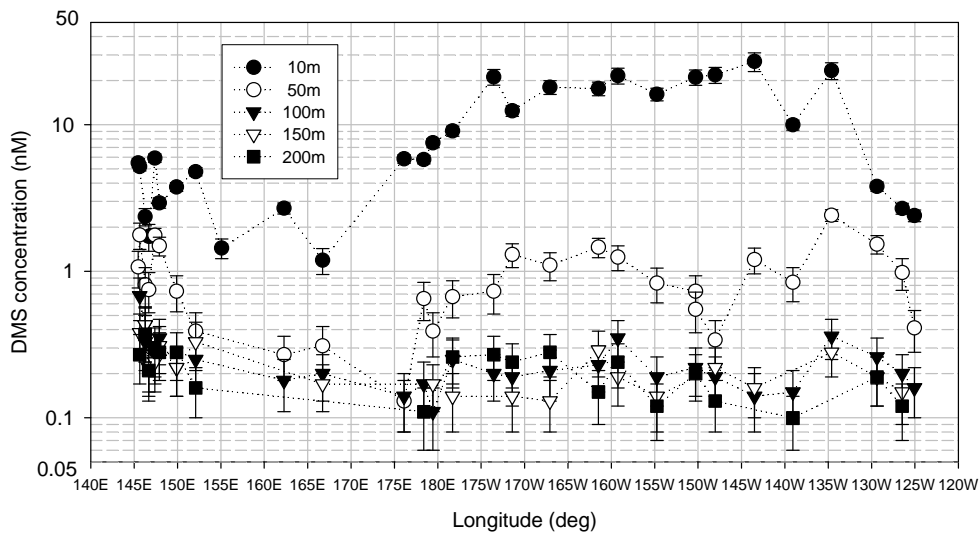
Figure 2.7.3 Longitudinal distributions of the seawater DMS concentrations at 5 depths. The DMS concentration was dependent on the calibration curves, and error bars in this figure indicate this dependency.
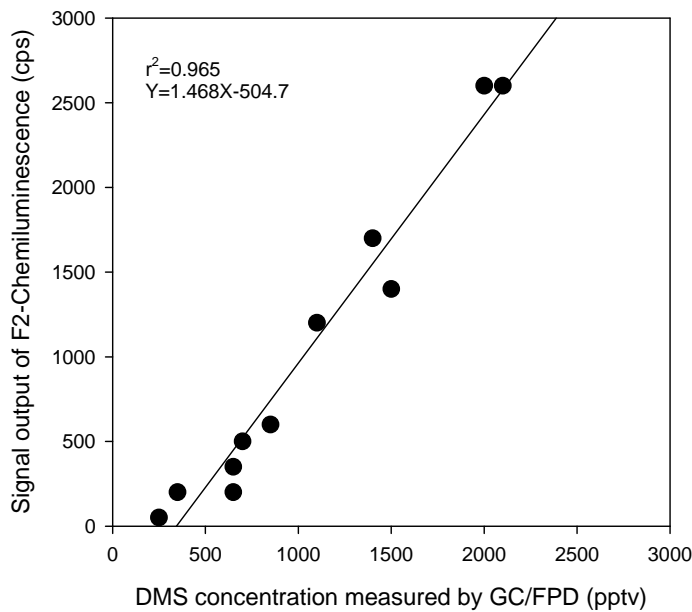

Figure 2.7.4 Scatter plot of the atmospheric DMS concentration measured by GC/FPD system and the signal output of F2-chemiluminescence.

2.8 Aerosol and fog water flux measurement

September 3, 2007

(1) Personnel

> *Yoko Iwamoto (Ocean Research Institute, the Univ. of Tokyo)*
> *Kaori Kawana (Ocean Research Institute, the Univ. of Tokyo)*
> *Mitsuo Uematsu (Ocean Research Institute, the Univ. of Tokyo) (Not on board)*

(2) Objectives

The northern North Pacific has a high sea fog frequency during summer because the warm and wet air mass from the lower latitude of North Pacific passes over the cold sea surface of the northern North Pacific and is cooled down to sufficient low temperature for the formation of fog.   Sea fog plays an important role not only in reflection of solar radiation, but also in linkage of chemical material between surface ocean and lower atmosphere through scavenging anthropogenic or biogenic aerosols in marine boundary layer.

For detailed aerosol and fog water flux measurement, it is necessary that measuring size distribution of aerosols and fog droplets by high time resolution.   In this study, the eddy covariance method (10 Hz acquisition rate) in a unique integration of aerosols and fog droplets measuring equipment on a moving ship is employed in order to cover wide areas of the marine boundary layer. Simultaneously, aerosols, fog water, rainwater and seawater samples were collected during this cruise for post-chemical analysis.   In addition, the concentrations of ozone, carbon monoxide and sulfur dioxide, which are good parameters for characterization of air masses in marine boundary layer, have been measured.

(3) Measured parameters

i. Turbulent fluxes obtained by eddy covariance system located at the top of the foremast

- Atmospheric aerosol particle flux in one size class from 5 nm to 3 µm particle diameter
- Fog water fluxes in 40 size classes from 2 to 50 µm fog droplet diameter
- CO_2 and water vapor fluxes

ii. Property of trace gas and atmospheric aerosol particles measured at the compass deck

- Aerosol particle number distribution (particle size classes: 0.10, 0.15, 0.20, 0.30, 0.50, 1.0, 2.0, 5.0 µm< diameter)
- Sulfate concentration in aerosol (PM1.0: <1.0 µm in diameter)
- Ozone concentration
- Sulfur dioxide concentration
- Carbon monoxide concentration

iii. Aerosol, fog water, rainwater and seawater sampling for post-chemical analyses

- High volume filter samples of aerosol particles PM2.5 (<2.5 µm in diameter) and PM>2.5 at the compass deck
- Passive string fog water collection at the compass deck
- Two-stage fog impactor fog water collection at the compass deck
  Stage 1: Aero-dynamical droplet diameter of > 13 µm
  Stage 2: Aero-dynamical droplet diameter from 6 to 13 µm
- Rainwater collection at the compass deck
- Seawater sampling at depth of 0, 10, 50, 100, 150 and 200 m

(4) Instruments and methods
i. Turbulent fluxes obtained by eddy covariance system located at top of foremast

The configuration and the sensors of the eddy covariance system as deployed at the top of the foremast are depicted in Figure 2.8.1. Each sensor is connected via RS232 through an RS232-LAN server to the recording PC at the environmental research laboratory. The combination of serial communication and TCP/IP-protocol based system enable us to record the data free of noise as well as get besides the parameters also all available status information of the sensors for consecutively quality assurance.
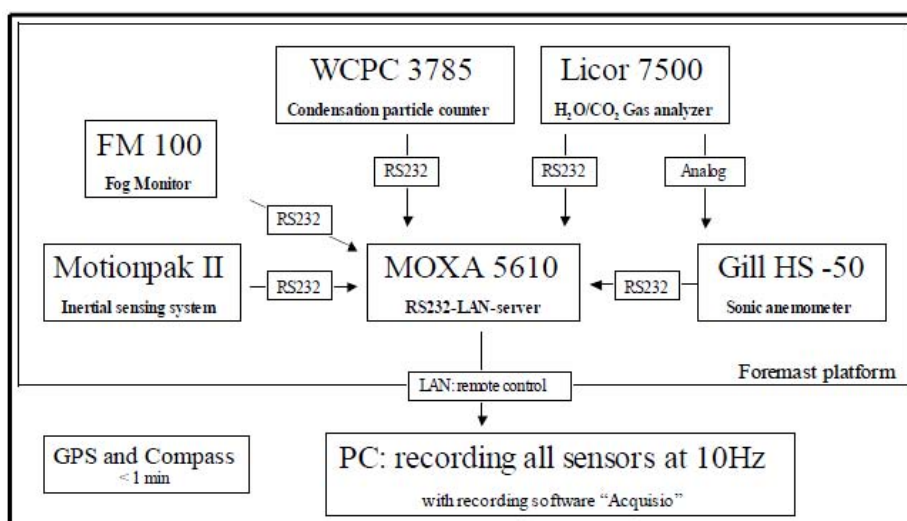

Fig. 2.8.1 Technical layout of the eddy covariance System

ii. Property of trace gas and atmospheric aerosol particles measured at compass deck

Aerosol particle number distribution was measured with 7 size ranges (0.10, 0.15, 0.20, 0.30, 0.50, 1.0, 2.0, 5.0 µm<diameter) by two particle counters (RION, model KC-18 and KC-01D) for every 5 minutes. The concentration of sulfate in aerosols was measured for every 10 minutes by using ambient particulate sulfate monitor (Rupprechet & patashnik Co. Inc., model 8400S). This instrument measured the mass concentration of ambient particulate sulfate contained in fine particles (PM1.0). Ozone concentration was measured every 12 seconds by an ozone monitor (Dylec Corp., model 1150). Carbon monoxide concentration was measured every 1 minute by a CO analyzer (Thermo Electron Co. Inc., model 48C). Sulfur dioxide concentration was measured every 1 minute by a sulfur dioxide analyzer (Kimoto Electronic Co. Ltd., model SA631).

iii. Aerosol, fog water, rainwater and seawater sampling for post-chemical analysis

Size-fractionated aerosols (PM2.5 and PM>2.5) were collected on Teflon filters (ADVANTEC, PF040, 90 mm) by High-volume virtual dichotomous impactors (Kimoto Electric Co. Ltd., model AS9) at 12 hours or 5 days intervals on the compass deck. In order to avoid contamination from ship exhaust, all aerosol samplers were automatically controlled by a wind sector to operate only when the relative wind direction ranged from -100º to 100º of the bow and relative wind speed was higher than 1 m s^{-1}. After collections, the samples were stored at 5 ℃ prior to analysis.

Bulk fog water samples were collected using a passive string fog sampler (Usui Co. Inc.,

FWG-400) on compass deck.　This device traps fog droplets by collision with Teflon strings (0.5 mm in diameter).　The fog droplets collide with the strings and drop along the strings into 500 ml Teflon bottle beneath the strings.　　Size-fractionated fog droplets (fog droplets diameter 6-13, >13 μm) samples were collected in plastic bottles using a two-stage fog impactor (Meßtechnik für Ummeltforschung, enviscope) on compass deck.　Rainwater samples were collected in PTFE bottles using rainwater sampler (Shibata Co. Inc., W-102) on the compass deck.　Table 2.8.1 and 2.8.2 shows time and location when fog water or rainwater sampling started, respectively.　After the collection, pH and electrical conductivity were measured, and samples were filtered by 0.4 μm pore size Nucrepore filters. The filtered fog water and rainwater were stored in plastic bottles (5 ℃), the filters were also stored at 5 ℃.

　　　　Seawater samples were collected with Niskin bottles from 5 layers (10, 50, 100, 150 and 200 m) at stns P01-013, 040, 044, 058, 069, 078, 088, 098, 107 and 111.　Surface seawater samples were collected using plastic buckets at stns P01-013, 017, 020, 024, 028, 040, 044, 058, 060, 061, 063, 067, 069, 073, 078, 080, 084, 088, 090, 094, 098, 102, 107, 111 and 114.　These samples were filtered by 10 and 0.4 μm pore size Nucrepore filters and the filters stored at 5 ℃.

Table 2.8.1　　Starting time and location of fog water sampling.

Smpl #	Time UTC	Location Lat. [N]	Location Long. [E]	Duration [hh:mm]	Smpl volume [mL]	pH	Conductivity [uS]
21	2007/7/26 14:44	42.8490	145.5423	4:12	202	3.362	72.9
22	2007/7/26 18:56	42.6468	145.6978	4:44	132	3.192	228
23	2007/7/27 6:00	42.2353	146.0650	1:00	98	4.334	38.6
24	2007/7/27 17:21	41.9687	146.2730	0:54	100	3.518	180.6
26	2007/7/28 0:31	41.7330	146.4002	0:45	54	3.139	272
27	2007/7/28 13:13	41.6293	146.5552	2:06	300	3.012	230
28	2007/7/30 15:24	40.0352	148.4100	2:56	398	3.517	117
29	2007/7/30 22:04	40.4128	149.0132	0:56	78	3.551	112.1
30	2007/7/31 11:24	41.0218	150.0167	1:16	152	4.073	54.5
31	2007/8/2 4:38	42.7782	152.9485	1:57	124	2.96	317
32	2007/8/2 6:35	42.7313	153.0128	2:10	300	3.436	162.4
33	2007/8/2 12:31	42.3847	153.0492	1:58	170	3.982	130.8
34	2007/8/2 14:29	42.2812	153.0497	2:16	356	3.809	139.6
35	2007/8/4 2:44	40.1825	153.0028	2:14	182	3.258	185.8
36	2007/8/4 4:58	40.0497	153.0162	2:55	86	3.384	129.3
37	2007/8/11 13:45	45.0497	158.6782	2:13	92	3.194	93
38	2007/8/11 15:58	45.4397	159.4138	2:30	234	3.652	50.1
39	2007/8/15 13:40	47.0032	181.9202	4:15	355	4.366	53.8
40	2007/8/16 10:48	46.9977	185.1507	2:47	184	3.612	167.7
41	2007/8/16 23:45	46.9947	187.3018	1:16	134	3.627	68.1
42	2007/8/17 1:01	46.9908	187.3197	2:13	109	3.576	229
43	2007/8/17 16:23	46.9943	189.9505	2:34	206	4.04	70.3
44	2007/8/17 18:59	46.9958	190.6553	3:31	700	4.618	69.1
45	2007/8/21 14:45	46.9922	205.2310	2:30	172	4.074	58.4
46	2007/8/21 18:34	46.9940	205.6678	1:50	95	3.701	113.8
47	2007/8/21 21:25	47.0000	206.3687	2:23	167	3.876	99.7
48	2007/8/22 0:37	46.9977	206.5158	2:12	118	3.638	204
49	2007/8/22 5:44	46.9867	207.4800	0:56	62	4.014	194.5
50	2007/8/23 9:06	46.9843	210.0860	1:33	70	3.162	315
51	2007/8/23 11:47	46.9943	210.8542	2:00	71	3.961	68.4
52	2007/8/23 15:16	46.9795	211.0132	2:19	42	3.299	141.7
53	2007/8/23 18:31	47.0103	211.9605	2:36	95	3.643	132.5
54	2007/8/24 1:05	47.0077	212.9323	2:10	289	3.681	103.1
55	2007/8/24 7:24	46.9982	214.1895	2:16	200	4.076	109.1
56	2007/8/29 8:31	47.0638	234.7152	4:16	277	4.25	38.3

Table 2.8.2   Starting time and location of rainwater sampling.

Smpl #	Time UTC	Location Lat. [N]	Long. [E]	Duration [hh:mm]	Smpl volume [mL]	pH	Conductivity [uS]
21	2007/8/15 3:42	46.9952	180.5705	2:10	42	4.284	153.5
22	2007/8/15 5:32	47.0047	180.5703	4:58	34	4.244	233
23	2007/8/15 10:50	46.9983	181.6945	7:05	53	4.195	267
24	2007/8/15 17:55	46.9997	182.7900	3:25	34	4.086	149.4
25	2007/8/16 14:27	46.9985	186.2017	4:14	132	4.201	70.2
26	2007/8/16 18:44	46.9970	186.5625	1:46	192	4.49	26.9
27	2007/8/17 4:05	47.0068	188.4443	4:13	77	4.112	42.2
28	2007/8/17 18:59	46.9958	190.6553	3:31	40	4.126	77.7

(5) Preliminary Results

As examples, concentration of ozone, carbon monoxide, aerosol number and sulfate were shown in Figure 2.8.2 – 2.8.5.   The data can be used for further discussions after the elimination of data during the contaminated periods.
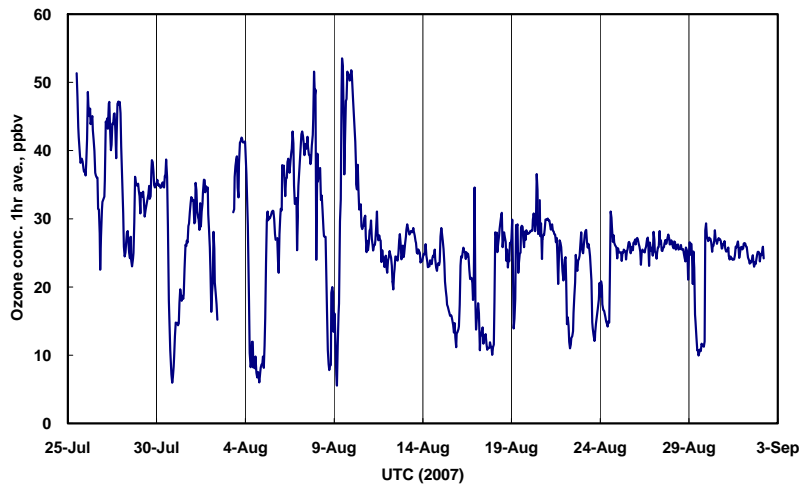

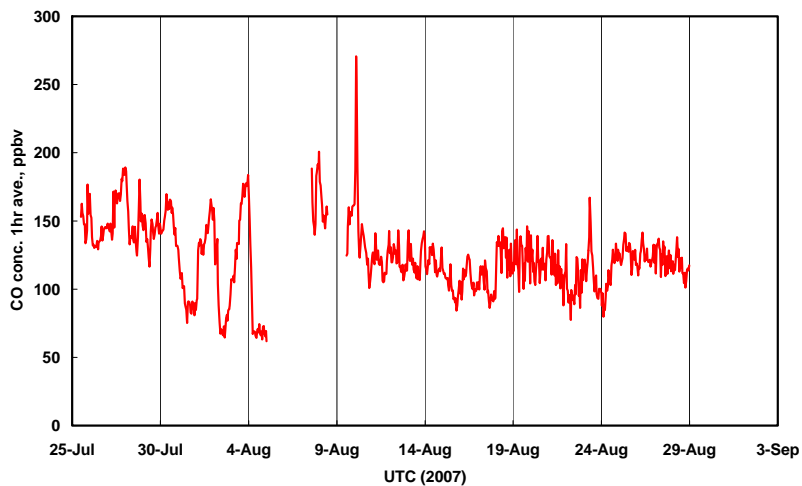Fig. 2.8.2   Temporal variation of ozone concentration.

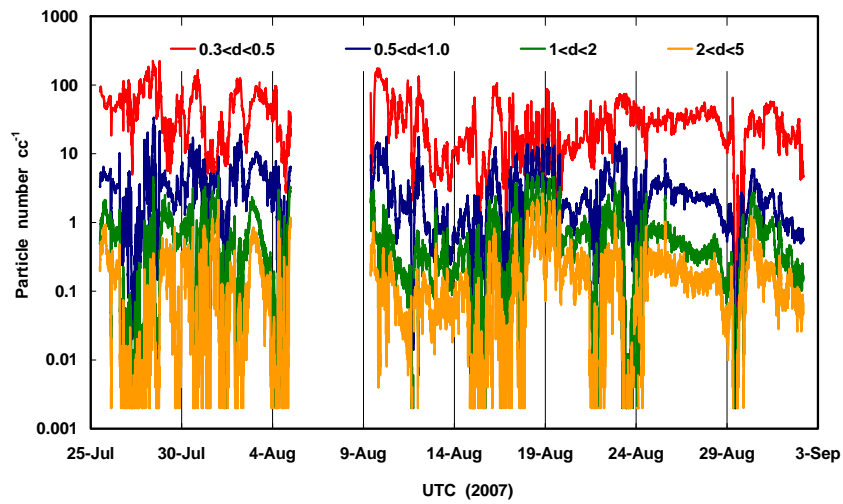Fig. 2.8.3   Temporal variation of carbon monoxide concentration.
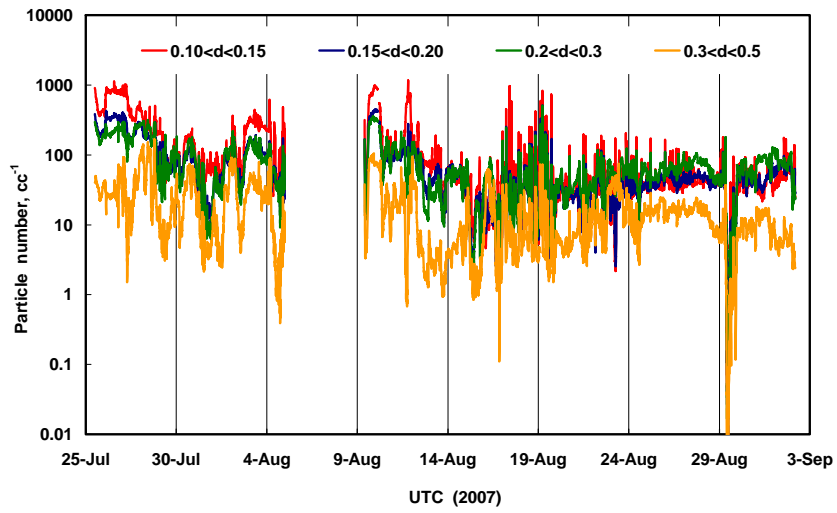
Fig. 2.8.4   Temporal variation of aerosol number concentrations.
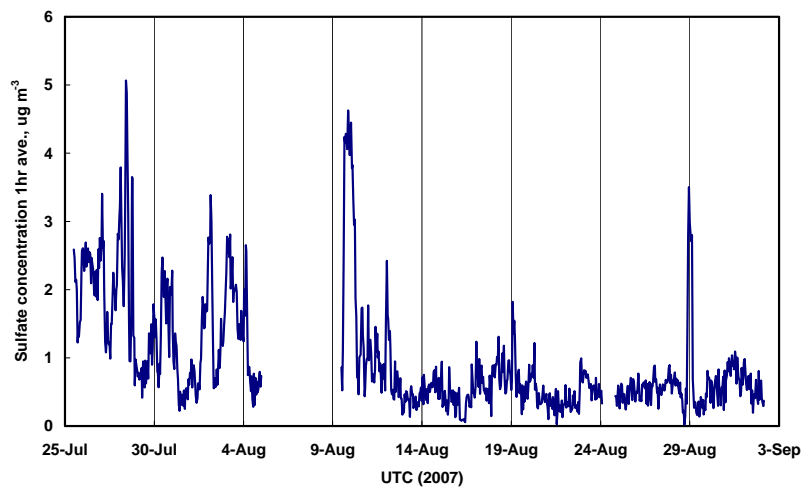

Fig. 2.8.5   Temporal variation of sulfate concentration.

(6) Future Plan

      Aerosol samples, fog water samples and rainwater samples will be analyzed for major inorganic ions and trace metals. Seawater samples will be analyzed for size and chemical composition of suspended particles by individual particle analysis and bulk chemical analysis. After the determination of data quality, the separation of air masses will be attempted by meteorological data and/or backward air mass trajectories for each atmospheric sample. It may be possible to discuss the interaction processes between atmosphere and surface seawater over the northern North Pacific Ocean.

(7) Data archives

      The data obtained during MR06-04 will be accessible upon request at Ocean Research Institute, The University of Tokyo.

2.9 Studies of marine organic carbon cycles associated with microbiological activity

(1) Personnel
Masao Uchida (NIES)
Yasuyuki Shibata (NIES)
Motoo Utsumi (Tsukuba University)
Yukiko Kuroki (Tsukuba University)
Chen Gang (Tsukuba University)

(2) Objectives

    Marine microbes, especially bacteria, are large and essential components of food webs and elemental cycles in the oceans. Marine bacteria include the two deepest divisions, or domains, Bacteria and Archaea. These domains are identified by genetic distance in the composition of the 16S rRNA gene (Woose et al. 1990). Marine bacteria are morphologically simple: microscopic rods, spheres and filaments generally less than 1-2 μ m in size, but bacteria are highly diverse in terms of both taxonomy and metabolism. There are many different varieties of bacteria existing in the oceans, but it has been long noted a discrepancy of several orders of magnitude between the number of bacterial cells that can be seen in the oceans by direct count (by epifluorescence microscopy) and the number of colonies that appear on agar plates (e.g. Jannasch and Jones, 1959).

In terms of carbon cycling, one of the most important activities of bacteria in marine systems is aerobic heterotrophy. Heterotrophic bacteria served primarily as a pathway for regeneration of organic nitrogen, phosphorus, and other bioactive elements, and represented a shunt of carbon and energy from the main phytoplankton-based food web. In addition, it is reported that nonthermophilic archaea represent up to 40% of the free-living prokaryotic community in the water column of the world's oceans (ex. Delong, 1992), and some of their population is chemoautotrophy (ex. Pearson et al. 2001). Therefore, it is important to study the relationship between carbon cycling and bacterial community structure in the sea-water column. The key aim of this study is to analyze the relationship between community structures of microorganisms and dissolved organic carbon cycling in surface ocean . The objectives of this study are as follow: 1) to collect mega volume of surface sea-water using auto filtration device for measuring radioactive isotope ratio of DOC and bacterial cell membrane lipids, and 2) to collect large volume of sea-water samples from CTD systems for measuring radio isotope ratio of DOC and POC.

(3) Methods

. Surface sea-water

To study diversity of bacteria community, radioactive isotope ratio of DOC and bacterial cell membrane lipid, we filtered mega volume surface sea-water using auto filtration device during the cruise. Then, we got samples of DOC fraction (Table 2.9.1).

To measure for carbon14 ratio of DOC, POC and DIC in surface, we collected surface sea-water samples at Stn. P01-010, 019, 027, 066, 072, X15, 081, X16, X17, 097, 101, 108 .

DOC : DOC samples were filtrated 2 L surface-water with quartz filters (Whatman
Cat No. 1851-047, Grade QMA , 47 mm in diameter). These samples collected in plastic bottles after washing nitric acid and were frozen at -20 oC during cruse.

POC: POC samples were filtrated 100 L surface-water with glass fiber filter filters (Whatman GF/F, with a operational pore size of 0.7 μ m, 110 mm in diameter). And these Filter samples were frozen at -20 oC during cruse.

DIC: Surface-water was collected in a 250 mL glass bottles. Then a head-space of 2 % of the bottle volume was left by remove sea-water sample with a plastic syringe. After added HgCl 200 μL, the bottle was sealed using a greased ground glass and a clip was secured.

. CTD sampling

To study radio isotope ratio of DOC, 2 L sea-water sampled from Niskin bottles at each sampling station (Table 2.9.2). Each water samples were filtered with quartz filters and collected plastic bottles after washing in nitric acid. The filtrated water samples and filters were frozen at -20oC during the cruise. In addition to, we filtrated large volume sea-water (about 40 – 80 L) what collected by extra Niskin bottles at same layer for measuring radiocarbon ratio of POC.

(4) References

Delong, E.F. (1992) Proc. Natl. Acad. Sci. USA 89: 5685-5689.

Jannasch, H. W., and Jones, G. E. (1959) Limnol. Oceanogr. 4:128-139.

Pearson, A., McNichol, A.P., Bentitez-Nelson, B.C., Hayes, J.M. and Eglinton, T.I. (2001) Geochim. Cosmochim. Acta 65: 3123-3137.

Woese, C. R., Kandler, O., and Wheelis, M. L. (1990) Proc. Natl. Acad. Sci. USA 87:4576-4579.

Table 6.9.1. DOC fraction sample list

Sample No.	Pore size of filter μm	Filtrated volum L	Date (UTC)	Start latitude	Start longitude	Stop latitude	Stop longitude
1	0.50	12263	25 July - 27 July	41-02.08N	143-15.32E	41-59.49N	146-13.56E
2	0.50	11400	27 July - 29 July	41-59.49N	146-13.56E	40-23.32N	147-23.42E
3	0.50	8655	29 July - 31 July	40-23.32N	147-23.42E	41-10.25N	150-.12.98E
4	0.50	8655	29 July - 31 July	40-23.32N	147-23.42E	41-10.25N	150-.12.98E
5	0.50	6660	31 July - 3 Aug	41-10.25N	150-.12.98E	41-37.07N	153-04.64E
6	0.50	6660	31 July - 3 Aug	41-10.25N	150-.12.98E	41-37.07N	153-04.64E
7	0.20	54294	25 July - 3 Aug	41-02.08N	143-15.32E	41-37.07N	153-04.64E
8	0.50	10466	3 Aug - 4 Aug	41-36.52N	153-04.64E	40-00.36N	153-01.63E
9	0.50	11992	4 Aug - 6 Aug	40-00.36N	153-01.63E	40-18.88N	149-32.08E
10	0.65	10877	6 Aug - 8 Aug	40-18.88N	149-32.08E	40-30.01N	144-02.92E
11	0.20	33355	6 Aug - 8 Aug	40-18.88N	149-32.08E	40-30.01N	144-02.92E
12	0.50	11706	12 Aug - 15 Aug	46-59.89N	162-15.89E	46-59.67N	179-25.77W
13	0.50	11706	12 Aug - 15 Aug	46-59.89N	162-15.89E	46-59.67N	179-25.77W
14	0.50	7597	15 Aug -17 Aug	46-59.76N	179-25.80W	46-59.61N	168-58.27W
15	0.50	7597	15 Aug -17 Aug	46-59.76N	179-25.80W	46-59.61N	168-58.27W
16	0.20	47161	12 Aug - 20 Aug	46-59.89N	162-15.89E	46-58.82N	159-15.24W
17	0.50	9276	17 Aug - 23 Aug	46-59.61N	168-58.27W	46-59.66N	151-04.75W
18	0.50	9276	17 Aug - 23 Aug	46-59.61N	168-58.27W	46-59.66N	151-04.75W
19	0.50	11012	23 Aug - 26 Aug	46-59.66N	150-59.17W	47-00.36N	135-49.91W
20	0.50	11013	24 Aug - 26 Aug	46-59.67N	150-59.18W	47-00.37N	135-49.92W
21	0.20	36450	20 Aug - 28 Aug	46-58.78N	159-15.23W	46-59.87N	127-55.23W
22	0.50	4329	27 Aug - 1 Sep	47-00.37N	135-49.92W	53-40.47N	154-04.11W
23	0.50	4329	27 Aug - 1 Sep	47-00.37N	135-49.92W	53-40.47N	154-04.11W
24	0.20	14226	27 Aug - 1 Sep	46-59.87N	127-55.23W	53-40.47N	154-04.11W

Table 6.9.2. CTD sampling

Stn.	Start Date (UTC)	Position latitude	Position longitude	Depth	layer	DOC filtrated volum	POC (Extra Niskins) Sampling depth	POC (Extra Niskins) filtrated volume
P01-010	27.Jul	41-52.60N	146-18.20E	6678	36	2.0 L	Non.	-
P01-027	1.Aug	41-56.50N	151-28.10E	5140	33	2.0 L	Non.	-
P01-072	18.Aug	47-00.20N	168-12.70W	5400	34	2.0 L	5250	23.0 L
P01-081	20.Aug	47-00.50N	158-07.80W	5229	34	2.0 L	5250	26.0 L
P01-X17	24.Aug	46-53.94N	144-25.74W	4677	31	2.0 L	7580	51.5 L
P01-101	26.Aug	47-00.10N	135-44.20W	4134	29	2.0 L	4000	82.0 L

3. Hydrography

3.1 CTDO$_2$ Measurements
14 September 2007

(1) Personnel

> Hiroshi Uchida (JAMSTEC)
> Satoshi Ozawa (MWJ)
> Hirokatsu Uno (MWJ)
> Tomoyuki Takamori (MWJ)
> Kenichi Katayama (MWJ)

(2) Winch arrangements

The CTD package was deployed by using 4.5 Ton Traction Winch System (Dynacon, Inc., Bryan, Texas, USA), which was installed on the R/V Mirai in April 2001 (Fukasawa et al., 2004). Primary system components include a complete CTD Traction Winch System with up to 7000 m of 9.53 mm armored cable (Ocean Cable and Communications Co., Yokohama, Kanagawa, Japan).

(3) Overview of the equipment

The CTD system was SBE 911plus system (Sea-Bird Electronics, Inc., Bellevue, Washington, USA). The SBE 911plus system controls 36-position SBE 32 Carousel Water Sampler. The Carousel accepts 12-litre Niskin-X water sample bottles (General Oceanics, Inc., Miami, Florida, USA). The SBE 9plus was mounted horizontally in a 36-position carousel frame. SBE's temperature (SBE 3) and conductivity (SBE 4) sensor modules were used with the SBE 9plus underwater unit. The pressure sensor is mounted in the main housing of the underwater unit and is ported to outside through the oil-filled plastic capillary tube. A modular unit of underwater housing pump (SBE 5T) flushes water through sensor tubing at a constant rate independent of the CTD's motion, and pumping rate (3000 rpm) remain nearly constant over the entire input voltage range of 12-18 volts DC. Flow speed of pumped water in standard TC duct is about 2.4 m/s. Two sets of temperature and conductivity modules were used. An SBE's dissolved oxygen sensor (SBE 43) was placed between the primary conductivity sensor and the pump module. Auxiliary sensors, a Deep Ocean Standards Thermometer (SBE 35), an altimeter (PSA-916T; Teledyne Benthos, Inc., North Falmous, Massachusetts, USA), an oxygen optode (Oxygen Optode 3830; Aanderaa Data Instruments AS, Bergen, Norway), and a fluorometer (Seapoint sensors, Inc., Kingston, New Hampshire, USA) were also used with the SBE 9plus underwater unit. In addition, a prototype of oxygen optode (RINKO; Alec Electronics Co. Ltd., Kobe, Hyogo, Japan) was also used. To minimize motion of the CTD package, a heavy stainless frame (total weight of the CTD package without sea water in the bottles is about 1000 kg) was used with an aluminum plate (54 × 90 cm) (Fig. 3.1.1).

Summary of the system used in this cruise

Deck unit:
> SBE 11plus, S/N 0272

Under water unit:
> SBE 9plus, S/N 79492 (Pressure sensor: S/N 0575)

Temperature sensor:

SBE 3plus, S/N 4216 (primary from Stn. 1_1 to 44_1)

SBE 3plus, S/N 4188 (primary from Stn. 58_1)

SBE 3, S/N 1464 (secondary: from Stn. 1_1 to 29_1)

SBE3, S/N 1525 (secondary: from Stn. 40_1)

Conductivity sensor:

SBE 4, S/N 1203 (primary: from Stn. 1_1 to 10_1)

SBE 4, S/N 3064 (primary: from Stn. 11_1)

SBE 4, S/N 2854 (secondary)

Oxygen sensor:

SBE 43, S/N 0949 (primary)

AANDERAA Oxygen Optode 3830, S/N 612

ALEC oxygen optode (RINKO, prototype)

Pump:

SBE 5T, S/N 4598 (primary: from Stn. 1_1 to 58_2, secondary from Stn. 60_1)

SBE 5T, S/N 4595 (secondary: from Stn. 1_1 to 58_2, primary from Stn. 60_1)

Altimeter:

PSA-916T, S/N 1157

Deep Ocean Standards Thermometer:

SBE 35, S/N 0045

Fluorometer:

Seapoint Sensors, Inc., S/N 2579

(removed from Stn. 9_1 to 12_1 due to lacking of proof pressure)

Carousel Water Sampler:

SBE 32, S/N 0391

Water sample bottle:

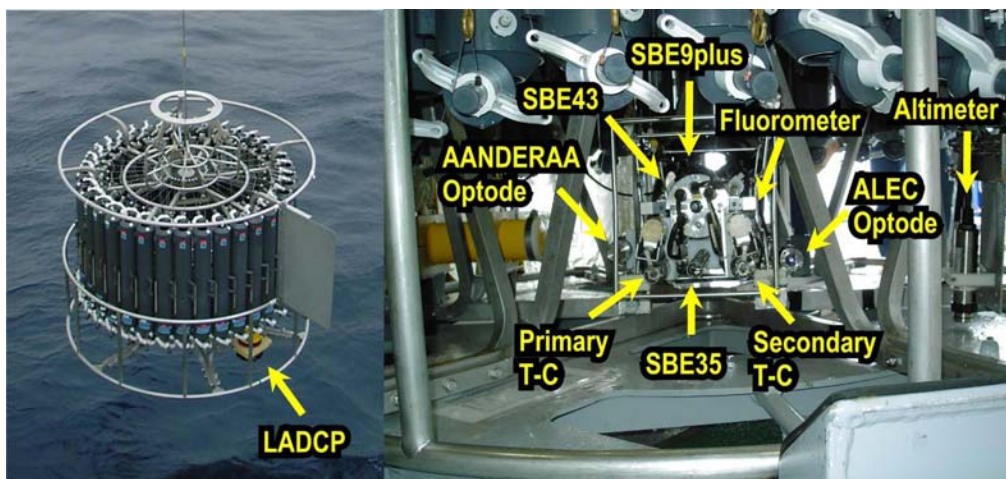12-litre Niskin-X (no TEFLON coating)

Fig. 3.1.1 The CTD package (left) and the position of the sensors (right).

(4) Pre-cruise calibration

i. Pressure

The Paroscientific series 4000 Digiquartz high pressure transducer (Model 415K-187: Paroscientific, Inc., Redmond, Washington, USA) uses a quartz crystal resonator whose frequency of oscillation varies

with pressure induced stress with 0.01 per million of resolution over the absolute pressure range of 0 to 15000 psia (0 to 10332 dbar). Also, a quartz crystal temperature signal is used to compensate for a wide range of temperature changes at the time of an observation. The pressure sensor has a nominal accuracy of 0.015 % FS (1.5 dbar), typical stability of 0.0015 % FS/month (0.15 dbar/month), and resolution of 0.001 % FS (0.1 dbar). Since the pressure sensor measures the absolute value, it inherently includes atmospheric pressure (about 14.7 psi). SEASOFT subtracts 14.7 psi from computed pressure automatically.

Pre-cruise sensor calibrations for linearization were performed at SBE, Inc.

S/N 0575, 27 October 1999

The time drift of the pressure sensor is adjusted by periodic recertification corrections against a dead-weight piston gauge (Model 480DA, S/N 23906; Bundenberg Gauge Co. Ltd., Irlam, Manchester, UK). The corrections are performed at JAMSTEC, Yokosuka, Kanagawa, Japan by Marine Works Japan Ltd. (MWJ), Yokohama, Kanagawa, Japan, usually once in a year in order to monitor sensor time drift and linearity.

S/N 0575, 5 July 2007

slope = 0.99980507

offset = 2.33363

Result of the pre-cruise pressure sensor calibration against the dead-weight piston gauge is shown in Fig. 3.1.2.
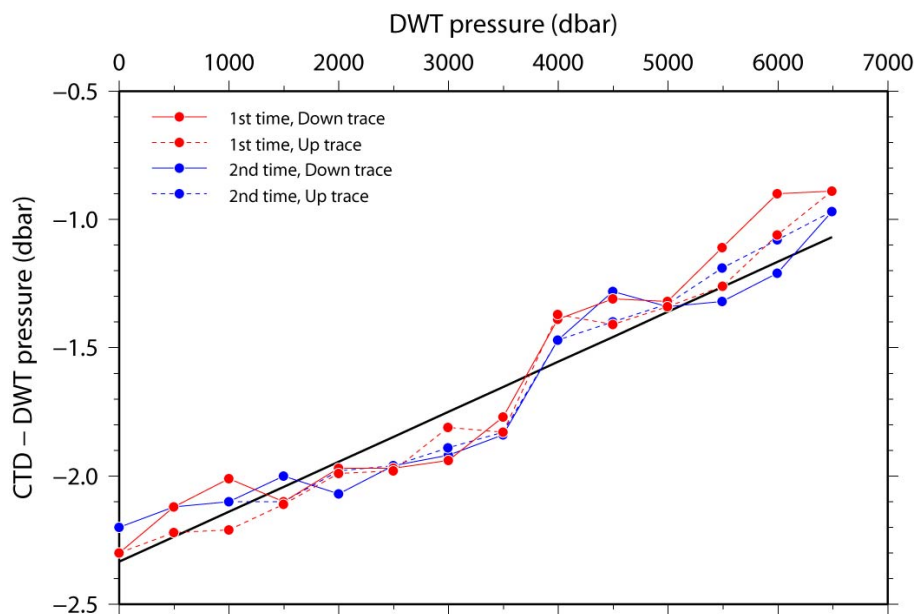
Fig. 3.1.2 Difference between the dead-weight piston gauge and the CTD pressure. The calibration line (black line) is also shown.

ii. Temperature (SBE 3)

The temperature sensing element is a glass-coated thermistor bead in a stainless steel tube, providing a pressure-free measurement at depths up to 10500 (6800) m by titanium (aluminum) housing. The SBE 3 thermometer has a nominal accuracy of 1 mK, typical stability of 0.2 mK/month, and resolution of 0.2 mK at 24 samples per second. The premium temperature sensor, SBE 3plus, is a more rigorously tested

and calibrated version of standard temperature sensor (SBE 3).

Pre-cruise sensor calibrations were performed at SBE, Inc.

        S/N 4216, 16 May 2007

        S/N 4188, 16 May 2007

        S/N 1464, 14 June 2007

        S/N 1525, 14 June 2007

Pressure sensitivity of SBE 3 was corrected according to a method by Uchida et al. (2007), for the following sensor.

        S/N 4188, $-2.946675e{-}7$ [°C/dbar]

Time drift of the SBE 3 temperature sensors based on the laboratory calibrations is shown in Fig. 3.1.3.
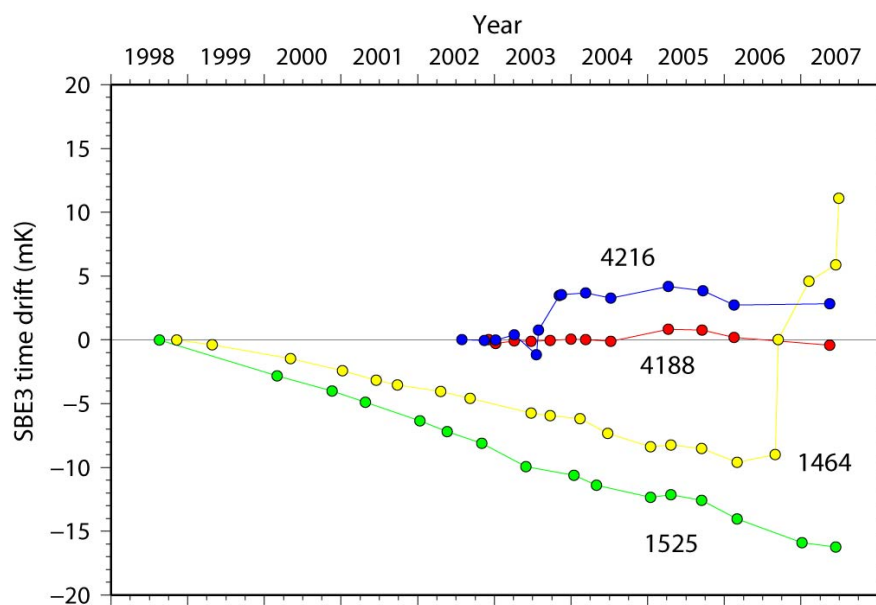

Fig. 3.1.3 Time drift of SBE 3 temperature sensors based on laboratory calibrations.

iii. Conductivity (SBE 4)

The flow-through conductivity sensing element is a glass tube (cell) with three platinum electrodes to provide in-situ measurements at depths up to 10500 (6800) m by titanium (aluminum) housing. The SBE 4 has a nominal accuracy of 0.0003 S/m, typical stability of 0.0003 S/m/month, and resolution of 0.00004 S/m at 24 samples per second.

Pre-cruise sensor calibrations were performed at SBE, Inc.

        S/N 1203, 14 June 2007

        S/N 3064, 14 June 2007

        S/N 1088, 14 June 2007

The value of conductivity at salinity of 35, temperature of 15 °C (IPTS-68) and pressure of 0 dbar is 4.2914 S/m.

iv. Oxygen (SBE 43)

The SBE 43 oxygen sensor uses a Clark polarographic element to provide in-situ measurements at depths up to 7000 m. The range for dissolved oxygen is 120 % of surface saturation in all natural waters, nominal accuracy is 2 % of saturation, and typical stability is 2 % per 1000 hours.

Pre-cruise sensor calibrations were performed at SBE, Inc.

    S/N 0949, 1 June 2007

v. Deep Ocean Standards Thermometer

Deep Ocean Standards Thermometer (SBE 35) is an accurate, ocean-range temperature sensor that can be standardized against Triple Point of Water and Gallium Melt Point cells and is also capable of measuring temperature in the ocean to depths of 6800 m. The SBE 35 was used to calibrate the SBE 3 temperature sensors in situ (Uchida et al., 2007).

Pre-cruise sensor linearization was performed at SBE, Inc.

    S/N 0045, 27 October 2002

Then the SBE 35 is certified by measurements in thermodynamic fixed-point cells of the TPW (0.0100 °C) and GaMP (29.7646 °C). The slow time drift of the SBE 35 is adjusted by periodic recertification corrections. Pre-cruise sensor calibration was performed at SBE, Inc.

    S/N 0045, 29 May 2007 (slope and offset correction)

The time required per sample = $1.1 \times$ NCYCLES + 2.7 seconds. The 1.1 seconds is total time per an acquisition cycle. NCYCLES is the number of acquisition cycles per sample and was set to 4. The 2.7 seconds is required for converting the measured values to temperature and storing average in EEPROM.

When using the SBE 911 system with SBE 35, the deck unit receives incorrect signal from the under water unit for confirmation of firing bottle #16. In order to correct the signal, a module (Yoshi Ver. 1; EMS Co. Ltd., Kobe, Hyogo, Japan) was used between the under water unit and the deck unit.

Time drift of the SBE 35 based on the fixed point calibrations is shown in Fig. 3.1.4.
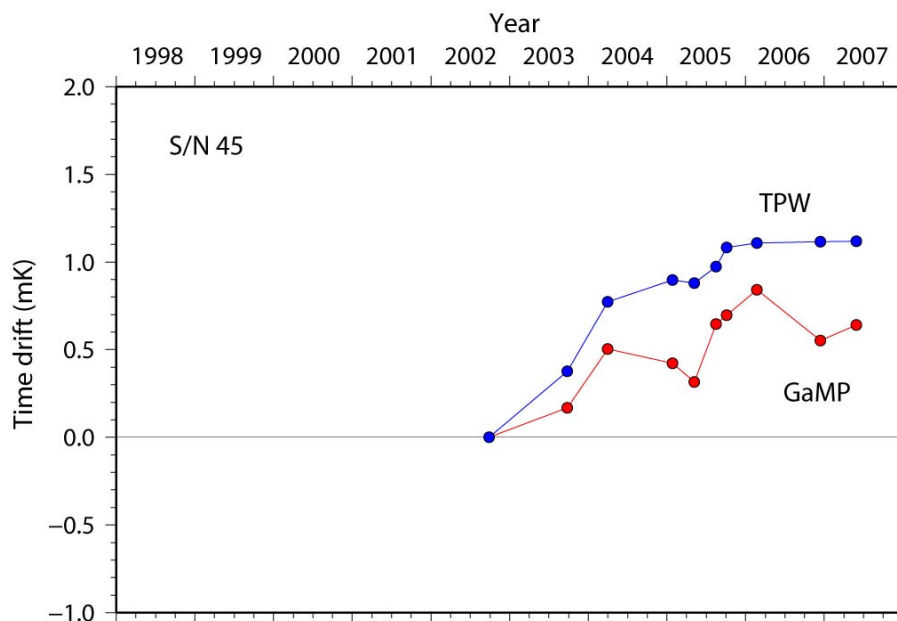
Fig. 3.1.4 SBE35 time drift based on laboratory fixed point calibrations (triple point of water, TPW and gallium melt point, GaMP) performed by SBE, Inc.

vi. Altimeter

Benthos PSA-916T Sonar Altimeter (Teledyne Benthos, Inc.) determines the distance of the target from the unit by generating a narrow beam acoustic pulse and measuring the travel time for the pulse to bounce back from the target surface. It is rated for operation in water depths up to 10000 m. The PSA-916T uses the nominal speed of sound of 1500 m/s.

vii. Oxygen Optode

Oxygen Optode 3830 (Aanderaa Instruments AS) is based on the ability of selected substances to act as dynamic fluorescence quenchers. In order to use with the SBE 911plus CTD system, an analog adaptor (3966) is connected to the oxygen optode (3830). The analog adaptor is packed into titanium housing made by Alec Electronics Co. Ltd., Kobe, Hyogo, Japan. The sensor is designed to operate down to 6000 m and the titanium housing for the analog adaptor is designed to operate down to 7000 m. The range for dissolved oxygen is 120 % of surface saturation in all natural waters, nominal accuracy is less than 5 % of saturation, and setting time (68%) is shorter than 25 seconds.

Outputs from the sensor are the raw phase shift and temperature. The optode oxygen can be calibrated by the Stern-Volmer equation, according to a method by Uchida et al. (submitted manuscript):

$$O_2 \ (\mu mol/l) = (\tau_0 / \tau - 1) / K_{sv}$$

where τ is decay time, τ_0 is decay time in the absence of oxygen and K_{sv} is Stern-Volmer constant. The τ_0 and the K_{sv} are assumed to be functions of temperature as follows.

$$K_{sv} = C_{11} + C_{12} \times t + C_{13} \times t^2$$
$$\tau_0 = C_{21} + C_{22} \times t$$
$$\tau = C_{31} + C_{32} \times P_b$$

where t is CTD temperature (°C) and P_b is raw phase measurement (degrees). The oxygen concentration is calculated using temperature data from the first responding CTD temperature sensor instead of temperature data from slow responding optode temperature sensor. The calibration coefficients were preliminary determined using the results from Stn. 1 to 15 and used during the cruise.

$$C_{11} = 2.606649508949701e–03$$
$$C_{12} = 1.116597645632670e–04$$
$$C_{13} = 1.600852291743077e–06$$
$$C_{21} = 60.10653405006491$$
$$C_{22} = 9.810613061511041e–02$$
$$C_{31} = –5.316195492754106$$
$$C_{32} = 1.078473950879603$$

viii. Fluorometer

The Seapoint Chlorophyll Fluorometer (Seapoint Sensors, Inc., Kingston, New Hampshire, USA) provides in-situ measurements of chlorophyll-a at depths up to 6000 m. The instrument uses modulated blue LED lamps and a blue excitation filter to excite chlorophyll-a. The fluorescent light emitted by the chlorophyll-a passes through a red emission filter and is detected by a silicon photodiode. The low level signal is then processed using synchronous demodulation circuitry, which generates an output voltage proportional to chlorophyll-a concentration.

ix. Prototype oxygen optode

The prototype of oxygen optode (RINKO: Alec Electronics Co. Ltd.) provides the raw phase shift and temperature at depths up to 7000 m. Pre-cruise calibration was not performed for the prototype sensor.

(5) Data collection and processing
i. Data collection

CTD system was powered on at least 20 minutes in advance of the data acquisition and was powered off at least two minutes after the operation in order to acquire pressure data on the ship's deck.

The package was lowered into the water from the starboard side and held 10 m beneath the surface for about one minute in order to activate the pump. After the pump was activated, the package was lifted to the surface and lowered at a rate of 1.0 m/s to 200 m (or 300 m when significant wave height is high) then the package was stopped to operate the heave compensator of the crane. The package was lowered again at a rate of 1.2 m/s to the bottom. For the up cast, the package was lifted at a rate of 1.1 m/s except for bottle firing stops. At each bottle firing stops, the bottle was fired after waiting from the stop for 30 seconds and the package was stayed at least 5 seconds for measurement of the SBE 35. At 200 m (or 300 m) from the surface, the package was stopped to stop the heave compensator of the crane.

Water samples were collected using a 36-bottle SBE 32 Carousel Water Sampler with 12-litre Nisken-X bottles. Before a cast taken water for CFCs, the 36-bottle frame and Niskin-X bottles were wiped with acetone.

Data acquisition software
SEASAVE-Win32, version 5.27b

ii. Data collection problems

The primary conductivity sensor was shifted during the down cast of station 7_1, 8_1, 9_1, and 10_1. Therefore the conductivity sensor was replaced after the station 10_1.

At station 23_1, bottle #15 did not trip because of failure of the bottle setting.

At station 29_1, a longline for fishery was caught in a propeller at about 5000 dbar of the down cast. Therefore the cast was quitted and no water was sampled.

At station 58_1, primary temperature signal was lost at 2400 dbar of the down cast. Therefore the cast was quitted and the connection cable was replaced.

At stations 81_1, 105_1 and 111_1, Jellyfish was in secondary T-C duct, and data quality from the secondary temperature and conductivity sensors was bad. The secondary T-C duct was cleaned with Triton-X after the casts.

At station 115_1, there was a fishing boat near the planned location. Therefore the station location was changed a little to the north.

iii. Data processing

SEASOFT consists of modular menu driven routines for acquisition, display, processing, and archiving of oceanographic data acquired with SBE equipment. Raw data are acquired from instruments and are stored as unmodified data. The conversion module DATCNV uses instrument configuration and calibration coefficients to create a converted engineering unit data file that is operated on by all SEASOFT post processing modules. The following are the SEASOFT and original software data processing module sequence and specifications used in the reduction of CTD data in this cruise.

Data processing software
SEASOFT-Win32, version 5.27b

DATCNV converted the raw data to engineering unit data. DATCNV also extracted bottle information where scans were marked with the bottle confirm bit during acquisition. The duration was set to 4.4 seconds, and the offset was set to 0.0 second.

TCORP (original module, version 1.0) corrected the pressure sensitivity of the SBE 3 for both profile and bottle information data. One SBE 3 (S/N 4188) was corrected because it had relatively large pressure sensitivity (about +1.8 mk per 6000 dbar).

ROSSUM created a summary of the bottle data. The data were averaged over 4.4 seconds.

ALIGNCTD converted the time-sequence of sensor outputs into the pressure sequence to ensure that all calculations were made using measurements from the same parcel of water. For a SBE 9plus CTD

with the ducted temperature and conductivity sensors and a 3000-rpm pump, the typical net advance of the conductivity relative to the temperature is 0.073 seconds. So, the SBE 11plus deck unit was set to advance the primary and the secondary conductivity for 1.73 scans (1.75/24 = 0.073 seconds). Oxygen data are also systematically delayed with respect to depth mainly because of the long time constant of the oxygen sensor and of an additional delay from the transit time of water in the pumped plumbing line. This delay was compensated by 6 seconds advancing oxygen sensor output (oxygen voltage) relative to the temperature data. Prototype of the oxygen optode data (RINKO) are also delayed by slightly slow response time of the sensor. The delay was compensated by 2 seconds advancing sensor output relative to the temperature data.

ALIGNOPT (original module, version 0.1) also compensated the delay of the AANDERAA optode sensor by advancing relative to the CTD temperature data as a function of temperature (t).

$$\text{align (sec)} = 25 \times \exp(-0.13 \times t) \quad \text{(for } 0 \leq t \leq 16.3\ ^\circ\text{C)}$$
$$= 25 \quad \text{(for } t < 0\ ^\circ\text{C)}$$
$$= 3 \quad \text{(for } t > 16.3\ ^\circ\text{C)}$$

WILDEDIT marked extreme outliers in the data files. The first pass of WILDEDIT obtained an accurate estimate of the true standard deviation of the data. The data were read in blocks of 1000 scans. Data greater than 10 standard deviations were flagged. The second pass computed a standard deviation over the same 1000 scans excluding the flagged values. Values greater than 20 standard deviations were marked bad. This process was applied to all variables.

CELLTM used a recursive filter to remove conductivity cell thermal mass effects from the measured conductivity. Typical values used were thermal anomaly amplitude alpha = 0.03 and the time constant 1/beta = 7.0.

FILTER performed a low pass filter on pressure with a time constant of 0.15 seconds. In order to produce zero phase lag (no time shift) the filter runs forward first then backwards.

WFILTER performed as a median filter to remove spikes in Fluorometer data. A median value was determined by 49 scans of the window.

SECTION (or original module of SECTIONU, version 1.0) selected a time span of data based on scan number in order to reduce a file size. The minimum number was set to be the start time when the CTD package was beneath the sea-surface after activation of the pump. The maximum number was set to be the end time when the package came up from the surface. Data for estimation of the CTD pressure drift were prepared before SECTION.

LOOPEDIT marked scans where the CTD was moving less than the minimum velocity of 0.0 m/s (traveling backwards due to ship roll).

DESPIKE (original module, version 1.0) removed spikes of the data. A median and mean absolute deviation was calculated in 1-dbar pressure bins for both down- and up-cast, excluding the flagged values. Values greater than 4 mean absolute deviations from the median were marked bad for each bin. This process was performed 2 times for temperature, conductivity and oxygen voltage data.

DERIVE was used to compute oxygen.

BINAVG averaged the data into 1-dbar pressure bins. The center value of the first bin was set equal to the bin size. The bin minimum and maximum values are the center value plus and minus half the bin size. Scans with pressures greater than the minimum and less than or equal to the maximum were averaged. Scans were interpolated so that a data record exist every dbar.

DERIVE was re-used to compute salinity, potential temperature, and density (σ_θ).

SPLIT was used to split data into the down cast and the up cast.

The shift of the primary conductivity data of station 7_1, 8_1, 9_1, and 10_1 were corrected by using original module SHIFTCORR. The conductivity sensor gradually shifted from 1000 dbar to the following

depth of the down cast. Magnitude of the shift at the following depth was estimated and the conductivity data between 1000 dbar and the following depth was linearly corrected.

Station	Maximum depth of the shift	Magnitude of the shift at the maximum depth
7_1	4170 dbar	–0.00003 S/m
8_1	3774 dbar	–0.00001 S/m
9_1	5850 dbar	–0.00002 S/m
10_1	5820 dbar	–0.00004 S/m

Remaining spikes in temperature, salinity and oxygen data were manually eliminated from the 1-dbar-averaged data. The following data gaps over 1-dbar were linearly interpolated with a quality flag of 6.

Station	Pressure (dbar)	Parameters
2_1	348	Salinity
4_1	70	Salinity
5_1	413, 435-440, 456, 475, 485, 485, 503-504	Salinity
12_1	173	Salinity
21_1	826	Salinity
25_1	108, 416	Salinity
70_1	202, 207	Salinity
72_1	384	Salinity
X15_1	480	Salinity
79_1	141	Salinity
82_1	1776-1780	Salinity
84_1	26	Temperature, Salinity
114_1	284-290	Salinity
115_1	20	Salinity

(6) Post-cruise calibration
i. Pressure

The CTD pressure sensor offset in the period of the cruise was estimated from the pressure readings on the ship deck. For best results the Paroscientific sensor was powered on for at least 20 minutes before the operation. In order to get the calibration data for the pre- and post-cast pressure sensor drift, the CTD deck pressure was averaged over first and last one minute, respectively. Then the atmospheric pressure deviation from a standard atmospheric pressure (14.7 psi) was subtracted from the CTD deck pressure. The atmospheric pressure was measured at the captain deck (20 m high from the base line) and sub-sampled one-minute interval as a meteorological data. Time series of the CTD deck pressure is shown in Fig. 3.1.5.

The CTD pressure sensor offset was estimated from the deck pressure obtained above. Mean of the pre- and the post-casts data over the whole period gave an estimation of the pressure sensor offset from the pre-cruise calibration. Mean residual pressure between the dead-weight piston gauge and the calibrated CTD data at 0 dbar of the pre-cruise calibration was subtracted from the mean deck pressure. Estimated mean offset of the pressure data is listed in Table 3.1.1. The post-cruise correction of the pressure data is not deemed necessary for the pressure sensor.
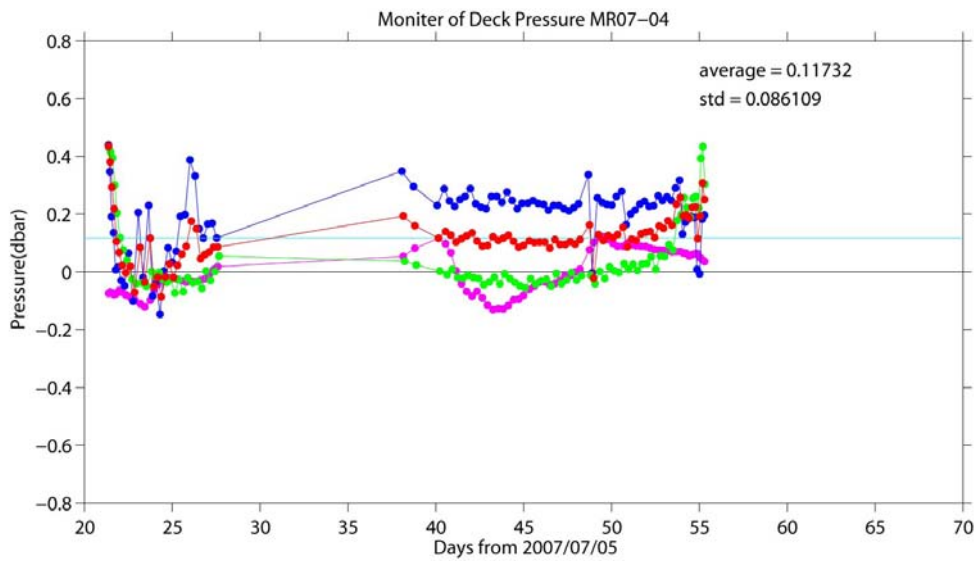
Fig. 3.1.5 Time series of the CTD deck pressure. Pink dot indicates atmospheric pressure anomaly. Blue and green dots indicate pre- and post-cast deck pressures, respectively. Red dot indicates an average of the pre- and the post-cast deck pressures.

Table 3.1.1 Offset of the pressure data. Mean and standard deviation are calculated from time series of the average of the pre- and the post-cast deck pressures.

===

Serial number	Mean deck pressure	Standard deviation	Residual pressure	Estimated offset
0575	0.12 dbar	0.09 dbar	0.06 dbar	0.06 dbar

----

ii. Temperature

The CTD temperature sensors (SBE 3) were calibrated with the SBE 35 under the assumption that discrepancies between SBE 3 and SBE 35 data were due to pressure sensitivity, the viscous heating effect, and time drift of the SBE 3, according to a method by Uchida et al. (2007).

Post-cruise sensor calibrations for the SBE 35 will be performed at SBE, Inc., after MR07-06 cruise. The CTD temperature was preliminary calibrated as

$$\text{Calibrated temperature} = T - (c_0 \times P + c_1 \times t + c_2)$$

where T is CTD temperature in °C, P is pressure in dbar, t is time in days from pre-cruise calibration date of CTD temperature and c_0, c_1, and c_2 are calibration coefficients. The coefficients were determined using the data for the depths deeper than 1950 dbar.

The number of data used for the calibration and the mean absolute deviation from the SBE 35 are listed in Table 3.1.2 and the calibration coefficients are listed in Table 3.1.3. The results of the post-cruise calibration for the CTD temperature are summarized in Table 3.1.4 and shown in Fig. 3.1.6.
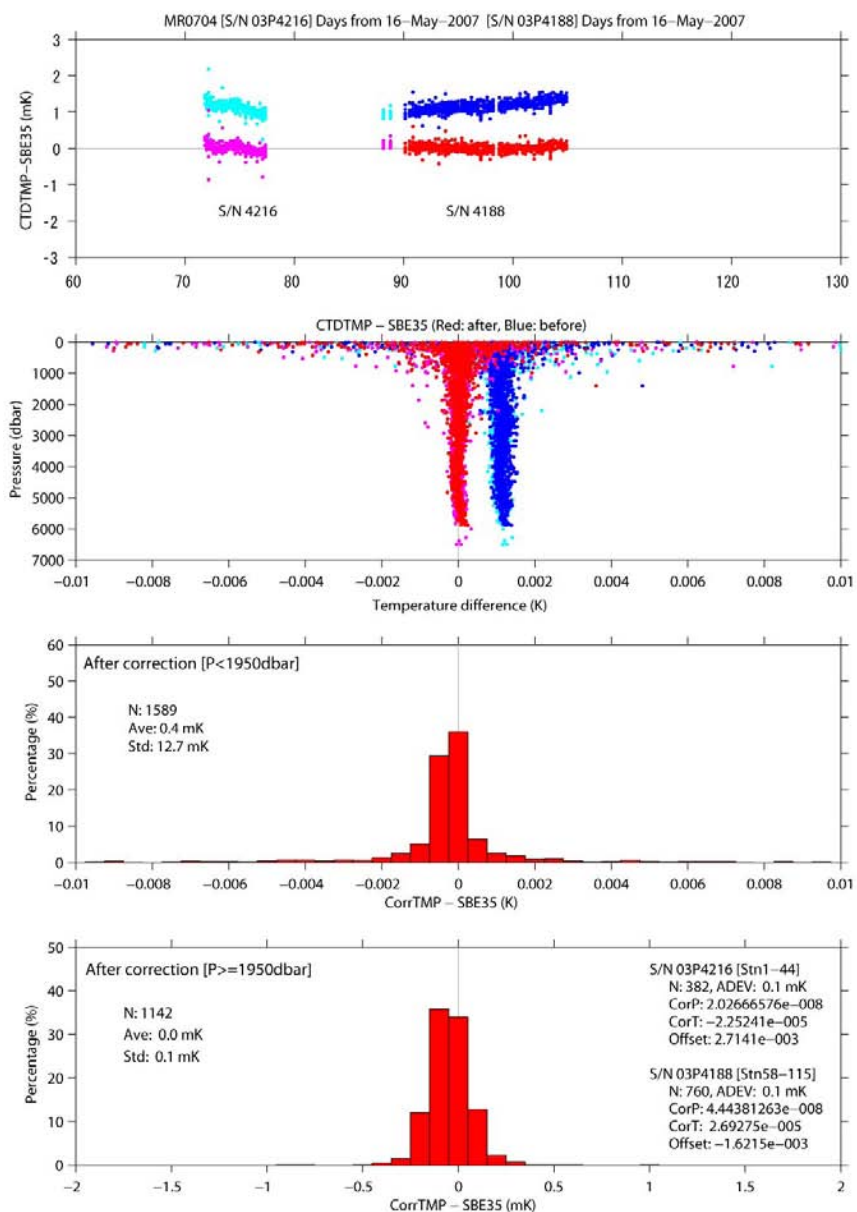
Fig. 3.1.6 Difference between the CTD temperature and the SBE 35. Blue/cyan and red/magenta dots indicate before and after the post-cruise calibration using the SBE 35 data, respectively. Top panel shows for P ≥ 1950 dbar. Lower two panels show histogram of the difference after the calibration.

Table 3.1.2 Number of data used for the calibration (pressure ≥ 1950 dbar) and mean absolute deviation between the CTD temperature and the SBE 35.

Serial number	Number	Mean absolute deviation	Note
4216	382	0.1 mK	Stn. 1_1 to 44_1
4188	760	0.1 mK	Stn. 58_1 to 115_1

Table 3.1.3 Calibration coefficients for the CTD temperature sensors.

Serial number	c_0 (°C/dbar)	c_1 (°C/day)	c_2 (°C)
4216	2.02667e–8	–2.25241e–5	0.0027
4188	4.44381e–8	2.69275e–5	–0.0016

Table 3.1.4 Difference between the CTD temperature and the SBE 35 after the post-cruise calibration. Mean and standard deviation (Sdev) are calculated for the data below and above 1950 dbar. Number of data used is also shown.

Pressure ≥ 1950 dbar			Pressure < 1950 dbar		
Number	Mean (mK)	Sdev (mK)	Number	Mean (mK)	Sdev (mK)
1142	0.00	0.1	1589	0.35	12.7

iii. Salinity

The discrepancy between the CTD salinity and the bottle salinity is considered to be a function of conductivity and pressure. The CTD salinity was calibrated as

$$\text{Calibrated salinity} = S - (c_0 \times P + c_1 \times C + c_2 \times C \times P + c_3)$$

where S is CTD salinity, P is pressure in dbar, C is conductivity in S/m and c_0, c_1, c_2 and c_3 are calibration coefficients. The best fit sets of coefficients were determined by minimizing the sum of absolute deviation with a weight from the bottle salinity data. The MATLAB® function FMINSEARCH was used to determine the sets. The weight was given as a function of vertical salinity gradient and pressure as

$$\text{Weight} = \min[4, \exp\{\log(4) \times Gr / Grad\}] \times \min[4, \exp\{\log(4) \times P^2 / PR^2\}]$$

where Grad is vertical salinity gradient in PSU dbar^{-1}, and P is pressure in dbar. Gr and PR are threshold of the salinity gradient (0.5 mPSU dbar^{-1}) and pressure (1000 dbar), respectively. When salinity gradient is small (large) and pressure is large (small), the weight is large (small) at maximum (minimum) value of 16 (1). The salinity gradient was calculated using up cast CTD salinity data. The up cast CTD salinity data was low-pass filtered with a 3-point (weights are 1/4, 1/2, 1/4) triangle filter before the calculation.

The primary conductivity data created by the software module ROSSUM were used after the post-cruise calibration for the primary temperature data. The coefficients were determined for some groups of the CTD stations. The results of the post-cruise calibration for the CTD salinity are summarized in Table 3.1.5 and shown in Fig. 3.1.7. And the calibration coefficients and number of data used for the calibration are listed in Table 3.1.6.
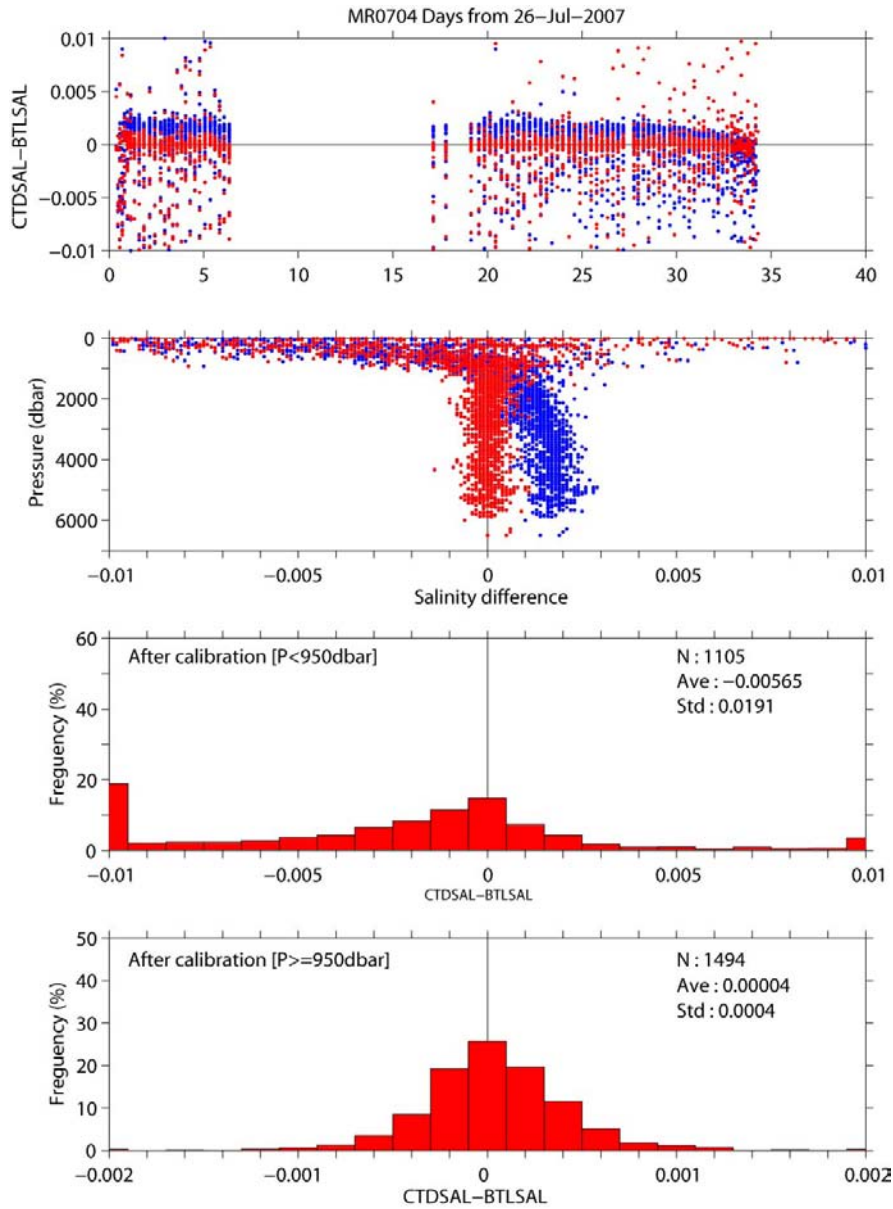
Fig. 3.1.7 Difference between the CTD salinity and the bottle salinity. Blue and red dots indicate before and after the post-cruise calibration using the bottle salinity data, respectively. Top panel shows for P ≥ 950 dbar. Lower two panels show histogram of the difference after the calibration.

Table 3.1.5 Difference between the CTD salinity and the bottle salinity after the post-cruise calibration. Mean and standard deviation (Sdev) are calculated for the data below and above 950 dbar. Number of data used is also shown.

Pressure $\geq$ 950 dbar			Pressure < 950 dbar		
Number	Mean (mPSU)	Sdev (mPSU)	Number	Mean (mPSU)	Sdev (mPSU)
1494	0.0	0.4	1105	–5.7	19.1

Table 3.1.6 Calibration coefficients for the CTD salinity. Number of data used is also listed.

Station	Number	c_0	c_1	c_2	c_3
1_1~28_1	824	1.0331764015e–5	1.6322214271e–3	–3.1041705576e–6	
–5.2179231380e–3					
40_1~82_2	845	5.5743728228e–6	–7.5153334807e–3	–1.5802276835e–6	
2.3338375432e–2					
83_2~92_1	357	–2.6365673251e–6	–1.7948408615e–2	9.9643702860e–7	
5.6418293029e–2					
X17_1~115_1	568	–6.8043279569e–7	–1.1413741305e–2	3.6019288465e–7	
3.5439131977e–2					

iv. Oxygen (SBE 43)

The CTD oxygen from the SBE 43 sensor was not calibrated for this cruise, because relatively high-quality oxygen data were obtained from the oxygen optode sensors.

v. Oxygen optode (AANDERAA)

The optode oxygen was calibrated by the Stern-Volmer equation, according to a method by Uchida et al. (submitted manuscript):

$$O_2 \text{ (μmol/l)} = (\tau_0 / \tau - 1) / K_{sv}$$

where τ is decay time, τ_0 is decay time in the absence of oxygen and K_{sv} is Stern-Volmer constant. The τ_0 and the K_{sv} are assumed to be functions of temperature as follows.

$$K_{sv} = C_{11} + C_{12} \times t + C_{13} \times t^2$$
$$\tau_0 = C_{21} + C_{22} \times t$$
$$\tau = C_{31} + C_{32} \times P_b$$

where t is CTD temperature (°C) and P_b is raw phase measurement (deg). The oxygen concentration was calculated using temperature data from the first responding CTD temperature sensor instead of temperature data from slow responding optode temperature sensor.

The calibration was performed for the up cast phase data created by the software module ROSSUM after the post-cruise calibration for the CTD temperature and salinity. The calibration coefficients (C_{11}, C_{12}, C_{13}, C_{21}, C_{22}, C_{31} and C_{32}) were determined for all CTD stations. The offset (C_{31}) for the phase shift

was slightly changed for the 6 groups of CTD casts. The results of the post-cruise calibration for the optode oxygen are summarized in Table 3.1.7 and shown in Fig. 3.1.8. And the calibration coefficients and number of data used for the calibration are listed in Table 3.1.8.

Although the up cast optode data was well calibrated in situ (Fig. 3.1.8), difference between the up and down cast was quite large in the surface layer (~150 dbar) (Fig. 3.1.9). Similar discrepancy was seen in the data obtained in the North Pacific subarctic region (MR06-03_2), and was not seen in the data obtained in the North Pacific subtropical region (MR05-05) (Uchida et al., submitted manuscript). Data quality of the in-situ calibrated down cast optode data was bad in the surface layer. Therefore the prototype oxygen optode (RINKO) data will be calibrated in situ and used as the CTD oxygen data.
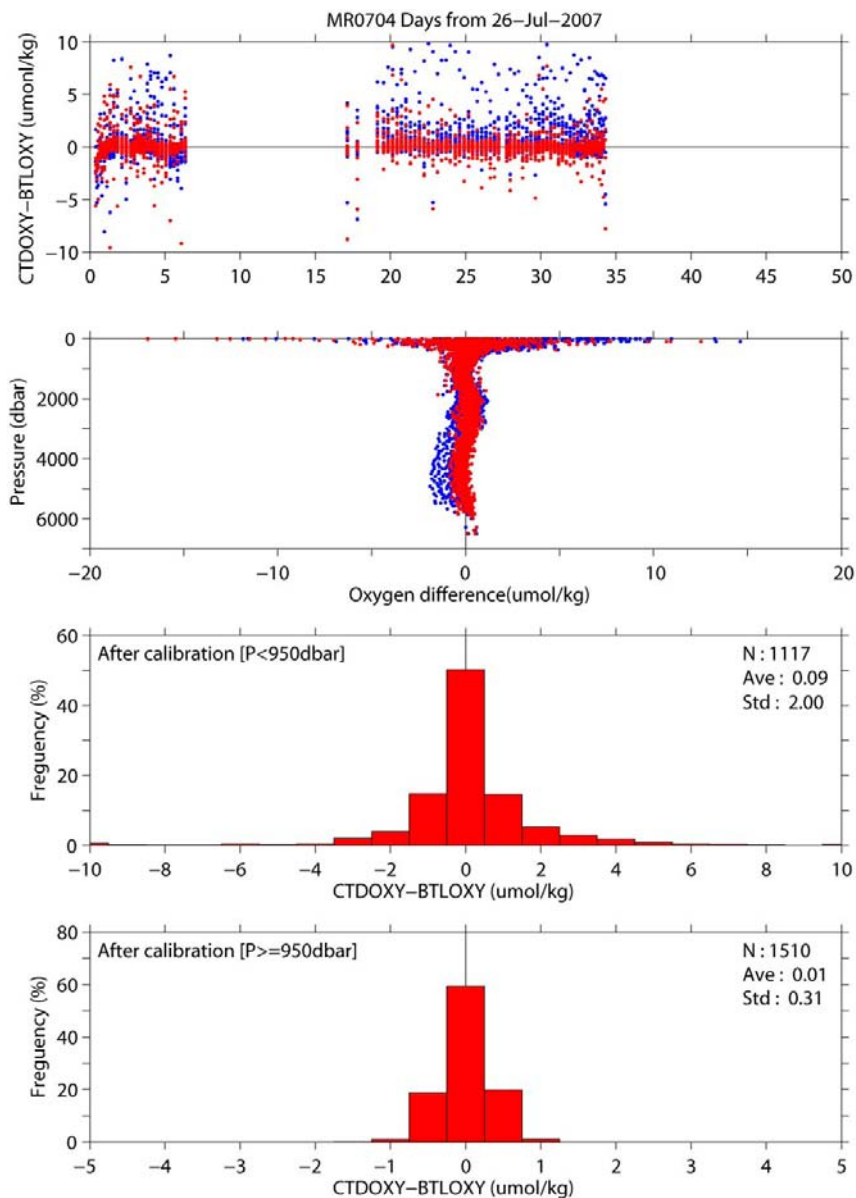

Fig. 3.1.8 Difference between the optode oxygen and the bottle oxygen. Blue and red dots indicate before and after the post-cruise calibration using the bottle salinity data, respectively. Top panel shows for P ≥ 950 dbar. Lower two panels show histogram of the difference after the calibration.

Table 3.1.7 Difference between the optode oxygen and the bottle oxygen after the post-cruise calibration. Mean and standard deviation (Sdev) are calculated for the data below and above 950 dbar. Number of data used is also shown.

==

Pressure $\geq$ 950 dbar			Pressure < 950 dbar		
Number	Mean (µmol/kg)	Sdev (µmol/kg)	Number	Mean (µmol/kg)	Sdev (µmol/kg)
1510	0.01	0.31	1117	0.09	2.00

Table 3.1.8 Calibration coefficients for the optode oxygen. Number of data used is also listed.

==

Number	Mean absolute deviation	Coefficients	Group of CTD casts
2627	0.60 µmol /kg	$C_{11} = 2.633748019016525e{-}03$	
		$C_{12} = 1.227335148555336e{-}04$	
		$C_{13} = 1.746113399901766e{-}06$	
		$C_{21} = 60.14088623607846$	
		$C_{22} = 8.962512697430804e{-}02$	
		$C_{31} = -6.046793385372612$	1_1 – 9_1
		$= -5.992731438527348$	10_1 – 17_1
		$= -6.043763970992551$	18_1 – 23_1
		$= -6.094002885258246$	24_1 – 28_1
		$= -6.005615328980936$	40_1 – 103_1
		$= -6.059440531429654$	104_1 – 115_1
		$C_{32} = 1.089750333374984$	

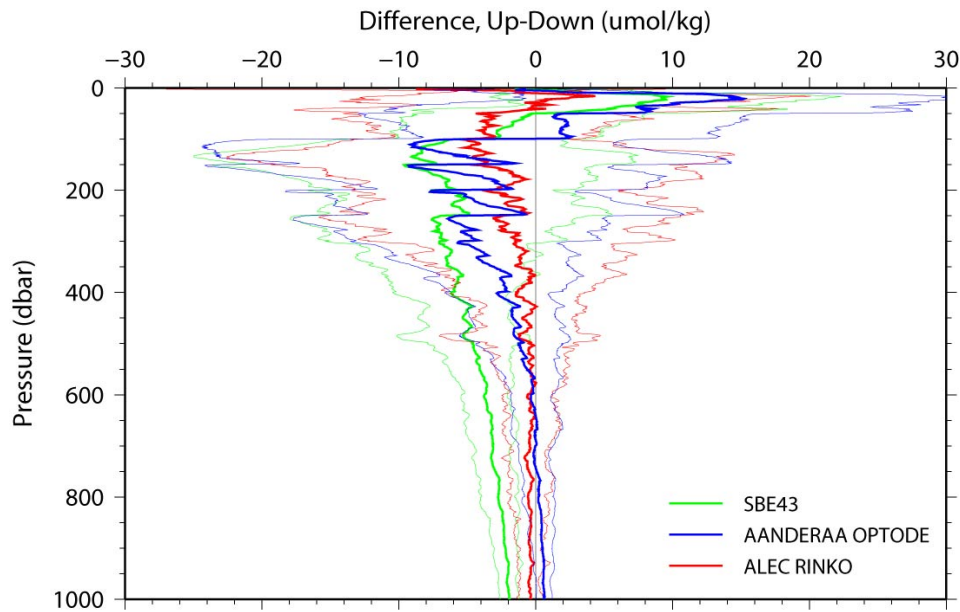
Fig. 3.1.9 Mean difference between the down and up cast oxygen data for the SBE 43 (green line), the oxygen optode (blue line) and the prototype oxygen optode (red line). Thin lines represent 1 standard deviation from the mean profile. Data before post-cruise calibration were used.

vi. Prototype oxygen optode (RINKO)

The prototype of oxygen optode will be also calibrated by the Stern-Volmer equation, according to a method by Uchida et al. (submitted manuscript). The calibration coefficients will be determined for post-cruise calibration.

References
Fukasawa, M., T. Kawano and H. Uchida (2004): Blue Earth Global Expedition collects CTD data aboard Mirai, BEAGLE 2003 conducted using a Dynacon CTD traction winch and motion-compensated crane, *Sea Technology*, 45, 14-18.

Uchida, H., K. Ohyama, S. Ozawa, and M. Fukasawa (2007): In-situ calibration of the Sea-Bird 9plus CTD thermometer, *J. Atmos. Oceanic Technol.* (in press)

Uchida, H., T. Kawano, I. Kaneko, and M. Fukasawa: In-situ calibration of optode-based oxygen sensors, submitted to *J. Atmos. Oceanic Technol.*

3.2 Bottle Salinity

September 2, 2007

(1) Personnel

Takeshi Kawano (JAMSTEC)

Naoko Takahashi(MWJ)

Tatsuya Tanaka (MWJ)

(2)Objectives

Bottle salinities were measured in order to be compared with CTD salinities to identify leaking bottles and calibrate CTD salinities.

(3)Instrument and Method

i. Salinity Sample Collection

The bottles in which the salinity samples are collected and stored are 250 ml Phoenix brown glass bottles with screw caps.　Each bottle was rinsed three times with sample water and was filled to the shoulder of the bottle. The caps were also thoroughly rinsed. Salinity samples were stored more than 12 hours in the same laboratory as the salinity measurement was made.

ii. Instruments and Method

The salinity analysis was carried out on Guildline Autosal salinometer model 8400B (S/N 62827), which was modified by addition of an Ocean Science International peristaltic-type sample intake pump and two Guildline platinum thermometers model 9450. One thermometer monitored an ambient temperature and the other monitored a bath temperature. The resolution of the thermometers was 0.001 deg C. The measurement system was almost same as Aoyama et al (2003).　The salinometer was operated in the air-conditioned ship's laboratory at a bath temperature of 24 deg C.

An ambient temperature varied from approximately 20.9 deg C to 24.4 deg C, while a bath temperature is very stable and varied within +/- 0.003 deg C on rare occasion except for the end of the cruise. A measure of a double conductivity ratio of a sample is taken as a median of thirty-one reading. Data collection was started after 5 seconds and it took about 10 seconds to collect 31 readings by a personal computer. Data were sampled for the sixth and seventh filling of the cell. In case the difference between the double conductivity ratio of this two fillings is smaller than 0.00002, the average value of the two double conductivity ratios was used to calculate the bottle salinity with the algorithm for practical salinity scale, 1978 (UNESCO, 1981). If the difference was grater than or equal to the 0.0003, we measured one more additional filling of the cell. In case the double conductivity ratio of the additional filling did not satisfy the criteria above, we measured two more filling of the cell and the median of the double conductivity ratios of five fillings are used to calculate the bottle salinity.

The measurement was conducted for about 16 hours per day (typically from 8:00 to 24:00) and the cell was cleaned with ethanol or soap or both after the measurement of the day. We measured more than 3,200 samples in total.

(4) Preliminary Result

i. Stand Seawater

Standardization control was set to 452 and all the measurements were done by this setting. STNBY was 5398 +/- 0001 and ZERO was 0.00001 +/- 0.00001. We used IAPSO Standard Seawater batch P148 whose conductivity ratio was 0.99982 (double conductivity ratio is 1.99964) as the standard for salinity. We measured 37 bottles of P148 during routine measurement from Stn.1 to Stn.28 and 78
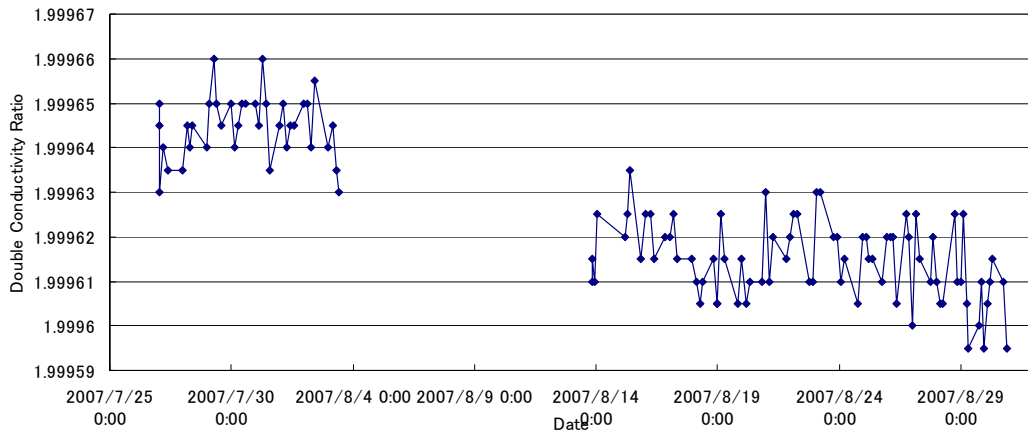
bottles from Stn.40 to Stn.115.

Fig.3.2.1 History of Double conductivity ratio of P148 during Leg.1. X and Y axes represents date and double conductivity ratio, respectively.

Fig.3.2.1 shows the history of double conductivity ratio of the Standard Seawater batch P148. During the period from 27, July to 4, August, the average of double conductivity ratio was 1.99985 and no drifts was calculated. Therefore we subtract 0.00001 from double conductivity ratio of samples measured during this period. Because of the trouble described in Section.1, measurement was interrupted for about 10 days. During the period from 13 August, double conductivity ratio of SSW was around 1.99862, however, after 28 August, it became smaller, probably due to cooling of room temperature. Therefore, we added 0.00002 to double conductivity ratio of samples measured from 13 August to 28 August, and 0.00003 to it measured after 28 August. Correction for the history of double conductivity ration after this correction was shown in Fig.3.2.2. After correction, the average of double conductivity ratio of 115 bottles of SSW became 1.999636 and the standard deviation was 0.00008, which is equivalent to 0.0002 in salinity.
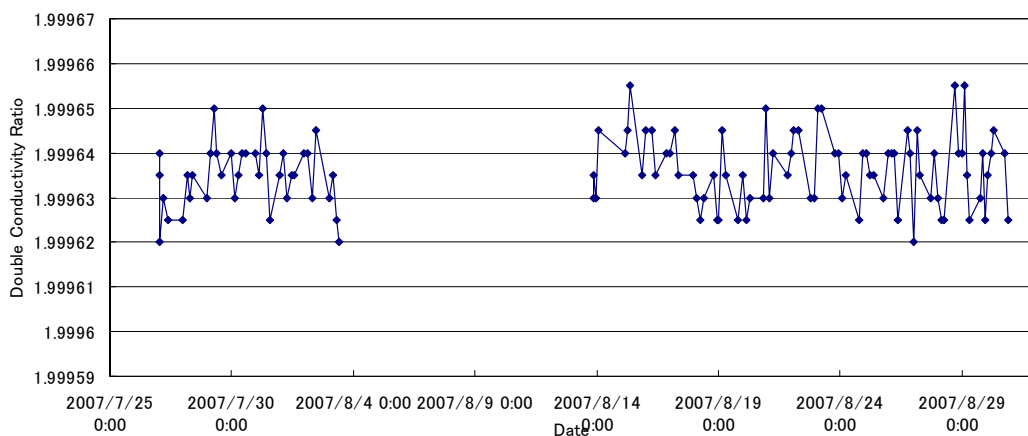

Fig.3.2.2 History of Double conductivity ratio of P148. X and Y axes represent time Date and double conductivity ratio, respectively. (after correction)

ii. Sub-Standard Seawater

We also used sub-standard seawater which was deep-sea water filtered by pore size of 0.45 micrometer and stored in a 20 liter cubitainer made of polyethylene and stirred for at least 24 hours before measuring. It was measured every six samples in order to check the possible sudden drift of the salinometer. During the whole measurements, there was no detectable sudden drift of the salinometer.

iii. Replicate and Duplicate Samples

We took 491 pairs of replicate. Fig.3.2.3 shows the histogram of the absolute difference between replicate samples. There were 4 bad measurements and 5 questionable measurements of replicate samples. Excluding these bad and questionable measurements, the average and standard deviation of the absolute deference of 482 pairs of replicate samples was 0.0018 and 0.00019 in salinity, respectively.
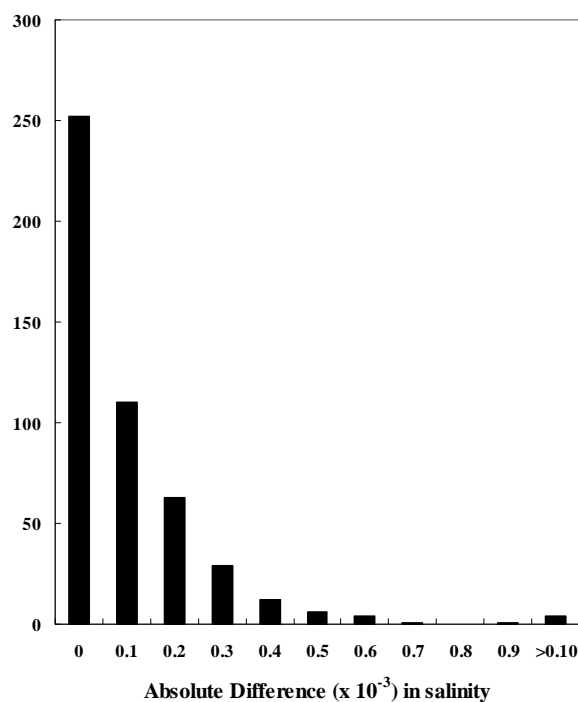
Fig.3.2.3 The histogram of the absolute difference between replicate samples.

(5) Further data quality check

All the data will be checked once again in detail with other parameters such as dissolved oxygen and nutrients.

Reference

Aoyama, M., T. Joyce, T. Kawano and Y. Takatsuki : Standard seawater comparison up to P129. Deep-Sea Research, I, Vol. 49, 1103 1114, 2002

UNESCO : Tenth report of the Joint Panel on Oceanographic Tables and Standards. UNESCO Tech. Papers in Mar. Sci., 36, 25 pp., 1981

3.3   Bottle Oxygen

September 03, 2007

(1) Personnel

Yuichiro KUMAMOTO [1], *Kimiko NISHIJIMA* [2], *Keisuke WATAKI* [2], and *Miyo Ikeda* [2]

    1) Japan Agency for Marine Earth Science and Technology

    2) Marine Works Japan Co. Ltd

(2) Objectives

Dissolved oxygen is one of good tracers for the ocean circulation.   Recent studies in the subarctic North Pacific indicated that dissolved oxygen concentration in intermediate layers decreased in basin wide scale during the past decades.   The causes of the decrease, however, are still unclear.   During MR07-04, conducted from 24-Jul-07 to 03-Sep-07, we measured dissolved oxygen concentration from surface to bottom layers at 88 hydrocast stations along around 47°N from Japan to the North America. These stations reoccupied the WHP-P01 stations in 1985 and 1999.   Our purpose is to evaluate decadal change of dissolved oxygen in the subarctic North Pacific between 1999 and 2007.

(3) Reagents

    Pickling Reagent I: Manganous chloride solution (3M)

    Pickling Reagent II: Sodium hydroxide (8M) / sodium iodide solution (4M)

    Sulfuric acid solution (5M)

    Sodium thiosulfate (0.025M)

    Potassium iodate (0.001667M)

    CSK standard of potassium iodate: Lot EWL3818, Wako Pure Chemical Industries Ltd., 0.0100N

(4) Instruments

    Burette for sodium thiosulfate and potassium iodate;

      APB-510 manufactured by Kyoto Electronic Co. Ltd. / 10 cm^3 of titration vessel

    Detector;

      Automatic photometric titrator, DOT-01 manufactured by Kimoto Electronic Co. Ltd.

(5) Seawater sampling

Following procedure is based on a determination method in the WHP Operations Manual (Dickson, 1996). Seawater samples were collected from 12-liters Niskin sampler bottles attached to the CTD-system. Seawater for bottle oxygen measurement was transferred from the Niskin sampler bottle to a volume calibrated glass flask (ca. 100 cm^3).   Three times volume of the flask of seawater was overflowed. Sample temperature was measured by a thermometer during the overflowing.   Then two reagent solutions (Reagent I, II) of 0.5 cm^3 each were added immediately into the sample flask and the stopper was inserted carefully into the flask. The sample flask was then shaken vigorously to mix the contents and to disperse the precipitate finely throughout.   After the precipitate has settled at least halfway down the flask, the flask was shaken again vigorously to disperse the precipitate.   The sample flasks containing pickled samples were stored in a laboratory until they were titrated.

(6) Sample measurement

At least two hours after the re-shaking, the pickled samples were measured on board.   A magnetic

stirrer bar and 1 cm^3 sulfuric acid solution were added into the sample flask and stirring began. Samples were titrated by sodium thiosulfate solution whose molarity was determined by potassium iodate solution. Temperature of sodium thiosulfate during titration was recorded by a thermometer. We measured dissolved oxygen concentration using two sets of the titration apparatus, named DOT-1 and DOT-3. Dissolved oxygen concentration (μmol kg^{-1}) was calculated by the sample temperature during the sampling, CTD salinity, flask volume, and titrated volume of the sodium thiosulfate solution.

(7) Standardization

Concentration of sodium thiosulfate titrant (ca. 0.025M) was determined by potassium iodate solution. Pure potassium iodate was dried in an oven at 130°C. 1.7835 g potassium iodate weighed out accurately was dissolved in deionized water and diluted to final volume of 5 dm^3 in a calibrated volumetric flask (0.001667M). 10 cm^3 of the standard potassium iodate solution was added to a flask using a volume-calibrated dispenser. Then 90 cm^3 of deionized water, 1 cm^3 of sulfuric acid solution, and 0.5 cm^3 of pickling reagent solution II and I were added into the flask in order. Amount of titrated volume of sodium thiosulfate (usually 5 times measurements average) gave the molarity of the sodium thiosulfate titrant. Table 3.3.1 shows result of the standardization during this cruise. Error (C.V.) of the standardization was 0.02±0.01 %, c.a. 0.05 μmol kg^{-1}.

(8) Determination of the blank

The oxygen in the pickling reagents I (0.5 cm^3) and II (0.5 cm^3) was assumed to be 3.8 x 10^{-8} mol (Murray *et al.*, 1968). The blank from the presence of redox species apart from oxygen in the reagents (the pickling reagents I, II, and the sulfuric acid solution) was determined as follows. 1 and 2 cm^3 of the standard potassium iodate solution were added to two flasks respectively. Then 100 cm^3 of deionized water, 1 cm^3 of sulfuric acid solution, and 0.5 cm^3 of pickling reagent solution II and I each were added into the two flasks in order. The blank was determined by difference between the two times of the first (1 cm^3 of KIO$_3$) titrated volume of the sodium thiosulfate and the second (2 cm^3 of KIO$_3$) one. The results of 3 times blank determinations were averaged (Table 3.3.1). The averaged blank of DOT-3 was –0.010 cm^3. The pickling reagents for DOT-1 were changed on July 31. After that, the blank of DOT-1 slightly decreased to be about –0.009 cm^3.

Table 3.3.1 Results of the standardization and the blank determinations during MR07-04.

Date (UTC)	#	KIO$_3$ ID No.	DOT-1 (cm^3) Na$_2$S$_2$O$_3$	E.P.	blank	DOT-3 (cm^3) Na$_2$S$_2$O$_3$	E.P.	blank	Samples (Stations)
2007/07/26	1	20070619-05-02	20070613-01-03	3.960	-0.002	20070613-01-04	3.952	-0.011	Stn.1,2,3,4,5,6,7
2007/07/27		20070619-05-03	20070613-02-03	3.959	-0.003	20070613-02-04	3.951	-0.012	Stn.8,9,10,11,12
2007/07/28		20070619-05-04	20070413-03-01	3.969	-0.003	20070413-03-02	3.962	-0.011	Stn.13,14,15,16,17,18
2007/07/30		20070619-05-05	20070413-03-01	3.968	-0.003	20070413-03-02	3.961	-0.010	Stn.19,20,21,22,23,24 (DOT-01)
2007/07/30		20070619-05-06	-	-	-	20070413-03-02	3.961	-0.011	Stn.19,20,21,22,23,24 (DOT-03)
2007/07/31		20070619-05-07	20070613-03-03	3.961	-0.011	20070613-03-04	3.961	-0.011	Stn.25,26,27,28
2007/08/12		20070619-06-01	20070413-03-03	3.960	-0.009	20070413-03-04	3.962	-0.011	Stn.40,44
2007/08/14		20070619-06-02	20070413-04-01	3.960	-0.010	20070413-04-02	3.960	-0.011	Stn.58,60,61,62,63
2007/08/15		20070619-06-03	20070413-04-01	3.962	-0.009	20070413-04-02	3.962	-0.010	Stn.64,65,66,67,68
2007/08/17	2	20070619-06-04	20070413-04-03	3.960	-0.012	20070413-04-04	3.963	-0.011	Stn.69,70,71,72,73,74
2007/08/19		20070619-06-05	20070413-04-03	3.962	-0.006	20070413-04-04	3.963	-0.010	Stn.X15,76,77,78,79,80
2007/08/21		20070619-06-06	20070413-05-01	3.961	-0.009	20070413-05-02	3.958	-0.010	Stn.81,82,83,84,85,86
2007/08/23		20070619-06-07	20070413-05-01	3.961	-0.008	20070413-05-02	3.959	-0.009	Stn.X16,87,88,89
2007/08/24		20070619-06-08	20070413-05-03	3.959	-0.009	20070413-05-04	3.961	-0.010	Stn.90,92,X17,94,95
2007/08/25	3	20070619-07-01	20070413-05-03	3.960	-0.008	20070413-05-04	3.961	-0.011	Stn.96,97,98,99,100,101
2007/08/27		20070619-07-02	20070413-06-01	3.958	-0.010	20070413-06-02	3.958	-0.011	Stn.102,103,104,105,106,107
2007/08/28		20070619-07-03	20070413-06-01	3.958	-0.012	20070413-06-02	3.961	-0.008	Stn.108,109,110,111,112,113,114,115

Batch number of the KIO$_3$ standard solution

(9) Replicate sample measurement

Replicate samples were taken from every CTD cast. Total amount of the replicate sample pairs in good measurement (flagged 2) was 236. The standard deviation of the replicate measurement was 0.10 μmol kg^{-1} and there was no significant difference between DOT-1 and DOT-3 measurements. The standard deviation was calculated by a procedure (SOP23) in DOE (1994). Although the differences of

the replicate sample pairs at surface (10 m depth) were slightly large, relation between the difference and sampling depth was unknown (Figure 3.3.1). The differences did not depend on measurement date (Figure 3.3.2). In the hydrographic data sheet, a mean of replicate sample pairs will be presented with the flag 2.
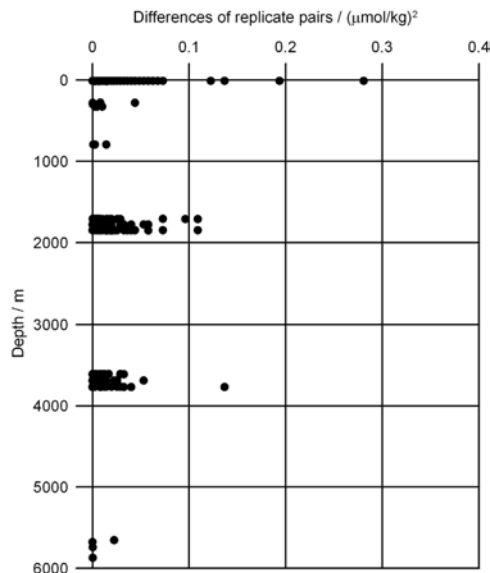
Figure 3.3.1   Differences of replicate pairs against sampling depth.
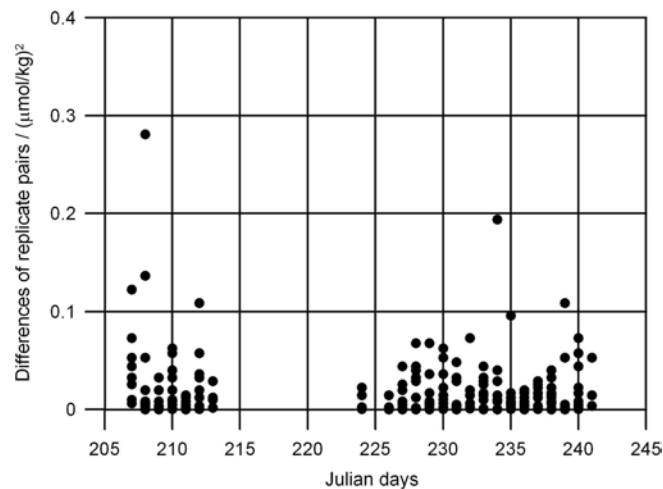
Figure 3.3.2   Differences of replicate pairs against measurement date (Julian days).

(10) CSK standard measurements

The CSK standard solution is commercial potassium iodate solution (0.0100 N) for analysis of dissolved oxygen. In the cruise, we measured the two CSK standard solutions (Lot EWL3818) against our KIO_3 standards as samples (Table 3.3.2). A good agreement among them confirms that there was no systematic error in our oxygen measurements in this cruise. Those values agree with those measured in the previous cruise, MR07-03, suggesting comparability in oxygen measurements between MR07-04 and MR07-03 cruises. In addition, we compared a new KIO_3 standard series prepared in 2007 with those in 2006 and 2005 using the same lot of the CSK standard (Table 3.3.2). Except one measurement against "20060419-05-11" KIO_3 solution, all of them agree well, which implies that oxygen measurements during

the cruises in 2005 and 2006 are also comparable with those in 2007.

Table 3.3.2 Results of the CSK standard (Lot EWL3818) measurements.

Date (UTC)	KIO$_3$ ID No.	DOT-1		DOT-3		Remarks
		Conc. (N)	error (N)	Conc. (N)	error (N)	
2007/07/23	20070619-05-01	0.009999	0.000001	0.010002	0.000002	MR07-04
2007/08/29	20070619-07-04	0.010004	0.000001	0.010006	0.000003	
2007/06/10	20070424-01-08	–	–	0.010006	0.000002	MR07-03
2007/07/24	20070425-01-06	0.010006	0.000003	0.010005	0.000002	
2007/06/27	20070424-01-10	0.010001	0.000004	–	–	check in June/2007 for 2007 series
2007/06/29	20070425-01-10	0.009994	0.000006	–	–	
2007/06/28	20070425-02-10	0.010001	0.000002	–	–	
2007/06/28	20070618-04-10	0.010003	0.000006	–	–	
2007/06/29	20070619-05-10	0.009995	0.000008	–	–	
2007/06/27	20070619-06-10	0.009997	0.000002	–	–	
2007/06/28	20070619-07-10	0.009999	0.000002	–	–	
2007/06/29	20070619-08-10	0.009998	0.000001	–	–	
2007/06/28	20070619-09-10	0.010000	0.000002	–	–	
2007/06/27	20070619-10-10	0.009996	0.000003	–	–	
2007/06/27	20060419-02-11	0.010004	0.000002	–	–	check in June/2007 for 2006 series
2007/06/27	20060419-05-11	0.010015	0.000010	–	–	
2007/06/28	20060419-07-11	0.010009	0.000003	–	–	
2007/06/27	20060419-10-11	0.009998	0.000002	–	–	
2007/06/29	20060419-11-11	0.010000	0.000001	–	–	
2007/06/28	20050829-10	0.010003	0.000002	–	–	check in June/2007 for 2005 series
2007/06/28	20050829-22	0.010000	0.000002	–	–	
2007/06/29	20050829-34	0.010000	0.000002	–	–	
2007/06/28	20050829-46	0.009996	0.000001	–	–	
2007/06/28	20050829-94	0.009999	0.000002	–	–	

(11) Quality control flag assignment

Quality flag values were assigned to oxygen measurements using the code defined in Table 0.2 of WHP Office Report WHPO 91-1 Rev.2 section 4.5.2 (Joyce *et al*., 1994). Measurement flags of 2 (good), 3 (questionable), 4 (bad), and 5 (missing) have been assigned (Table 3.3.3). The replicate data were averaged and flagged 2 if both of them were flagged 2. If either of them was flagged 3 or 4, a datum with "younger" flag was selected. Thus we did not use flag of 6 (replicate measurements). For the choice between 2, 3, or 4, we basically followed a flagging procedure as listed below:

　　a. Bottle oxygen concentration and difference between bottle oxygen and CTD oxygen at the sampling were plotted against CTD pressure. Any points not lying on a generally smooth trend were noted.

　　b. Dissolved oxygen was then plotted against sampling pressure or sigma-theta. If a datum deviated from a group of plots, it was flagged 3.

　　c. Vertical sections against pressure and potential density were drawn. If a datum was anomalous on the section plots, datum flag was degraded from 2 to 3, or from 3 to 4.

　　d. If the bottle flag was 4 (did not trip correctly), a datum was flagged 4 (bad). In case of the bottle flag 3 (leaking) or 5 (unknown problem), a datum was flagged based on steps a, b, and c.

Table 3.3.3   Summary of assigned quality control flags.

Flag	Definition	
2	Good	2,628
3	Questionable	1
4	Bad	0
5	Not report (missing)	1
	Total	2,630

(12) Preliminary Results

i. Overview

    Fig. 3.3.3 shows zonal transects of dissolved oxygen along WHP-P01 in 2007.   Although most of hydrocasts between stations 028 and 060 in the western North Pacific were canceled, difference in dissolved oxygen distribution between the eastern and western North Pacific can be distinguished.   The boundary between the east and west is likely to be lying between 170°W and 160°W.   Dissolved oxygen concentrations in bottom waters in the west are higher than those in the east.   The minimum concentration around 1000 m depth in the east was lower than that in the west.   These features are derived from the meridional ocean circulation in the global scale.

ii. Comparison with the WHP-P01 oxygen data in 1999 and 1985

    We compared dissolved oxygen in deep waters below 1000 dbar in 2007 with those in 1985 and 1999 (Fig.3.3.4).   The oxygen data in 2007 were systematically lower than those in 1985 and 1999 by 1.8 ± 1.8 and 2.3 ± 3.3 µmol kg^{-1}, respectively.   Causes of the about 2 µmol kg^{-1} offset between the data in 2007 and the historical ones are unknown.   Despite of this offset, dissolved oxygen concentrations in the thermocline in 2007 were significantly higher than those in 1999.   Distribution of differences in Apparent Oxygen Utilization (AOU) against water density between 1999 and 2007 (Fig. 3.3.5b) indicates that AOU (dissolved oxygen) decreased (increased) in waters just below seasonal mixing layer from 1999 to 2007.   Although there were not enough data in the west of the date line, the AOU decrease was found between 180° and 135°W approximately and its minimum (about −60 µmol kg^{-1}) appeared around 175°W and 26.6 σ_θ.   This AOU changes between 1999 and 2007 are completely opposite to those between 1985 and 1999 (Fig. 3.3.5a, Watanabe *et al.*, 2001).   These results suggest that dissolved oxygen in the intermediate water in the subarctic North Pacific decreased between 1985 and 1999 and increased between 1999 and 2007.
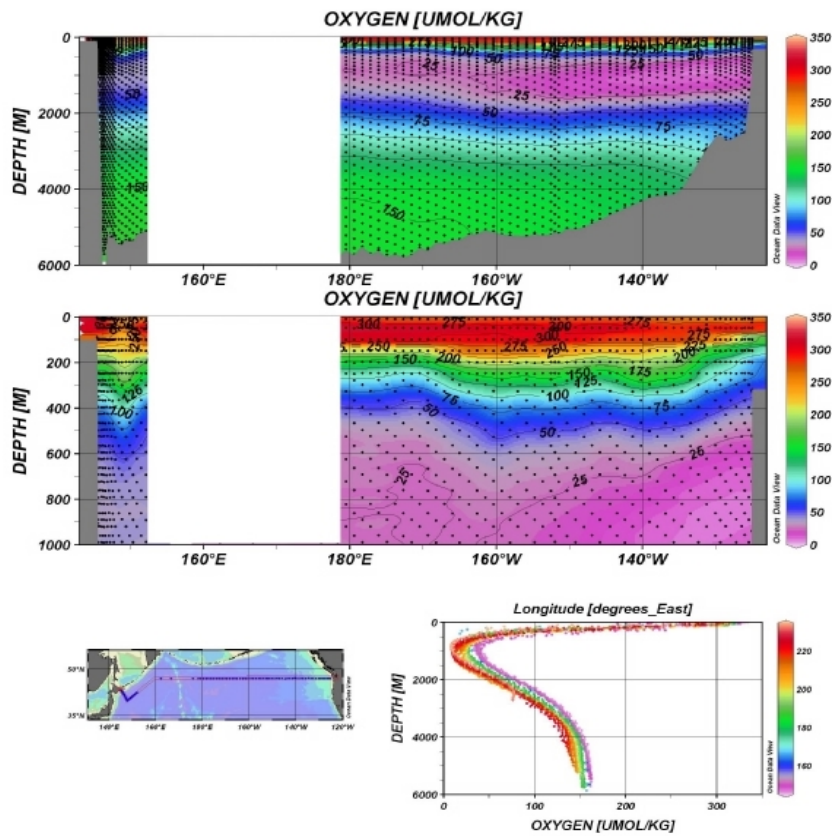
Figure 3.3.3   Zonal transects of dissolved oxygen (μmol kg^{-1}) along the WHP-P01 in 2007.   The transect between station 028 and 060 was concealed because of sparse data.
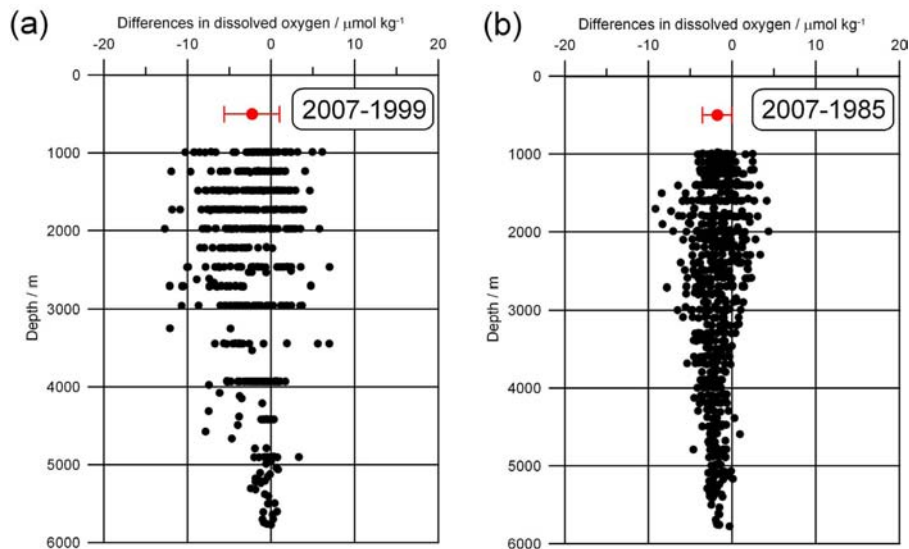
Figure 3.3.4   Differences of dissolved oxygen (μmol kg^{-1}) between 1999 and 2007 (a) and between 1985 and 2007 (b) in deep waters below 1000 dbar.   The data are restricted within the area to the east of the date line (180°).   Red circles denote the mean of the differences with the standard deviations.

(a) ΔAOU / μmol kg⁻¹ WHP-P01 (47°N) 1999 - 1985

(b) ΔAOU / μmol kg⁻¹ WHP-P01 (47°N) 2007 - 1999

Figure 3.3.5   Distributions of differences of Apparent Oxygen Utilization, AOU (μmol kg⁻¹) against density (σ_θ) between 1985 and 1999 (a) and between 1999 and 2007 (b).   Contour intervals are 10 μmol kg⁻¹.   Small dots indicate sampling layers of dissolved oxygen.   Sparse data hinder the comparison between 1999 and 2007 in shallow layers in the area to the east of 150°W (shaded area).

References

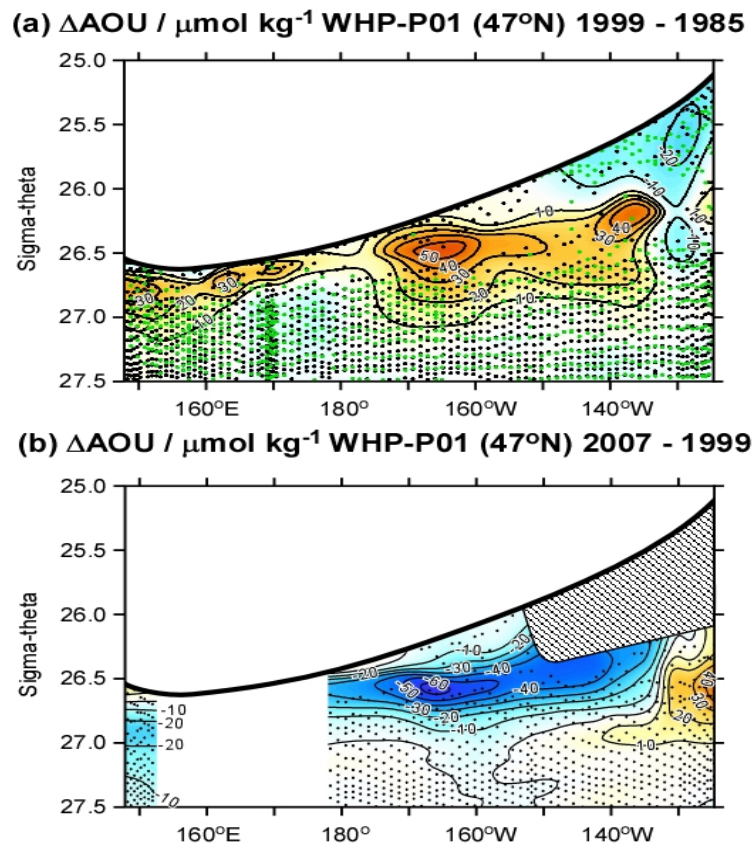Dickson, A. (1996) Determination of dissolved oxygen in sea water by Winkler titration, in WHPO Pub. 91-1 Rev. 1, November 1994, Woods Hole, Mass., USA.

DOE (1994) Handbook of methods for the analysis of the various parameters of the carbon dioxide system in sea water; version 2. A.G. Dickson and C. Goyet (eds), ORNL/CDIAC-74.

Joyce, T., and C. Corry, eds., C. Corry, A. Dessier, A. Dickson, T. Joyce, M. Kenny, R. Key, D. Legler, R. Millard, R. Onken, P. Saunders, M. Stalcup, contrib. (1994) Requirements for WOCE Hydrographic Programme Data Reporting, WHPO Pub. 90-1 Rev. 2, May 1994 Woods Hole, Mass., USA.

Murray, C.N., J.P. Riley, and T.R.S. Wilson (1968) The solubility of oxygen in Winkler reagents used for determination of dissolved oxygen, Deep-Sea Res., 15, 237-238.

Watanabe, Y.W., T. Ono, A. Shimamoto, T. Sugimoto, M. Wakita and S. Watanabe (2001) Probability of a reduction in the formation rate of subsurface water in the North Pacific during the 1980s and 1990s. Geophys. Res. Letts., 28, 3298-3292.

3.4 Nutrients
draft as of 3 Sept. 2007 for MR0704 cruise

(1)Personnel

Michio AOYAMA (Meteorological Research Institute / Japan Meteorological Agency, Principal Investigator)
Ayumi TAKEUCHI (Department of Marine Science, Marine Works Japan Ltd.)
Takayoshi SEIKE (Department of Marine Science, Marine Works Japan Ltd.)
Shunsuke MIYABE(Department of OD Science Technical Support, Marine Works Japan Ltd.)

(2)Objectives

The objectives of nutrients analyses during the R/V Mirai MR0704 cruise, WOCE P1 revisited cruise in 2007, along 47N line in the Western North Pacific are as follows;

Describe the present status of nutrients concentration with excellent comparability.

The determinants are nitrate, nitrite, phosphate and silicate (Although silicic acid is correct, we use silicate because a term of silicate is widely used in oceanographic community.)

Study the temporal and spatial variation of nutrients concentration based on the previous high quality experiments data of WOCE previous P1 cruises in 1985 and 1999, GOESECS, IGY and so on.

Study of temporal and spatial variation of nitrate: phosphate ratio, so called Redfield ratio.

Obtain more accurate estimation of total amount of nitrate, phosphate and silicate in the interested area.

Provide more accurate nutrients data for physical oceanographers to use as tracers of water mass movement.

(3)Equipment and techniques

i. Analytical detail using TRAACS 800 systems (BRAN+LUEBBE)

The phosphate analysis is a modification of the procedure of Murphy and Riley (1962).

Molybdic acid is added to the seawater sample to form phosphomolybdic acid which is in turn reduced to phosphomolybdous acid using L-ascorbic acid as the reductant.

Nitrate + nitrite and nitrite are analyzed according to the modification method of Grasshoff (1970). The sample nitrate is reduced to nitrite in a cadmium tube inside of which is coated with metallic copper. The sample stream with its equivalent nitrite is treated with an acidic, sulfanilamide reagent and the nitrite forms nitrous acid which reacts with the sulfanilamide to produce a diazonium ion. N1-Naphthylethylene-diamine added to the sample stream then couples with the diazonium ion to produce a red, azo dye. With reduction of the nitrate to nitrite, both nitrate and nitrite react and are measured; without reduction, only nitrite reacts. Thus, for the nitrite analysis, no reduction is performed and the alkaline buffer is not necessary. Nitrate is computed by difference.

The silicate method is analogous to that described for phosphate. The method used is essentially that of Grasshoff et al. (1983), wherein silicomolybdic acid is first formed from the silicic acid in the sample and added molybdic acid; then the silicomolybdic acid is reduced to silicomolybdous acid, or "molybdenum blue," using ascorbic acid as the reductant. The analytical methods of the nutrients during this cruise are similar with previous cruises (Uchida and Fukasawa, 2005).

The flow diagrams and reagents for each parameter are shown in Figures 3.4.1-3.4.4.
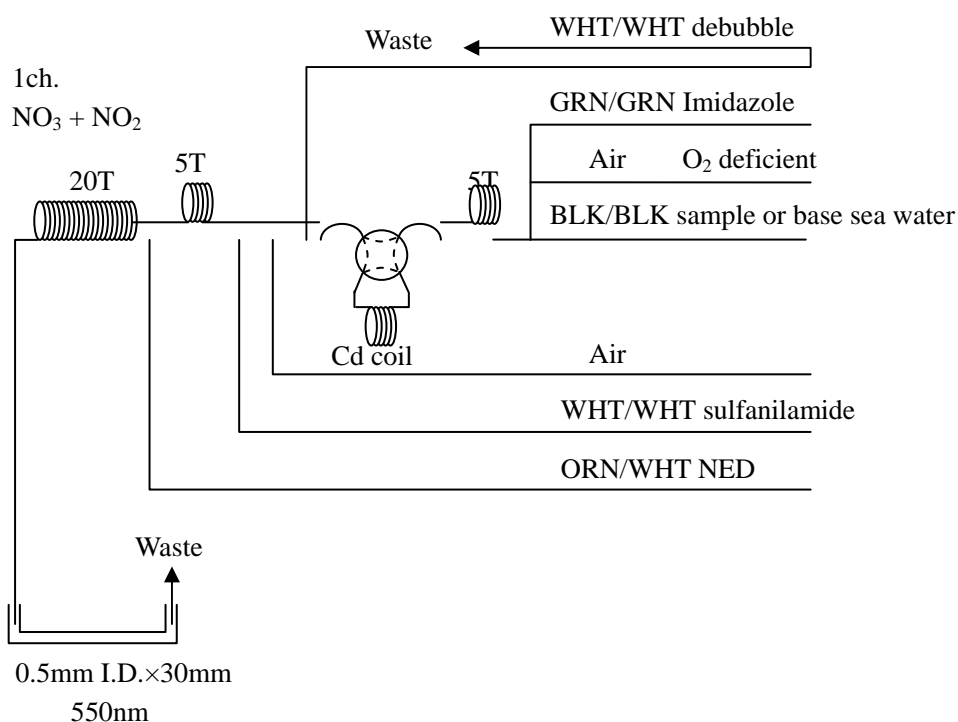
Figure3.4.1: 1ch. (NO_3+NO_2) Flow diagram.

---

ii. Nitrate Reagents

Imidazole (buffer), 0.06M (0.4% w/v)

Dissolve 4g imidazole, $C_3H_4N_2$, in ca. 900ml DIW; add 2ml concentrated HCl; make up to 1000ml with DIW. After mixing, 1ml Triton(R)X-100 (50% solution in ethanol) is added.

Sulfanilamide, 0.06M (1% w/v) in 1.2M HCl

Dissolve 10g sulfanilamide, $4\text{-}NH_2C_6H_4SO_3H$, in 1000ml of 1.2M (10%) HCl. After mixing, 2ml Triton(R)X-100 (50% solution in ethanol) is added.

N-1-Napthylethylene-diamine dihydrochloride, 0.004 M (0.1% w/v)

Dissolve 1 g NEDA, $C_{10}H_7NHCH_2CH_2NH_2$ 2HCl, in 1000ml of DIW; containing 10ml concentrated HCl.

Stored in a dark bottle.
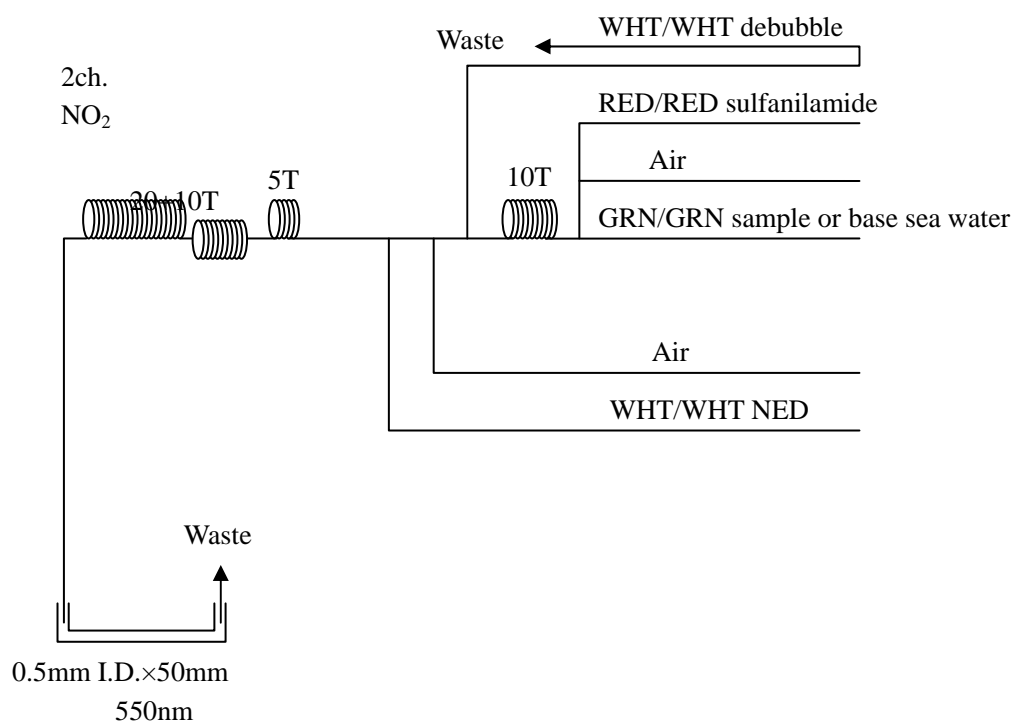
Figure 3.4.2: 2ch. (NO_2) Flow diagram.

iii. Nitrite Reagents

Sulfanilamide, 0.06M (1% w/v) in 1.2M HCl

Dissolve 10g sulfanilamide, $4-NH_2C_6H_4SO_3H$, in 1000ml of 1.2M (10%) HCl. After mixing, 2ml Triton(R)X-100 (50% solution in ethanol) is added.

N-1-Napthylethylene-diamine dihydrochloride , 0.004 M (0.1% w/v)

Dissolve 1 g NEDA, $C_{10}H_7NHCH_2CH_2NH_2$ 2HCl, in 1000ml of DIW; containing 10ml concentrated HCl.

Stored in a dark bottle.
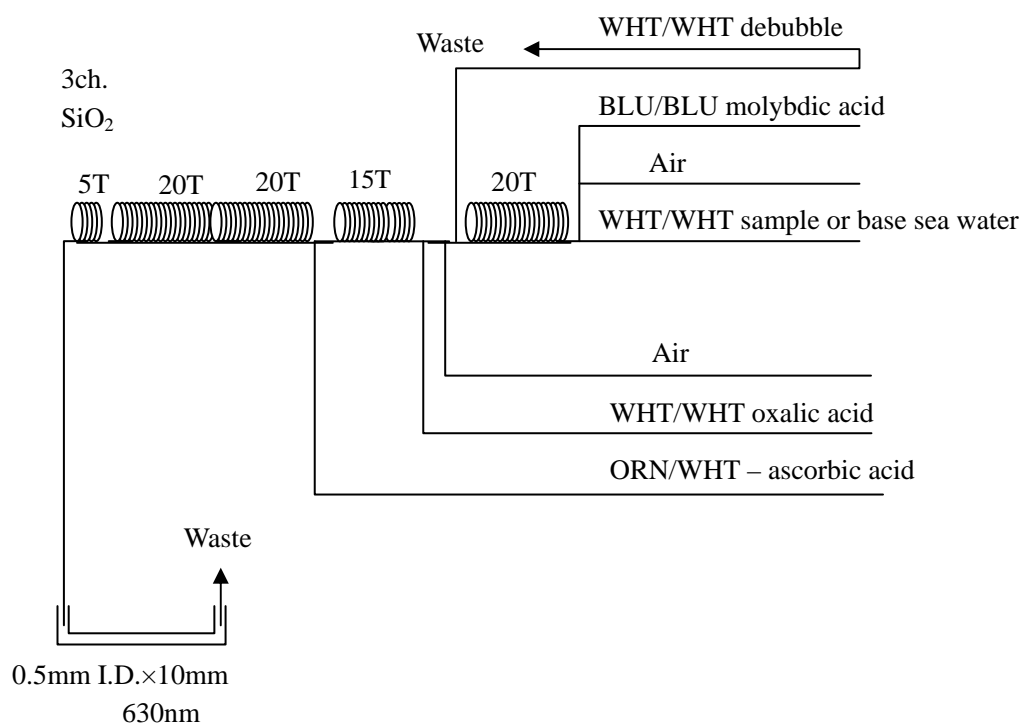
Figure 3.4.3: 3ch. (SiO$_2$) Flow diagram.

---

iv. Silicic Acid Reagents

Molybdic acid, 0.06M (2% w/v)

Dissolve 15g Disodium Molybdate(VI) Dihydrate, Na$_2$MoO$_4$ 2H$_2$O, in 1000ml DIW containing 8ml H$_2$SO$_4$. After mixing, 20ml sodium dodecyl sulphate (15% solution in water) is added.

Oxalic acid, 0.6M (5% w/v)

Dissolve 50g Oxalic Acid Anhydrous, HOOC: COOH, in 950ml of DIW.

Ascorbic acid, 0.01M (3% w/v)

Dissolve 2.5g L (+)-Ascorbic Acid, C$_6$H$_8$O$_6$, in 100ml of DIW. Stored in a dark bottle and freshly

prepared before every measurement.

4ch.
PO$_4$

WHT/WHT debubble

Waste

RED/RED PO$_4$dilution

20T   20T   20T   5T   Air

GRN/GRN sample or base sea water

Air

WHT/WHT PO$_4$ color reagent

Waste

0.5mm I.D.×50mm
880nm
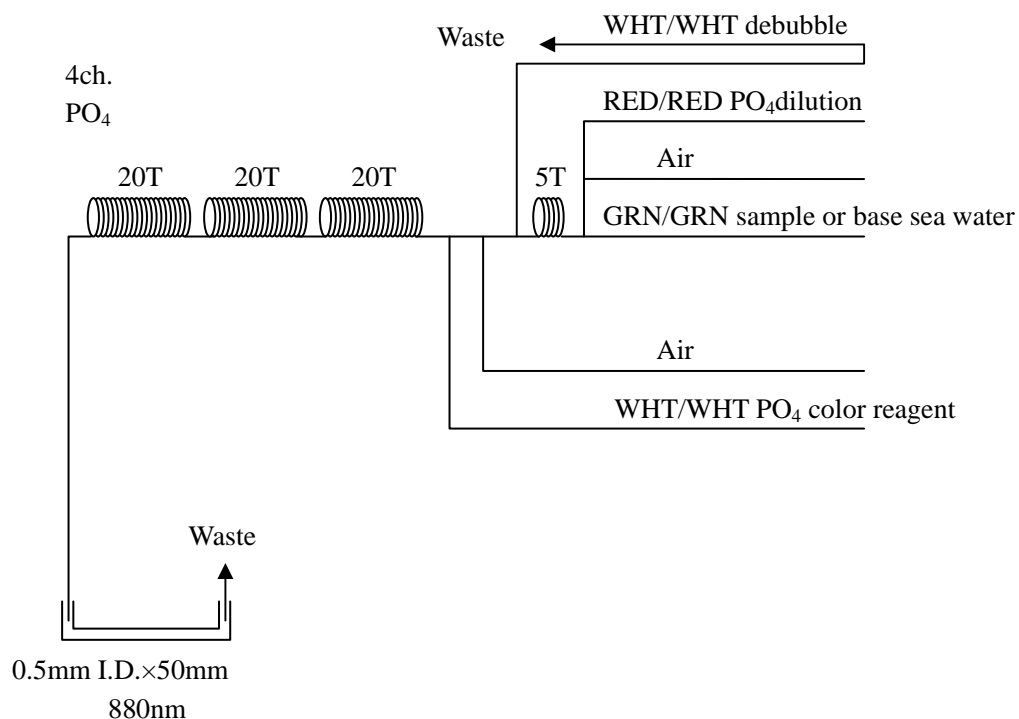
Figure 3.4.4: 4ch. (PO$_4$) Flow diagram.

v. Phosphate Reagents

Stock molybdate solution, 0.03M (0.8% w/v)

Dissolve 8g Disodium Molybdate(VI) Dihydrate, Na$_2$MoO$_4$ 2H$_2$O, and 0.17g Antimony Potassium Tartrate, C$_8$H$_4$K$_2$O$_{12}$Sb$_2$ 3H$_2$O, in 1000ml of DIW containing 50ml concentrated H$_2$SO$_4$.

Mixed Reagent

Dissolve 0.8g L (+)-Ascorbic Acid, C$_6$H$_8$O$_6$, in 100ml of stock molybdate solution. After mixing,   2ml sodium dodecyl sulphate (15% solution in water) is added. Stored in a dark bottle and freshly prepared before every measurement.

PO4 dilution

Dissolve Sodium Hydrate, NaCl, 10g in ca. 900ml, add 50ml Acetone and 4ml concentrated H$_2$SO$_4$, make up to 1000ml. After mixing, 5ml sodium dodecyl sulphate (15% solution in water) is added.

vi. Sampling procedures

Sampling of nutrients followed that oxygen, trace gases and salinity. Samples were drawn into two of virgin 10 ml polyacrylates vials without sample drawing tubes. These were rinsed three times before filling and vials were capped immediately after the drawing. The vials are put into water bath at 25 +-1deg. C in 10 minutes before use to stabilize the temperature of samples.

No transfer was made and the vials were set an auto sampler tray directly. Samples were analyzed after collection basically within 17 hours.

vii. Data processing.

Raw data from TRAACS800 were treated as follows;

Check baseline shift.

Check the shape of each peak and positions of peak values taken, and then change the positions of peak values taken if necessary.

Carry-over correction and baseline drift correction were applied to peak heights of each samples followed by sensitivity correction.

Baseline correction and sensitivity correction were done basically using liner regression.

Load pressure and salinity from CTD data to calculate density of seawater.

Calibration curves to get nutrients concentration were assumed second order equations.

(4) Nutrients standards
i. Volumetric Laboratory Ware of in-house standards

All volumetric glass- and polymethylpetene (PMP)-ware used were gravimetrically calibrated.   Plastic volumetric flasks were gravimetrically calibrated at the temperature of use within 2-3 K.

Volumetric flasks.

Volumetric flasks of Class quality (Class A) are used because their nominal tolerances are 0.05% or less over the size ranges likely to be used in this work. Class A flasks are made of borosilicate glass, and the standard solutions were transferred to plastic bottles as quickly as possible after they are made up to volume and well mixed in order to prevent excessive dissolution of silicic acid from the glass. High quality plastic (polymethylpentene, PMP, or polypropylene) volumetric flasks were gravimetrically calibrated and used only within 3-4 K of the calibration temperature.

The computation of volume contained by glass flasks at various temperatures other than the calibration temperatures were done by using the coefficient of linear expansion of borosilicate crown glass.

Because of their larger temperature coefficients of cubical expansion and lack of tables constructed for these materials, the plastic volumetric flasks were gravimetrically calibrated over the temperature range of intended use and used at the temperature of calibration within 3-4 K. The weights obtained in the calibration weightings were corrected for the density of water and air buoyancy.

Pipettes and pipettors.

All pipettes have nominal calibration tolerances of 0.1% or better. These were gravimetrically calibrated in order to verify and improve upon this nominal tolerance.

ii. Reagents, general considerations
General Specifications.

All reagents were of very high purity such as "Analytical Grade," "Analyzed Reagent Grade" and others.   And assay of nitrite was determined according JISK8019 and assays of nitrite salts were 99.1%. We use that value to adjust the weights taken.

For the silicate standards solution, we use Merck HC623465 solution. The silicate concentration is

certified by NIST-SRM3150 with the uncertainty of 0.5%. For nitrate and phosphate, we use Merck 99.999% powders.

Ultra pure water.

Ultra pure water (MilliQ water) freshly drawn was used for preparation of reagents, higher concentration standards and for measurement of reagent and system blanks.

Low-Nutrient Seawater (LNSW).

Surface water having low nutrient concentration was taken and filtered using 0.45 μm pore size membrane filter. This water is stored in 20 liter cubitainer with paper box. The concentrations of nutrient of this water were measured carefully in April 2007.

iii. Concentrations of nutrients for A, B and C standards

Concentrations of nutrients for A, B and C standards are set as shown in Table 3.4.1. The C standard is prepared according recipes as shown in Table 3.4.2. All volumetric laboratory tools were calibrated prior the cruise as stated in chapter (i). Then the actual concentration of nutrients in each fresh standard was calculated based on the ambient, solution temperature and determined factors of volumetric lab. wares.

Table 3.4.1: Nominal concentrations of nutrients for A, B and C standards

	A	B		C-1	C-2	C-3	C-4	C-5	C-6	C-7
$NO_3(\mu M)$	45000	900	0	BA	AY	AX	AV	BF	55	BG
$NO_2(\mu M)$	4000	20	0	BA	AY	AX	AV	BF	1.2	BG
$SiO_2(\mu M)$	36000	2880	0	BA	AY	AX	AV	BF	170	BG
$PO_4(\mu M)$	3000	60	0	BA	AY	AX	AV	BF	3.6	BG

Table 3.4.2: Working calibration standard recipes

C-STD	B-1 STD	B-2 STD
C-6	30 ml	30 ml

B-1 STD: Mixture of nitrate, silicate and phosphate

B-2 STD: Nitrite

iv. Renewal of in-house standard solutions.

In-house standard solutions as stated in (iii) were renewed as shown in Table 3.4.3.

Table 3.4.3: Timing of renewal of in-house standards.

NO_3, NO_2, SiO_2, PO_4	Renewal
A-1 Std. (NO_3)	maximum 1 month
A-2 Std. (NO_2)	maximum 1 month
A-3 Std. (SiO_2)	commercial prepared solution
A-4 Std. (PO_4)	maximum 1 month
B-1 Std. (mixture of NO_3, SiO_2, PO_4)	8 days
B-2 Std. (NO_2)	8 days

C Std	Renewal
C-6 Std (mixture of B1 and B2 Std.)	24 hours

Reduction estimation	Renewal
D-1 Std. (7200μM NO_3)	when A-1renewed
43μM NO_3	when C-std renewed
47μM NO_2	when C-std renewed

(5) Reference material of nutrients in seawater

To get the more accurate and high quality nutrients data to achieve the objectives stated above, huge numbers of the bottles of the reference material of nutrients in seawater (hereafter RMNS) are prepared (Aoyama et al., submitted ;Aoyama et al.,2007). In the previous world wide expeditions, such as WOCE cruises, the higher reproducibility and precision of nutrients measurements were required (Joyce and Corry, 1994). Since no standards were available for the measurement of nutrients in seawater at that time, the requirements were described in term of reproducibility.   The required reproducibility was 1%, 1-2%, 1-3% for nitrate, phosphate and silicate, respectively. Although nutrient data from the WOCE one-time survey was of unprecedented quality and coverage due to much care in sampling and measurements, the differences of nutrients concentration at crossover points are still found among the expeditions (Aoyama and Joyce, 1996, Mordy et al., 2000, Gouretski and Jancke, 2001). For instance, the mean offset of nitrate concentration at deep waters was 0.5 µmol kg^{-1} for 345 crossovers at world oceans, though the maximum was 1.7 µmol kg^{-1} (Gouretski and Jancke, 2001). At the 31 crossover points in the Pacific WHP one-time lines, the WOCE standard of reproducibility for nitrate of 1% was fulfilled at about half of the crossover points and the maximum difference was 7% at deeper layers below 1.6 deg. C in potential temperature (Aoyama and Joyce, 1996).

i. RMNSs for this cruise

RMNS lots BA, AY, AX, AV and BF, which covers full range of nutrients concentrations in the western North Pacific Ocean are prepared. 40 sets of BA,AY,AX,AV and BF are prepared.

Since silicate concentration along P1 section was expected to be very high, we also prepared RMNS lot BG, of which silicate concentration is 255 µmol kg^{-1}.   When silicate concentration expected to exceed 170 µmol kg^{-1}, we add RMNS lot BG as an additional standard as C7. These RMNSs were renewed daily and analyzed every 2 runs on the same day.

150 bottles of RMNS lot BC are prepared to use every analysis at every hydrographic station. These RMNS assignment were completely done based on random number. The RMNS bottles were stored at a room in the ship, REAGENT STORE, where the temperature was maintained around 24-26 deg. C.

ii. Assigned concentration for RMNSs

We assigned nutrients concentrations for RMNS lots BA, AY, AX, AV, BF, BC and BG as shown in table 3.4.4.

Table 3.4.4   Assigned concentration of RMNSs

unit: micro mol kg-1

	Phosphate	Nitrate	Silicate	Nitrite
AH	2.114	35.31	132.20	
BA	0.068	0.07	1.60	0.02
AY	0.516	5.60	29.42	0.62
AX	1.619	21.42	58.06	0.35
AV	2.516	33.36	154.14	0.10
BF	2.797	41.28	150.23	0.01
BC	2.782	40.71	156.13	0.02
BG	2.562	36.72	254.70	0.06

iii. The homogeneity of RMNSs

The homogeneity of lot BC and analytical precisions are shown in table 3.4.5. These are for the assessment of the magnitude of homogeneity of the RMNS bottles those are used during the cruise. As shown in table3.4.5 and table 3.4.6 the homogeneity of RMNS lot BC for nitrate and silicate are the same magnitude of analytical precision derived from fresh raw seawater in May2005. The homogeneity for phosphate, however, exceeded the analytical precision at some extent. In May 2007, analytical precisions become better less than 0.1% and the homogeneity at lot BF and BG for nitrate, phosphate and silicate were 0.11-0.14%, 0.17-0.21%, 0.08-0.10%, respectively.

Table 3.4.5:   Homogeneity of lot BC and previous lots derived from simultaneous 30 samples measurements and analytical precision onboard R/V Mirai in May 2005.

	Nitrate CV%	Phosphate CV%	Silicate CV%
BC	0.22	0.32	0.19
(AH)	(0.39%)	(0.83%)	(0.13)
(K)	(0.3%)	(1.0%)	(0.2%)
Precision	0.22%	0.22%	0.12%

Note: N=30 x 2

Table 3.4.6   Homogeneity of lot BF and BG derived from simultaneous 7 samples measurements and analytical precision onboard R/V Mirai in May 2007.

	Nitrate CV%	Phosphate CV%	Silicate CV%
BF	0.11	0.21	0.10
BG	0.14	0.17	0.08
Precision	0.05	0.07	0.06

Note: N=7 x 4

iv. Comparability of RMNSs during the periods from 2003 to 2007

Cruise-to-cruise comparability has examined based on the results of the previous results of RMNSs measurements obtained among cruises, and RMNS international comparison experiments in 2003 and 2007. As shown in Table 3.4.7, the nutrients concentration of RMNSs were in good agreement among the measurements during the period from 2003 to 2007. For the silicate measurements, we show lot numbers and chemical company names of each cruise/measurement in the footnote. As shown in table 3.4.7, there is less comparability among the measurements due to less comparability among the standard solutions provided by chemical companies in the silicate measurements.

Table   3.4.7   Comparability for phosphate, nitrate and silicate

Cruise/Lab	year	AH	BA	AY	AX	AV	BF	BC	BG
					Nitrate				
MR03-K01	2003	35.27							
MR03-ENG	2003	35.23							
MR03-K02	2003	35.28							
MR03-K04 Leg1	2003	35.25							
MR03-K04 Leg2	2003	35.37							
MR03-K04 Leg4	2003	35.37							
MR03-K04 Leg5	2003	35.34							
MR03-K04 Leg6	2003	35.31							
2003intercomparison	2003	35.23			21.39				
MR05-01	2005	35.53	0.10		21.50	33.40			
MR05-ENG	2005							40.80	
MR05-02	2005		0.10	5.60	21.40	33.30		40.70	
MR05-05_1 precruise	2005	35.70	0.10	5.60	21.40	33.40		40.70	
MR05-05_1	2005		0.07	5.61	21.43	33.36		40.62	
MR05-05_2 precruise	2005		0.08	5.58	21.39	33.36		40.72	
MR05-05_2	2005		0.07	5.62	21.44	33.36		40.73	
MR05-05_3 precruise	2005		0.06	5.62	21.49	33.39		40.79	
MR05-05_3	2005		0.07	5.62	21.45	33.37		40.74	
MR06-02	2006			5.62		33.36			
MR06-03 precruise	2006			5.59		33.42			
MR06-03_2precruise	2006			5.62		33.24			
MR06-04_1precruise	2006			5.60		33.33			

MR06-04_2	2006			5.63		33.12			
MR06-05_1	2006		0.04	5.58	21.40	33.32		40.63	
2006intercompariosn	2006		0.04	5.58	21.40	33.32		40.63	
2003intercomp_revisit	2006	35.40							
MR07-02	2007		0.04	5.62	21.44	33.40	41.36		36.85
MR0704_precruise_1	2007	35.75	0.08	5.66	21.57	33.49	41.50	40.85	36.91
MR0704_precruise_2	2007	35.85	0.08	5.66	21.63	33.54	41.61	40.98	37.02

Phosphate

MR03-K01	2003	2.100							
MR03-ENG	2003	2.117							
MR03-K02	2003	2.104							
MR03-K04 Leg1	2003	2.110							
MR03-K04 Leg2	2003	2.110							
MR03-K04 Leg4	2003	2.110							
MR03-K04 Leg5	2003	2.110							
MR03-K04 Leg6	2003	2.100							
2003intercomp	2003	2.100							
MR05-01	2005	2.126	0.070		1.620	2.520			
MR05-02	2005		0.070	0.520	1.620	2.520		2.770	
MR05-05_1 precruise	2005	2.140	0.050	0.510	1.620	2.520		2.780	
MR05-05_1	2005		0.062	0.515	1.614	2.515		2.774	
MR05-05_2 precruise	2005		0.066	0.519	1.608	2.510		2.784	
MR05-05_2	2005		0.064	0.517	1.614	2.516		2.781	
MR05-05_3 precruise	2005		0.060	0.519	1.620	2.517		2.788	
MR05-05_3	2005		0.061	0.515	1.615	2.515		2.778	
MR06-02	2006			0.516		2.515			
MR06-03 precruise	2006			0.496		2.499			
MR06-03_2 precruise	2006			0.504		2.515			
MR06-04_1precruise	2006			0.502		2.501			
MR06-04_2	2006			0.510		2.507			
MR06-05_1	2006		0.071	0.527	1.623			2.791	
2006intercomparison	2006		0.071	0.524	1.623	2.515		2.791	
2003intercomp_revisit	2006	2.141							
MR07-01	2007			0.524		2.521			
MR07-02	2007		0.080	0.593	1.646	2.553	2.832		2.599
MR0704_pre_test1	2007	2.143	0.062	0.518	1.622	2.515	2.815	2.786	2.574
MR0704_pre_test2	2007	2.148	0.057	0.515	1.622	2.520	2.815	2.792	2.582

Silicate

MR03-K01*	2003	133.9
MR03-ENG**	2003	134.1
MR03-K02**	2003	133.9
MR03-K04 Leg1**	2003	133.8
MR03-K04 Leg2**	2003	134.0

MR03-K04 Leg4**	**2003**	**134.0**							
MR03-K04 Leg5**	**2003**	**133.9**							
MR03-K04 Leg6**	**2003**	**133.8**							
2003intercomparison**	**2003**	**133.97**							
MR05-01#	**2005**	**135.5**	**1.6**		**59.4**	**157.7**			
MR05-02#	**2005**		**1.6**	**30.1**	**59.5**	**157.9**		**159.9**	
MR05-05_1precruise##	**2005**	**135.9**	**1.6**	**30.1**	**59.5**	**157.9**		**160.1**	
MR05-05_1##	**2005**		**1.6**	**30.1**	**59.5**	**158.0**		**160.0**	
MR05-05_2 precruise##	**2005**		**1.6**	**30.1**	**59.5**	**158.0**		**160.2**	
MR05-05_2##	**2005**		**1.6**	**30.1**	**59.5**	**158.0**		**160.1**	
MR05-05_3 precruise##	**2005**		**1.6**	**30.1**	**59.5**	**158.0**		**160.1**	
MR05-05_3##	**2005**		**1.6**	**30.1**	**59.5**	**157.9**		**160.1**	
MR06-02##	**2006**			**30.1**		**157.9**			
MR06-03 precruise ✝	**2006**			**29.4**		**154.5**			
MR06-03_2precruise ✝	**2006**			**29.6**		**154.5**			
MR06-04_1precruise ✝	**2006**			**29.5**		**154.3**			
MR06-04_1 ✝	**2006**								
MR06-04_2 ✝	**2006**			**30.2**		**154.0**			
MR06-05_1***	**2006**		**1.61**	**29.5**	**58.20**	**154.16**		**156.31**	
2006intercomparison ✝	**2006**		**1.64**	**29.5**	**58.18**	**154.33**			
2003intercomp_revisit ✝	**2006**	**132.55**							
MR07-01 ✝	**2007**			**29.4**		**154.53**			
MR07-02 ✝	**2007**		**1.65**	**29.6**	**58.37**	**154.55**	**150.57**		**254.95**
MR0704_precruise_1$	**2007**	**133.41**	**1.63**	**29.52**	**58.36**	**154.92**	**151.11**	**157.08**	**256.15**
MR0704_precruise_2$	**2007**	**133.39**	**1.70**	**29.60**	**58.44**	**155.18**	**151.33**	**157.19**	**256.61**

List of lot numbers: *: Kanto 306F9235; **: Kanto 402F9041; #: Kanto 502F9205; ##: Kanto 609F9157;

✝ Merck OC551722; ***: Merck HC694149, $:   Merck HC623465

(5) Quality control

i. Precision of nutrients analyses during the cruise

Precision of nutrients analyses during the cruise was evaluated based on the 11 measurements, which are measured every 12 samples, during a run at the concentration of C-6. We also evaluated the reproducibility based on the replicate analyses of five samples in each run. Summary of precisions are shown in Table 3.4.8. As shown in Table 3.4.8 and Figures 3.4.5-3.4.7, the precisions for each parameter are generally good considering the analytical precisions estimated from the simultaneous analyses of 12 samples in May 2007. Analytical precisions previously evaluated were 0.07% for phosphate, 0.05% for nitrate and 0.06% for silicate, respectively. During this cruise, analytical precisions were 0.10% for phosphate, 0.06% for nitrate and 0.07% for silicate in terms of median of precision, respectively. Then we can conclude that the analytical precisions for phosphate, nitrate and silicate were maintained throughout this cruise. The time series of precision are shown in Figures 3.4.5-3.4.7.

Table 3.4.8: Summary of precision based on the replicate analyses of 11 samples in each run through out cruise.

	Nitrate CV%	Phosphate CV%	Silicate CV%
Median	0.06	0.10	0.07
Mean	0.06	0.10	0.07
Maximum	0.12	0.19	0.12
Minimum	0.02	0.03	0.01
N	90	90	90
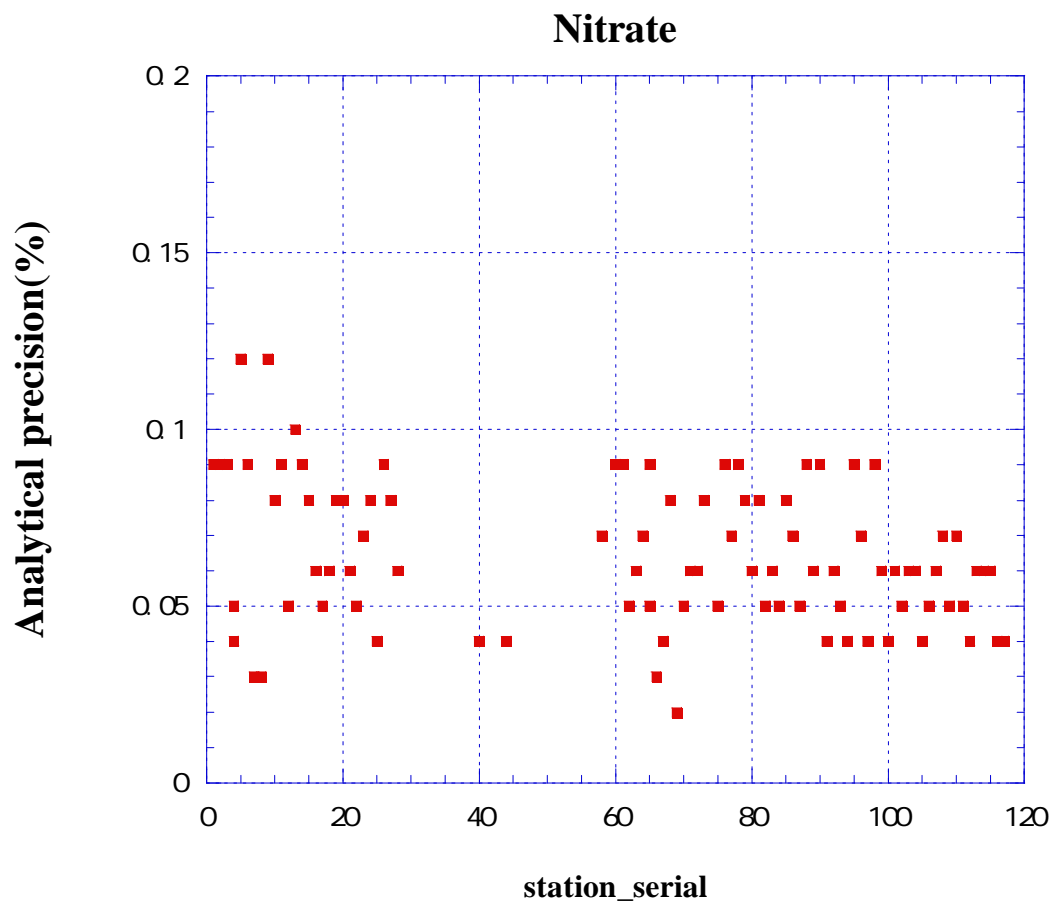
Figure: 3.4.5 Time series of precision of nitrate
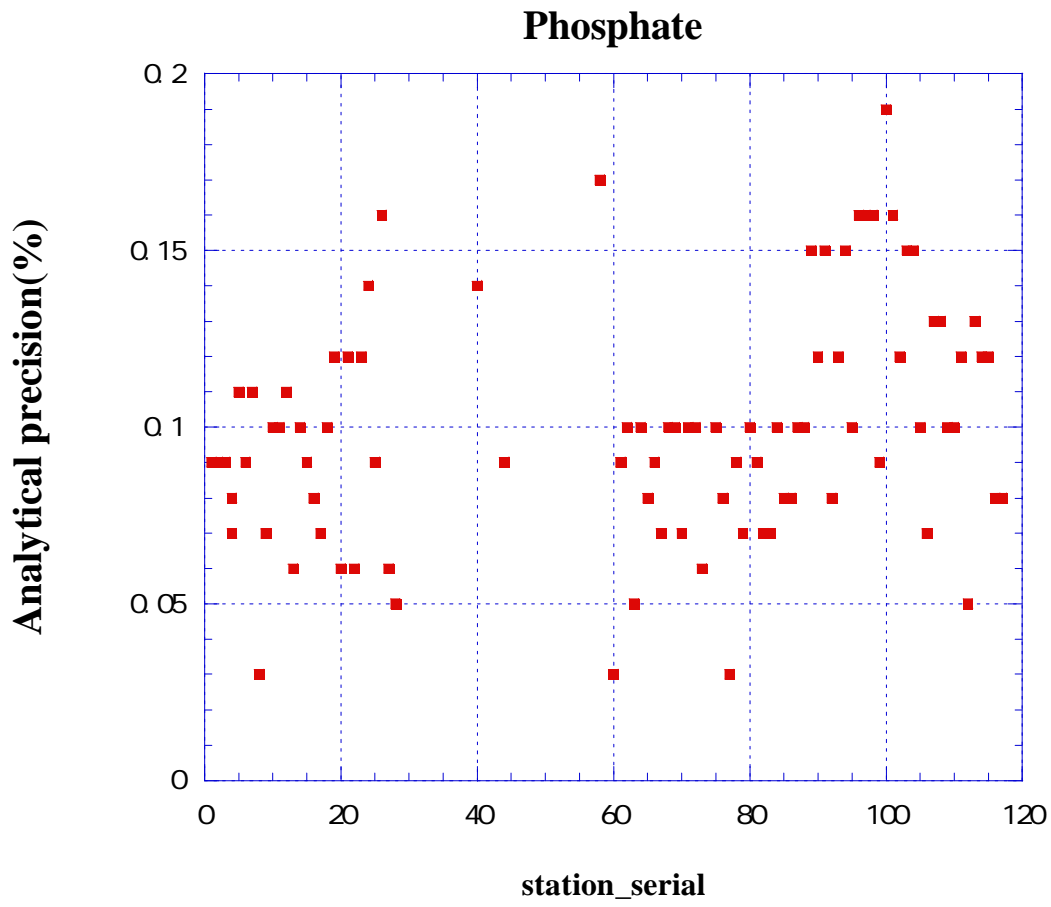
Phosphate

Figure: 3.4.6 Time series of precision of phosphate
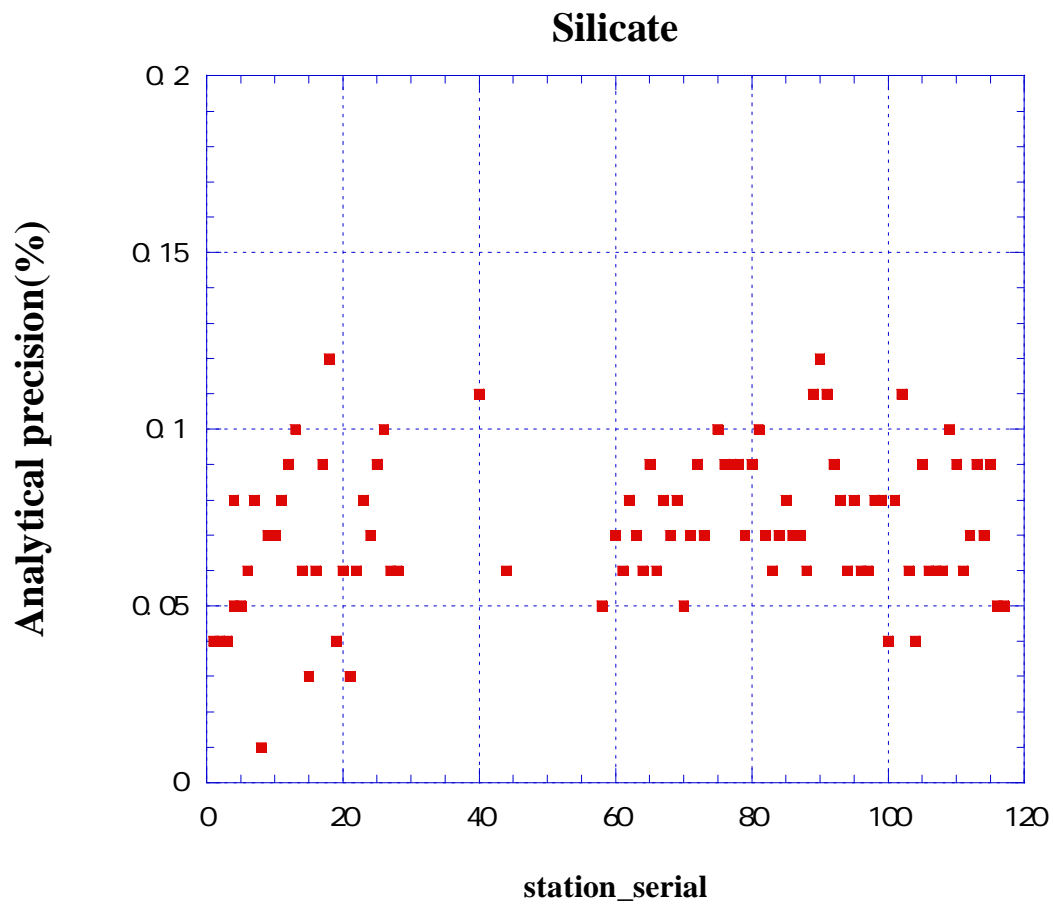
Silicate

Figure: 3.4.7 Time series of precision of silicate

ii. Carry over

We can also summarize the magnitudes of carry over throughout the cruise. These are small enough within acceptable levels as shown in Table 3.4.9.

Table 3.4.9: Summary of carry over through out cruise.

	Nitrate CV%	Phosphate CV%	Silicate CV%
Median	0.16	0.11	0.19
Mean	0.16	0.13	0.20
Maximum	0.28	0.44	0.36
Minimum	0.02	0.00	0.07
N	90	90	90

(6) Evaluation of Z-scores of RMNSs

Since we used RMNSs throughout the cruise, we can evaluate the trueness of our analysis in terms of Z-score of RMNSs.
Z-score for each analysis of RMNS is defined as follows;

$$Zpar = ABS((Cpar - Cnominal)/Ppar) \qquad (1)$$

Where
Zpar is Z-score for an analysis
Cpar is obtained concentration of a RMNS for interested parameter, nitrate, phosphate or silicate.
Cnominal is assigned concentration of RMNS for interested parameter, nitrate, phosphate or silicate.
Ppar is analytical precision at the concentration of RMNS for interested parameter, nitrate, phosphate or silicate.

Averages of these Z-scores were obtained for three parameters, nitrate, phosphate and silicate based on Z-scores for 7 RMNSs used at each run and shown in figure 3.4.8. Means of Z-score based on the Z-score of three parameters were also obtained and shown in figure 3.4.9.
These Z-scores were less than 0.6 in general and indicating that our analyses were in excellent comparability throughout the cruise.

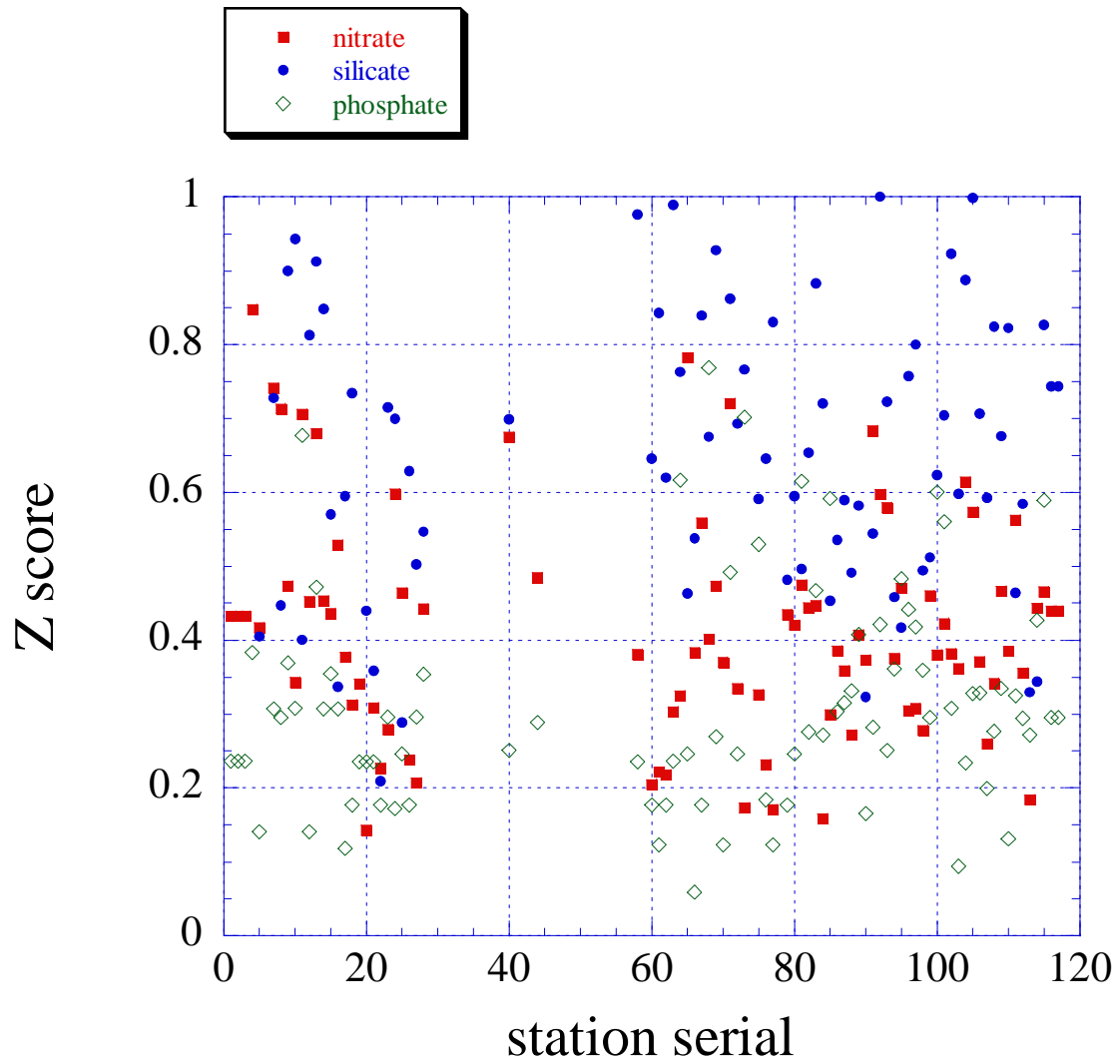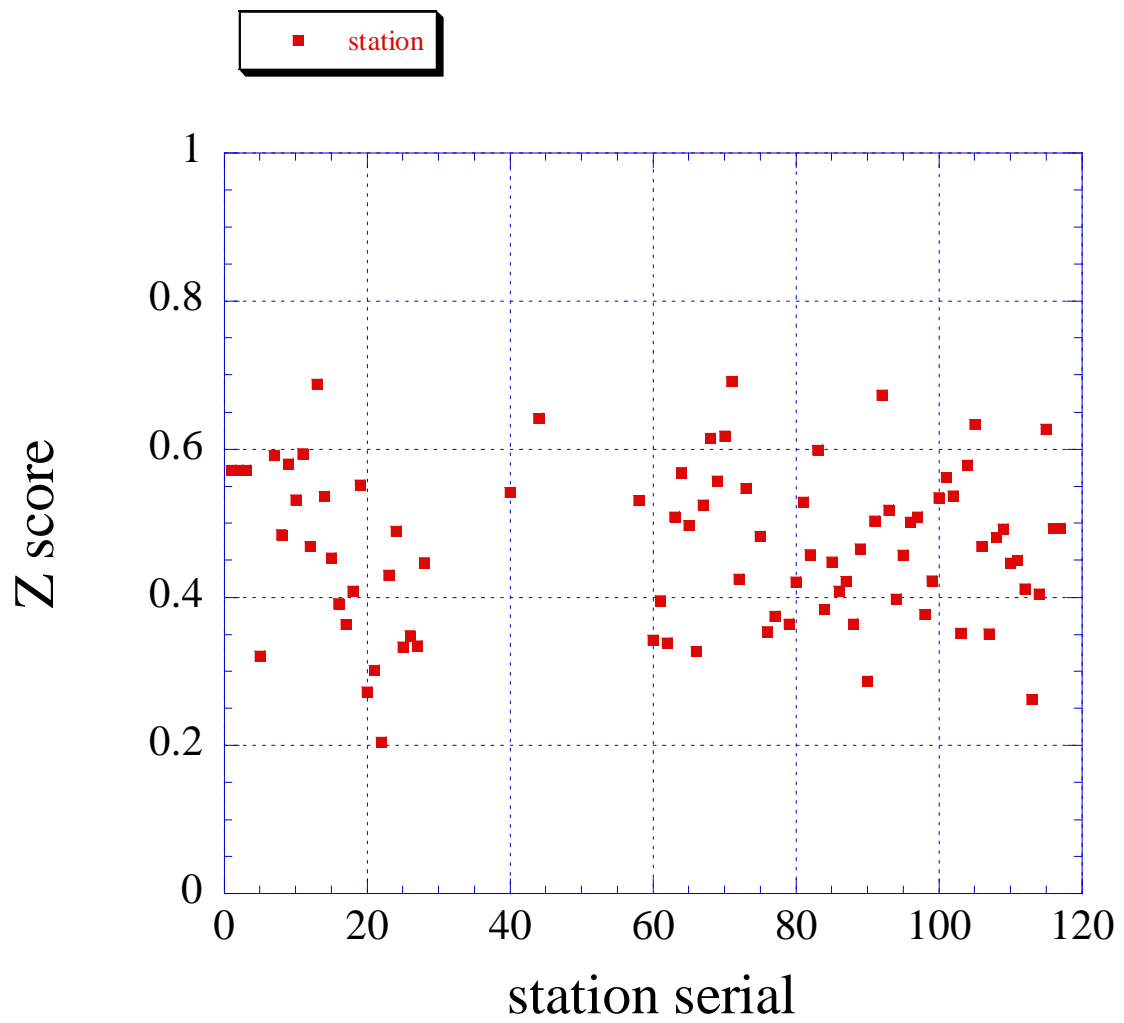**Figure 3.4.8. Z-score of nitrate, silicate and phosphate**

Figure 3.4.9. Means of Z-score at the stations

(7) Problems/improvements occurred and solutions.

During the analysis for the samples between station 8 and station 27, we got a problem on phosphate measurements.17 samples from 8 stations showed large difference on duplicate measurements exceeding uncertainty of 0.02 micro mol kg^{-1}.

Especially 12 samples showed 0.05 to 0.97 micro mol kg^{-1} higher values. We had judged that these higher values are contamination during the sampling from Niskin bottle or test tube itself. Therefore, we had checked probable source of this contamination including air-conditioners in the water sampling room and the laboratory. For the air-conditioners, we had cleaned up them. For the test tubes, **we had made blank test for 440 tubes**.

We did not see any contaminations on test tubes. Since higher phosphate concentration did not occur after we clean up the air-conditioners, we had concluded that the source of the contamination of phosphate might be one of air-conditioners in the Lab.

Reference

Aminot, A. and Kerouel, R. 1991. Autoclaved seawater as a reference material for the determination of nitrate and phosphate in seawater. Anal. Chim. Acta, 248: 277-283.

Aminot, A. and Kirkwood, D.S. 1995. Report on the results of the fifth ICES intercomparison exercise for nutrients in sea water, ICES coop. Res. Rep. Ser., 213.

Aminot, A. and Kerouel, R. 1995. Reference material for nutrients in seawater: stability of nitrate, nitrite, ammonia and phosphate in autoclaved samples. Mar. Chem., 49: 221-232.

Aoyama M., and Joyce T.M. 1996, WHP property comparisons from crossing lines in North Pacific. In Abstracts, 1996 WOCE Pacific Workshop, Newport Beach, California.

Aoyama, M., Ota, H., Iwano, S., Kamiya, H., Kimura, M., Masuda, S., Nagai, N., Saito, K., Tubota, H. 2004. Reference material for nutrients in seawater in a seawater matrix, Mar. Chem., submitted.

Aoyama et al.,2007. Recent Comparability of Oceanographic Nutrients Data: Results of a 2003 Intercomparison Exercise Using Reference Materials. Analytical Sciences in press.

Grasshoff, K., Ehrhardt, M., Kremling K. et al. 1983. Methods of seawater anylysis. 2nd rev. Weinheim: Verlag Chemie, Germany, West.

Uchida, H. & Fukasawa, M. WHP P6, A10, I3/I4 REVISIT DATA BOOK Blue Earth Global Expedition 2003 1, 2, (Aiwa Printing Co., Ltd., Tokyo, 2005).

Joyce, T. and Corry, C. 1994. Requirements for WOCE hydrographic programmed data reporting. WHPO Publication, 90-1, Revision 2, WOCE Report No. 67/91.

Kirkwood, D.S. 1992. Stability of solutions of nutrient salts during storage. Mar. Chem., 38 : 151-164.

Kirkwood, D.S. Aminot, A. and Perttila, M. 1991. Report on the results of the ICES fourth intercomparison exercise for nutrients in sea water. ICES coop. Res. Rep. Ser., 174.

Mordy, C.W., Aoyama, M., Gordon, L.I., Johnson, G.C., Key, R.M., Ross, A.A., Jennings, J.C. and Wilson. J. 2000. Deep water comparison studies of the Pacific WOCE nutrient data set. Eos Trans-American Geophysical Union. 80 (supplement), OS43.

Murphy, J., and Riley, J.P. 1962. Analytica chim. Acta 27, 31-36.

Gouretski, V.V. and Jancke, K. 2001. Systematic errors as the cause for an apparent deep water property variability: global analysis of the WOCE and historical hydrographic data　REVIEW ARTICLE, Progress In Oceanography, 48: Issue 4, 337-402.

3.5 Chlorofluorocarbons

(1) Personnel
Ken'ichi Sasaki (JAMSTEC)

Katsunori Sagishima (MWJ)

Yuichi Sonoyama (MWJ)

Shoko Tatamisashi (MWJ)

(2) Objectives

Chlorofluorocarbons (CFCs) are chemically and biologically stable gases that have been artificially synthesized at 1930's or later. The atmospheric CFCs can slightly dissolve in sea surface water by air-sea gas exchange and then are spread into the ocean interior. Three chemical species of CFCs, namely CFC-11 (CCl_3F), CFC-12 (CCl_2F_2), CFC-113 ($C_2Cl_3F_3$), and CFCs like compound, carbon tetrachloride (CCl_4) can be used as transient tracers for the decadal time scale ocean circulation. We measured these compounds in seawater on board.

(3) Instrument and Method

i. Instruments

Dissolved CFCs and CCl_4 are measured by an electron capture detector (ECD) – gas chromatograph attached with a purging & trapping system.

Table 3-5-1 Instruments for CFCs and CCl_4 analysis.

Gas Chromatograph:	GC-14B (Shimadzu Ltd.)
Detector:	ECD-14 (Shimadzu Ltd)
Analytical Columns: [For CFCs]:	
Pre-column:	Silica Plot capillary column [i.d.: 0.53mm, length: 8 m, thick: 0.25µm]
Main column:	Connected two capillary columns (Pola Bond-Q [i.d.: 0.53mm, length: 9 m, film thickness: 6.0µm] followed by Silica Plot [i. d.: 0.53mm, length: 15 m, film thickness: 0.25µm])
[For CCl_4]:	
Pre-column:	DB-624 capillary column [i.d.: 0.53mm, length: 30 m, film thickness: 0.25µm]
Main column:	DB-624 capillary column [i.d.: 0.53mm, length: 75 m, film thickness: 0.25µm]
Purging & trapping:	Developed in JAMSTEC. Cold trap columns are 1/16" SUS tubing packed Porapak T and Porpak N columns for CFCs and CCl_4 analyses, respectively.

ii. Sample Collection

Seawater sub-samples for CFCs and CCl_4 measurements were collected from 12 liter Niskin bottles to 300ml and 150 ml glass bottles (developed in JAMSTEC), respectively. The bottles were filled by nitrogen gas before sampling. Two times of the bottle volumes of seawater sample were overflowed. The seawater samples were kept in water bathes roughly controlled at in-situ sample temperature. The CFCs and CCl_4 concentrations were determined as soon as possible after sampling.

In order to confirm CFC concentrations of standard gases and their stabilities and also to check CFC saturation levels in sea surface water with respect to overlying air, CFC mixing ratios in background

air were periodically analyzed. Air samples were continuously led into the Environmental Research Laboratory using 10 mm OD Dekaron® tubing. The end of the tubing was put on a head of the compass deck and another end was connected onto a macro air pump in the laboratory. The tubing was relayed by a T-type union which had a small stop cock. Air sample was collected from the flowing air into a 100ml glass cylinder attached on the cock.

iii. Analysis

The analytical system is modified from the original design of Bullister and Weiss (1988). Constant volume of sample water (50ml for CFCs and 30 ml for CCl_4) is taken into the purging & trapping system. Dissolved CFCs and CCl_4 are de-gassed by N_2 gas purge and concentrated in a trap column cooled to -40 degree centigrade. The CFCs and CCl_4 are desorbed by electrically heating the trap column, and lead into the pre-column. CFCs and CCl_4 are roughly separated from other compounds in the pre-column and are sent to main analytical column. And then the pre-column is switched to another line and flushed buck by counter flow of pure nitrogen gas. CFCs and CCl_4 sent into main column are separated further and detected by an electron capture detector (ECD). Nitrogen gases used in this system was filtered by N_2 gas purifier (VICI) and gas purifier tube packed Molecular Sieve 13X (MS-13X).

Table 3-5-2 Analytical conditions of dissolved CFCs in seawater.

Temperature	
Analytical Column:	95 deg-C
Detector (ECD):	240 deg-C
Trap column:	-40 deg-C (at adsorbing) & 140 deg-C (at desorbing)
Mass flow rate of nitrogen gas (99.9999%)	
Carrier gas:	15 ml/min
Detector make-up gas:	22 ml/min
Back flush gas:	15 ml/min
Sample purge gas:	150 ml/min
Standard gas (Japan Fine Products co. ltd.)	
Base gas:	Nitrogen
CFC-11:	300 ppt (v/v)
CFC-12:	160 ppt (v/v)
CFC-113:	30 ppt (v/v)

Table 3-5-3 Analytical conditions of dissolved CCl_4 in seawater.

Temperature	
Analytical Column:	50 deg-C
Detector (ECD):	200 deg-C
Trap column:	-45 deg-C (at adsorbing) & 130 deg-C (at desorbing)
Mass flow rate of nitrogen gas (99.9999%)	
Carrier gas:	10 ml/min
Detector make-up gas:	27 ml/min
Back flush gas:	10 ml/min
Sample purge gas:	150 ml/min
Standard gas (Japan Fine Products co. ltd.)	
Base gas: Nitrogen	
CFC-10 (CCl4): 250 ppt (v/v)	

(4) Preliminary Result
i. Precisions

The analytical precisions are estimated from replicate sample analyses. The precisions of CFCs were calculated to be $\pm$ 0.009 pmol/kg (n = 163), $\pm$ 0.006 pmol/kg (n = 163) and $\pm$ 0.006 pmol/kg (n = 163) for CFC-11, -12 and -113, respectively. The precision of CCl_4 measurement was computed to be $\pm$ 0.1 pmol/kg (n = 18) but the sampling number is not enough to estimate statistical precision.

In the CCl_4 measurements, we had some problems relating accuracy. Our measurements of CCl_4 concentration in surface water and mixing ratio in background air were around 40 % higher than them expected values from the atmospheric CCl_4 history (Walker et al., 2000). A possible cause of this discrepancy is problem on calibration of the standard gasses. The standard gases will be calibrated with respect to other gasses in near future.

ii. Distribution of CFCs

Penetration depths of CFC-11 and -12 were deep in western region and relatively shallow in eastern region. In the almost all stations, maximum concentrations of the CFCs are found in 50 – 100 m depth. Significant increases in CFC-11 and -12 from 1985 (WOCE) to 2007 (this cruise) are detected in water mass of < 27.5 sigma theta.

(5) Further data quality check

Volumetric loops for seawater sample and standard gas (and air sample) will be calibrated after this cruise and CFC concentrations will be corrected. Variation of detector sensitivities will be taken into account. And then, all the data will be checked once again in detail by property to property plot and others.

(6) References

Bullister, J.L and R. F. Weiss: Determination of CCl_3F and CCl_2F_2 in seawater and air. Deep Sea Research, 35, 839-853, 1988.

Walker, S. J., R. F. Weiss, and P. K. Salameh, Reconstructed histories of the annual mean atmospheric mole flactions for the halocarbons CFC-11, CFC-12, CFC-113, and carbon tetrachloride. Journal of Geophysical Research, 105, 2000.

3.6. Carbon items

(1) Personnel

Akihiko Murata (JAMSTEC)

Fuyuki Shibata (MWJ)

Minoru Kamata (MWJ)

Yoshiko Ishikawa (MWJ)

Yasuhiro Arii (MWJ)

(2) Objectives

Concentrations of CO_2 in the atmosphere are now increasing at a rate of 1.5 ppmv y^{-1} owing to human activities such as burning of fossil fuels, deforestation, and cement production. It is an urgent task to estimate as accurately as possible the absorption capacity of the oceans against the increased atmospheric CO_2, and to clarify the mechanism of the CO_2 absorption, because the magnitude of the anticipated global warming depends on the levels of CO_2 in the atmosphere, and because the ocean currently absorbs 1/3 of the 6 Gt of carbon emitted into the atmosphere each year by human activities.

In this cruise, we are aimed at quantifying how much anthropogenic CO_2 absorbed in the ocean are transported and redistributed in the Pacific. For the purpose, we measured CO_2-system parameters such as dissolved inorganic carbon (C_T), total alkalinity (A_T) and pH.

(3) Apparatus

i. C_T

Measurements of C_T was made with two total CO_2 measuring systems (systems A and C; Nippon ANS, Inc.), which are slightly different from each other. The systems comprise of a seawater dispensing system, a CO_2 extraction system and a coulometer (Model 5012, UIC Inc.).

The seawater dispensing system has an auto-sampler (6 ports), which takes seawater in a 300 ml borosilicate glass bottle and dispenses the seawater to a pipette of nominal 20 ml volume by PC control. The pipette was kept at 20 °C by a water jacket, in which water from a water bath set at 20 °C is circulated.

CO_2 dissolved in a seawater sample is extracted in a stripping chamber of the CO_2 extraction system by adding phosphoric acid (10 % v/v). The stripping chamber is made approx. 25 cm long and has a fine frit at the bottom. To degass CO_2 as quickly as possible, a heating wire kept at 40 °C was rolled from the bottom to a 1/3 height of the stripping chamber. The acid is added to the stripping chamber from the bottom of the chamber by pressurizing an acid bottle for a given time to push out the right amount of acid. The pressrizing is made with nitrogen gas (99.9999 %). After the acid is transferred to the stripping chamber, a seawater sample kept in a pipette is introduced to the stripping chamber by the same method as in adding an acid. The seawater reacted with phosphoric acid is stripped of CO_2 by bubbling the nigrogen gas through a fine frit at the bottom of the stripping chamber. The CO_2 stripped in the chamber is carried by the nitrogen gas (flow rates is 140 ml min^{-1}) to the coulometer through a dehydrating module. The modules of system A and C consist of two electric dehumidifiers (kept at 1 - 2 °C) and a chemical desiccant ($Mg(ClO_4)_2$).

The measurement sequence such as system blank (phosphoric acid blank), 2 % CO_2 gas in a nitrogen base, sea water samples (6) was programmed to repeat. The measurement of 2 % CO_2 gas was made to monitor response of coulometer solutions (from UIC, Inc.).

ii. A_T

Measurement of A_T was made based on spectrophotometry using a custom-made system (Nippon

ANS, Inc.). The system comprises of a water dispensing unit, an auto-burette (765 Dosimat, Metrohm), and a spectrophotometer (Carry 50 Bio, Varian), which are automatically controlled by a PC. The water dispensing unit has a water-jacketed pipette and a water-jacketed titration cell. The spectrophotometer has a water-jacketed quartz cell, length and volume of which are 8 cm and 13 ml, respectively. To circulate sample seawater between the titration and the qaurtz cells, PFA tubes are connected to the cells.

A seawater of approx. 40 ml is transferred from a sample bottle (brosilicate glass bottle; 130 ml) into the water-jacketed (25 ℃) pipette by pressurizing the sample bottle (nitrogen gas), and is introduced into the water-jacketed (25 ℃) titration cell. The seawater is circulated between the titration and the quartz cells by a peristaric pump to rinse the route. Then, Milli-Q water is introduced into the titration cell, and is circulated in the route twice to rinse the route. Next, a seawater of approx. 40 ml is weighted again by the pipette, and is transferred into the titration cell. The weighted seawater is introduced into the quartz cell. Then, for seawater blank, absorbances are measured at three wavelengts (750, 616 and 444 nm). After the measurement, an acid titrant, which is a mixture of approx. 0.05 M HCl in 0.65 M NaCl and bromocresol green (BCG) is added (2.1 ml) into the titration cell. The seawater + acid titrant solution is circulated for 6 minutes between the titration and the quartz cells, with stirring by a stirring tip and bubbling by wet nitrogen gas in the titration cell. Then, absorbances at the three wavelengths are measured again.

Calculation of A_T was made by the following equation:

$$A_T = (-[H^+]_T V_{SA} + M_A V_A)/V_S,$$

where M_A is the molarity of the acid titrant added to the seawater sample, $[H^+]_T$ is the total excess hydrogen ion concentration in the seawater, and V_S, V_A and V_{SA} are the initial seawater volume, the added acid titrant volume, and the combined seawater plus acid titrant volume, respectively. $[H^+]_T$ is calculated from the measured absorbances based on the following equation (Yao and Byrne, 1998):

$$pH_T = -\log[H^+]_T = 4.2699 + 0.002578(35 - S) + \log((R - 0.00131)/(2.3148 - 0.1299R))$$
$$- \log(1 - 0.001005S),$$

where S is the sample salinity, and R is the absorbance ratio calculated as:

$$R = (A_{616} - A_{750})/(A_{444} - A_{750}),$$

where A_i is the absorbance at wavelength i nm.

The HCl in the acid titrant was standardized (0.049977 M) on land. The concentrations of BCG were estimated to be approx. 0.04×10^{-3} M, and 2.0×10^{-6} M in the acid titrant and in the sample seawater, respectively.

iii. pH

Measurement of pH was made by a pH measuring system (Nippon ANS, Inc.). For the detection of pH, spectrophotometry was adopted. The system comprises of a water dispensing unit and a spectrophotometer (Carry 50 Scan, Varian). For an indicator, *m*-cresol purple (2 mM) was used.

Seawater is transferred from borosilicate glass bottle (300 ml) to a sample cell in the spectrophotometer. The length and volume of the cell are 8 cm and 13 ml, respectively, and the sample cell is kept at 25.00 ± 0.05 ℃ in a thermostated compartment. First, absorbances of seawater only are measured at three wavelengths (730, 578 and 434 nm). Then the indicator is injected and circulated for about 4 minutes. to mix the indicator and seawater sufficiently. After the pump is stopped, the absorbances of seawater + indicator are maeasured at the same wavelengths. The pH is calculated based on the following equation (Clayton and Byrne, 1993):

$$pH = pK_2 + \log\left(\frac{A_1 / A_2 - 0.00691}{2.2220 - 0.1331(A_1 / A_2)} \right),$$

where A_1 and A_2 indicate absorbances at 578 and 434 nm, respectively, and pK_2 is calculated as a function of water temperature and salinity.

(4) Performances
i. C_T

The two systems worked well without a major malfunction. Replicate analysis was made approximately on every 9th seawater sample. The repeatability for systems A and C were estimated to be 1.3 ± 1.1 (n = 80 pairs) and 1.1 ± 1.0 (n = 80 pairs) µmol kg^{-1}, respectively. The combined result was 1.2 ± 1.0 µmol kg^{-1} (n = 160 pairs).

ii. A_T

The system showed a very good precision compared to systems used in previous studies. A few replicate samples were taken on every stations. The repeatability was estimated to be 0.4 ± 0.4 µmol kg^{-1} (n = 151 pairs).

iii. pH

The system worked well with no troubles. The average of absolute differences between replicate samples were 0.0008 ± 0.0007 pH unit (n = 199 pairs).

(5) Results

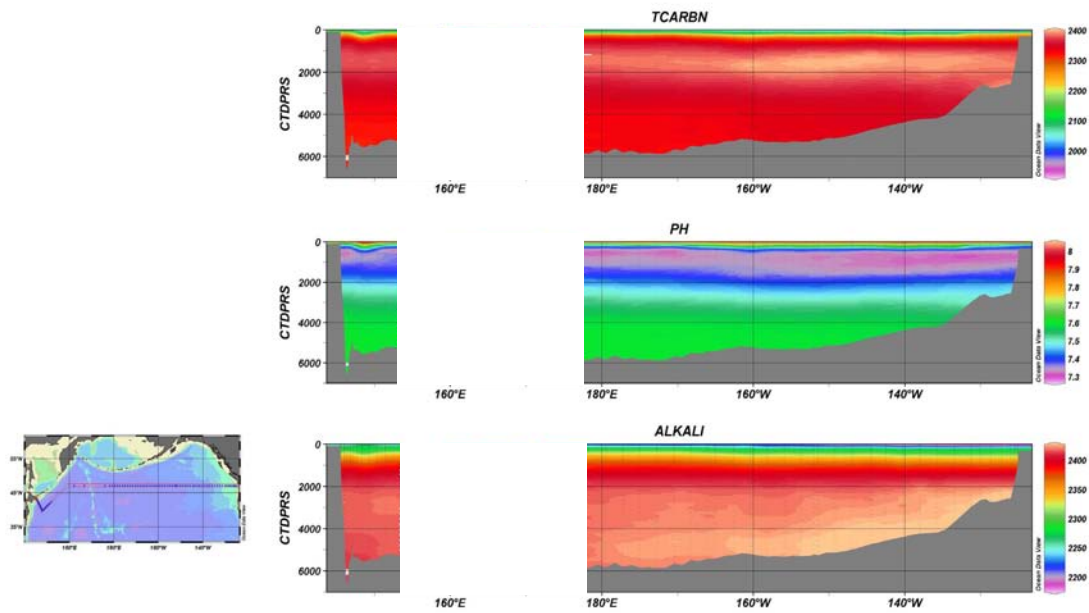Cross sections of C_T, pH, and A_T along WOCE P01 line are illustrated in Fig. 3.6.1.

Fig. 3.6.1. Distributions of C_T (upper), pH (middle), and A_T (bottom).

3.7 Samples taken for other chemical measurement

3.7.1 Carbon-13, -14

September 03, 2007

(1) Personnel

Yuichiro KUMAMOTO

Japan Agency for Marine Earth Science and Technology

(2) Objective

In order to investigate the water circulation and carbon cycle in the North Pacific, seawaters for carbon-14 (radiocarbon) and carbon-13 (stable carbon isotope) of total dissolved inorganic carbon (TDIC) were collected by the hydrocasts from surface to near bottom during MR07-04 cruise.

(3) Sample collection

The sampling stations and number of samples are summarized in Table 3.7.1.1. All samples for carbon isotope ratios were collected at 12 stations using 12-liter Niskin-X bottles. The seawater sample was siphoned into a 250 cm^3 glass bottle with enough seawater to fill the glass bottle 2 times. Immediately after sampling, 10 cm^3 of seawater was removed from the bottle and poisoned by 0.1 cm^3 μl of saturated $HgCl_2$ solution. Then the bottle was sealed by a glass stopper with Apiezon grease M and stored in a cool and dark space on board.

(4) Sample preparation and measurements

In our laboratory, dissolved inorganic carbon in the seawater samples will be stripped cryogenically and split into three aliquots: radiocarbon measurement (about 200 µmol), carbon-13 measurement (about 100 µmol), and archive (about 200 µmol). The extracted CO_2 gas for radiocarbon will be then converted to graphite catalytically on iron powder with pure hydrogen gas. The carbon-13 of the extracted CO_2 gas will be measured using Finnigan MAT252 mass spectrometer. The carbon-14 in the graphite sample will be measured by Accelerator Mass Spectrometry (AMS).

Table 3.7.1.1   The sampling stations and number of samples for carbon isotope ratios.

Station	No. samples	No. replicate samples	Max. sampling pressure /db
P01-010	36	2	6501
P01-019	34	2	5314
P01-027	34	2	5242
P01-066	36	2	5853
P01-072	34	2	5499
P01-X15	34	2	5430
P01-081	34	2	5324
P01-X16	33	2	5227
P01-X17	31	2	4742
P01-097	30	2	4399
P01-101	29	2	4202
P01-108	23	1	2752
Total	388	23	

References

Clayton T.D. and R.H. Byrne (1993) Spectrophotometric seawater pH measurements: total hydrogen ion concentrtaion scale calibration of m-cresol purple and at-sea results. Deep-Sea Research 40, 2115-2129.

Yao W. and R. H. Byrne (1998) Simplified seawater alkalinity analysis: Use of linear array spectrometers. Deep-Sea Research I 45, 1383-1392.

3.7.2 Radionuclides

draft as of 11 September, 2007

(1) Personnel

   Michio Aoyama (Meteorological Research Institute / Japan Meteorological Agency, Principal Investigator)

   Junji Matsushita (Department of Marine Science, Marine Works Japan Ltd.)

(2) Objectives

   . Study more about present distribution of ^{137}Cs in the subpolar region in the North Pacific Ocean originated mainly from atmospheric nuclear weapons tests conducted in the 1960s.

   . Provide detail artificial radionuclides database for general circulation model validation.

(3) Target radionuclides

Main target radionuclides are ^{137}Cs, and Pu.

(4) Sampling procedures

Sampling of seawater samples of radionuclides in water column were done followed that all parameters. The additional bottles were available by chance, then, the samples volumes for water column varied from 7 liter to 40 liter. Samples were drawn into 10 or 20 liter cubitainers from the Niskin bottles. Concentrated Nitric Acid was added to the samples to keep pH1.6.

Surface water samples were drawn through intake pump below several meters from the surface.

Seawater of 80 liter were collected for ^{137}Cs and Pu.

(5) Samples accomplished during the cruise

A total of 19 samples were collected for surface sample.

At the 15 stations, a total of 153 samples were collected for water column.

(6) Problem occurred and solutions.

No problem occurred.

(7) Sampling summary

Station#	Lat.	Long.	Sampling layer	Number of layers
6	42.485	145.84	Sur, 100-1000, 1930, 3182	9
11	41.71167	146.4117	Sur, 100-1000, 2070, 3080, 4080, 5080, 6500	12
18	40.12333	147.5633	Sur, 100-1000, 1930, 2930, 3920, 4920, 5379	12
22	40.32167	148.875	Sur, 100-1000, 2000, 3000, 4000, 5000, 5561	12
26	41.56167	150.8733	Sur, 100-1000, 2070, 3080, 4080, 5302	11
40	46.995	162.25667	Sur	1
44	47	166.74833	Sur	1
58	46.998333	176.095	Sur	1
60	47.00333	178.305	Sur	1
65	47.01167	183.9583	Sur, 100-1000, 1930, 2930, 3920, 4920, 5670, 5743.9	13
71	46.998333	190.65667	Sur, 100-1000, 1930, 2930, 3920, 4920, 5670, 5726	13
76	47.001667	196.28	Sur, 100-1000, 2070, 3080, 4080, 5294.1	11

82	47.00167	202.975	Sur, 100-1000, 2070, 3080, 4080, 5320.9	11
86	46.99167	207.4633	Sur, 100-1000, 1930, 2930, 3920, 4920, 5301.2	12
92	47	214.1917	Sur, 100-1000, 2000, 3000, 4000, 4881.4	11
96	46.99333	218.65	Sur, 100-1000, 2070, 3080, 4080, 4480.7	11
100	47	223.1517	Sur, 100-1000, 1930, 2930, 3920, 4228.3	11
104	47.001667	227.63833	Sur, 100-1000, 2000, 3000, 3286.6	10
109	46.99833	232.0783	Sur, 100-1000, 1930, 2724.0	9

100-1000 includes the layers of 100, 200, 400, 600, 800 and 1000 dbar

3.7.3 Nitrous oxide (N_2O), Methane (CH_4), Carbonyl sulfide (COS), and related substances
August 31, 2007

(1) Personnel

Osamu Yoshida[1], Kouhei Kawano[2], Tomohiro Miyafukuro[2], Sakae Toyoda[2], Keita Yamada[2], Keisuke koba[3], Yuichiro Ueno[4], Chisato Yoshikawa[2,5], and Naohiro Yoshida[2]*

[1] *Faculty of Environmental Systems, Rakuno Gakuen University*

[2] *Interdisciplinary Graduate School of Science and Engineering, Tokyo Institute of Technology*

[3] *Institute of Symbiotic Science and Technology, Tokyo University of Agriculture and Technology*

[4] *Global Edge Institute, Tokyo Institute of Technology*

[5] *Japan Society for the Promotion of Science*

* Principal Investigator

(2) Sampling elements

All sampling elements of Tokyo Institute of Technology and Rakuno Gakuen University group at hydrographic stations are listed below.

Table 1. Parameters and hydrographic station numbers for samples collection.

Parameters	Hydrographic station Numbers (WHP-P01)
1. Dissolved CH_4 (concentration)	1, 8, 12, 16, 21, 25, 40, 44, 58, 60, 62, 66, 70, 74, 79, 83, 87, 91, 95, 99, 105, 110, 114
2. Dissolved CH_4 (carbon isotope ratio)	1, 12, 21, 40, 58, 62, 70, 79, 87, 95, 105, 114
3. Dissolved N_2O (concentration and bulk isotope ratios)	1, 8, 12, 16, 21, 25, 40, 44, 58, 60, 62, 66, 70, 74, 79, 83, 87, 91, 95, 99, 105, 110, 114
4. Dissolved N_2O (isotopomers)	1, 12, 21, 40, 58, 62, 70, 79, 87, 95, 105, 114
5. Dissolved CH_4 (hydrogen isotope ratio)	1, 12, 21, 40, 58, 62, 70, 79, 87, 95, 105, 114
6. NO_3^- (isotope ratios)	1, 12, 21, 40, 58, 62, 70, 79, 87, 95, 105, 114
7. On-board incubation experiments (CH_4)	21, 40, 79
8. POM (isotope ratios)	1, 13, 21, 40, 58, 63, 70, 79, 87, 95, 105, 114
9. Chlorophyll *a*	1, 12, 21, 40, 58, 62, 70, 79, 87, 95, 105, 114
A. Air samples for air-sea flux of CH_4 and N_2O	1, 12, 21, 40, 58, 62, 70, 79, 87, 95, 105, 114
B. Concentration and sulfur isotope ratio of COS in the maritime air	1, 13, 22, 40, 58, 71, 87, 105, 114

(3) Nitrous oxide and related substances

Production, consumptions and air-sea flux of N_2O in the North Pacific Ocean

i. Introduction

Recently considerable attention has been focused on emission of biogenic trace gases from ecosystems, since the gases contain a significant amount of greenhouse gases such as carbon dioxide (CO_2), methane (CH_4) and nitrous oxide (N_2O). Isotopic signatures of these gases are well recognized to provide constraints for relative source strength and information on reaction dynamics concerning their formation and biological pathways. Nitrous oxide is a very effective heat-trapping gas in the atmosphere because it absorbs outgoing radiant heat in infrared wavelengths that are not captured by the other major greenhouse gases, such as water vapor and CO_2. The annual input of N_2O into the atmosphere is estimated to be about 16.4 Tg N_2O-N yr^{-1}, and the oceans are believed to contribute more than 17% of the total annual input (IPCC, 2001).

N_2O is produced by the biological processes of nitrification and denitrification (Dore et al., 1998; Knowles et al., 1981; Rysgaard et al., 1993; Svensson, 1998; Ueda et al., 1993). Depending on the redox conditions, N_2O is produced from inorganic nitrogenous compounds (NH_4 or NO_3^-), with subsequently different isotopic fractionation factors. The isotopic signatures of N_2O confer constraints on the relative source strength, and the reaction dynamics of N_2O biological production pathways are currently under investigation. Furthermore, isotopomers of N_2O contain more easily interpretable biogeochemical information as to their sources than obtained from conventional bulk ^{15}N and ^{18}O measurements (Yoshida and Toyoda, 2000).

The Pacific Ocean is the largest of the world's five oceans (followed by the Atlantic Ocean, Indian Ocean, Southern Ocean, and Arctic Ocean) (CIA, www) and expected to be important for the biogeochemical and biological cycles. Thus, the study of N_2O production and nutrients dynamics are very important to examine the origins of N_2O in seawater and to estimate the inventory of N_2O from this region with respect to the troposphere.

ii. Materials and methods

Samples were collected in the framework of MR07-04 research expedition on the *R/V Mirai* from July 24 to September 3, 2007. The purpose of the expedition was to study on the heat and material transports and their variability of the general ocean circulation and a study on chemical environment and its changes in the ocean. The production and consumption of dissolved N_2O in North Pacific was investigated by collecting seawater samples (12-23 stations), particulate organic matter (POM) (12 stations), samples for nitrate isotope ratios (12 stations) as shown in Table 1. The air Samples were sampled into pre-evacuated stainless-steel canisters (12 stations).

ii-a   Air-sea flux measurement

Concentration of N_2O at the surface water and ambient air will be measured using GC/C/IRMS at our laboratory.

ii-b N_2O concentration and isotope analyses

Water samplings were carried out at the indicated depths using a CTD water sampler. For N_2O analyses, water samples were introduced into two 125 ml glass vial and then sterilized with mercury chloride (100 μL saturated $HgCl_2$ solution per vial). The vial was then sealed with a butyl-rubber septum and an aluminum cap, taking care to avoid bubble formation, and then brought back to the laboratory and

stored at 4°C until the analyses were conducted. Dissolved N_2O concentrations and its isotopic compositions will be measured by using GC/C/IRMS.

ii-c Isotope ratios of POM

Water samples (3 L) for POM were collected at the depth of the chlorophyll *a* maximum and were filtrated through pre-combusted (450 °C, 4h) glass fiber filters (GF/F). The particles collected on the filter were stored at -30°C. Frozen particles were treated with 0.05 N hydrochloric acid, washed with Milli-Q water and then dried at 60°C for 48 hrs. Isotope ratios of POM will be measured by using EA/IRMS.

ii-d Isotope ratios of NO_3^-

For isotopic measurement of NO_3^-, water samples were collected in the same depth as N_2O concentration and isotope analyses. The water samples were filtrated using pre-combustion GF/F filter then collected in 60 ml polypropylene bottles and then sterilized with 1 mol l^{-1} NaOH (0.5 ml per vial). Isotope ratios of NO_3^- will be measured by using the chemical reduction method (Boontanon and Yoshida, 2004) and GC/C/IRMS

iii. Expected results

In the surface layer, N_2O concentration of water affects the sea-air flux directly (Dore et al., 1998). However the pathway of N_2O production in surface layer is also still unresolved. Usually N_2O production in surface layer is predominantly carried out nitrification, but denitrification also occurs in the case of oxygen concentration is low (Maribeb and Laura, 2004). Moreover it was reported that N_2O production by nitrification has photoinhibition (Olson, 1981). Therefore, this study is expected to reveal the pathway of N_2O production and N_2O production rate in the surface layer (especially euphotic zone).

In deeper layer during the settling particles or fecal pellets which may produce from phytoplankton or zooplankton, either directly or indirectly. In such pattern, N_2O could be produced through *in situ* biological processes of settling particles in subsurface layer and the maxima concentrations could be observed. Consequently, the isotopic measurement of these gases becomes a useful parameter for determining the origin and production pathway of N_2O under investigation. Additional, Pacific Ocean expected to be the large site of N_2O source to the troposphere. And at least three factors could be control the N_2O concentration and its isotopic compositions in these study areas are:

(a) The isotopic compositions of dissolved N_2O were governed through the gas exchange with the atmospheric N_2O in the surface layer.

(b) The N_2O production in subsurface layer through *in situ* biological processes and it should related to the isotopic compositions of POM and NO_3^-.

(c) The well mixing of N_2O in the deeper part may occur due to the transportation from upper layer or the transportation of N_2O from the other area by the occurrence of ocean current.

(d) The isotopic and isotopomeric compositions of surface and oxycline N_2O (tracer studies) could provide an information of N_2O production pathway especially in euphotic zone, and could be estimate for those N_2O production rate.

Furthermore, the relationship between the POM, N_2O production as well as N_2O isotope ratios and oxygen concentration in the surrounding water may be critically important for N_2O metabolism through nitrification, denitrification and coupling of nitrification-denitrification, because the O_2 gradient within the particle is likely to be regulated by the size of POM.

iv. References

Boontanon, N. and Yoshida, N.: Nitrogen and oxygen isotopic determination of nitrate by chemical reduction. *In* Proceedings of 2nd International Symposium on Isotopomers. Stresa, Italy, 208-211, 2004.

Campbell, L., Hongbin, L., Hector, A.N. and Vaulot, D.: Annual variability of phytoplankton and bacteria in the subtropical North Pacific Ocean at station ALOHA during the 1991-1994 ENSO event. Deep-Sea Research I, 44, 167-192, 1997.

Cohen, Y. and Gordon, L.I.: Nitrous oxide in the oxygen minimum of the eastern tropical North Pacific: evidence for its consumption during denitrification and possible mechanisms for its production. Deep Sea Research, 25, 509-524, 1978.

Dore, J.E., Popp, B.N., Karl, D.M. and Sansone, F.J.: A large source of atmospheric nitrous oxide from subtropical North Pacific surface water, Nature, 396, 63-66, 1998.

Intergovernmental Panel on Climate Change, Climate Change 2001.: The Scientific Basis. Contribution of Working Group I to the Third Assessment Report of the Intergovernmental Panel on Climate Change (IPCC), Cambridge Univ. Press, New York, 2001.

Knowles, R., Lean, D.R.S. and Chan, Y.K.: Nitrous oxide concentrations in lakes: variations with depth and time, Limnology and Oceanography, 26, 855-866, 1981.

Maribeb, C.-G. and Laura, F.: N_2O cycling at the core of the oxygen minimum zone off northern Chile, Marine Ecology Progress Series, 280, 1-11, 2004.

Olson, R.J.: Differential photoinhibition of marine nitrifying bacteria: a possible mechanism for the formation of the primary nitrite maximum, Journal of Marine Research, 39, 227-238, 1981.

Rysgaard, S., Risgaard-Petersen, N., Nielsen, L.P. and Revsbech, N.P.: Nitrification and denitrification in lake and estuarine sediments measured by the ^{15}N dilution technique and isotope pairing, Applied and Environmental Microbiology, 59, 2093-2098, 1993.

Svensson, J.M.: Emission of N_2O, nitrification and denitrification in a eutrophic lake sediment bioturbated by Chironomus plumosus, Aquatic Microbial Ecology, 14, 289-299, 1998.

Ueda, S., Ogura, N. and Yoshinari, T.: Accumulation of nitrous oxide in aerobic ground water, Water Research, 27, 1787-1792, 1993

www.cia.gov/cia/publications/factbook/geos/zn.html

Yoshida, N. and Toyoda, S.: Constraining the atmospheric N_2O budget from intramolecular site preference in N_2O isotopomers, Nature, 405, 330-334, 2000.

(4) Methane

Methane concentration and stable isotopic distribution as indicators of biogenic methane dynamics in the northern North Pacific Ocean

i. Dissolved CH_4
i-a Introduction

Atmospheric methane (CH_4) is a trace gas playing an important role in the global carbon cycle as a greenhouse gas. Its concentration has increased by about 1050 ppbv from 700 ppbv since the pre-industrial era (IPCC, 2001). In order to understand the current global methane cycle, it is necessary to quantify its sources and sinks. At present, there remain large uncertainties in the estimated methane fluxes from sources to sinks. The ocean's source strength for atmospheric methane should be examined in more detail, even though it might be a relatively minor source, previously reported to be 0.005 to 3% of the total input to the atmosphere (Cicerone and Oremland, 1988; Bange et al., 1994).

To estimate an accurate amount of the methane exchange from the ocean to the atmosphere, it

is necessary to explore widely and vertically. Distribution of dissolved methane in surface waters from diverse locations in the world ocean is often reported as a characteristic subsurface maximum representing a supersaturation of several folds (Yoshida et al., 2004). Although the origin of the subsurface methane maximum is not clear, some suggestions include advection and/or diffusion from local anoxic environment nearby sources in shelf sediments, and in situ production by methanogenic bacteria, presumably in association with suspended particulate materials (Karl and Tilbrook, 1994). These bacteria are thought to probable live in the anaerobic microenvironments supplied by organic particles or guts of zooplankton (Alldredge and Cohen, 1987).

So, this study investigates in detail profile of methane concentration and stable isotopic distribution in the water column in the North Pacific Ocean to clarify methane dynamics and estimate the flux of methane to the atmosphere.

i-b Materials and methods

Seawater samples are taken by CTD-CAROUSEL system attached Niskin samplers of 12 L at 5-23 layers and surface layer taken by plastic bucket at 12-23 hydrographic stations as shown in Table 1. Each sample was carefully subsampled into 30, 125, 600 ml glass vials to avoid air contamination for analysis of methane concentration, carbon isotope ratio, and hydrogen isotope ratio respectively. The seawater samples were poisoned by 20 μl (30 and 125 ml vials) or 100 μl (600 ml vial) of mercuric chloride solution (Tilbrook and Karl, 1995; Watanabe et al., 1995), and were closed with rubber and aluminum caps. These were stored in a dark and cool place until we got to land, where we conducted gas chromatographic analysis of methane concentration and mass spectrometric analysis of carbon and hydrogen isotopic composition at the laboratory.

The analytical method briefly described here: The system consists of a purge and trap unit, a desiccant unit, rotary valves, a gas chromatograph equipped with a flame ionization detector for concentration of methane, GC/C/IRMS for carbon isotope ratio of methane, GC/TC/IRMS for hydrogen isotope ratio of methane, and data acquisition units. The entire volume of seawater in each glass vial was processed all at once to avoid contamination and loss of methane. Precision obtained from replicate determinations of methane concentration was estimated to be better than 5% for the usual concentration of methane in seawater.

i-c Expected results

Subsurface maximum concentrations of methane (>3 nmol kg^{-1}) were expected to be observed in the North Pacific Ocean. A commonly-encountered distribution in the upper ocean with a methane peak within the pycnocline (e.g., Ward et al., 1987; Owens et al., 1991; Watanabe et al., 1995). Karl and Tilbrook (1994) suggested the suboxic conditions would further aid the development of microenvironments within particles in which methane could be produced. The organic particles are accumulated in the pycnocline, and methane is produced in the micro reducing environment by methanogenic bacteria. Moreover, in situ microbial methane production in the guts of zooplankton can be expected (e.g., Owens et al., 1991; de Angelis and Lee, 1994; Oudot et al., 2002). Watanabe et al. (1995) pointed out that the diffusive flux of methane from subsurface maxima to air-sea interface is sufficient to account for its emission flux to the atmosphere. In the mixed layer above its boundary, the methane is formed and discharged to the atmosphere in part, in the below its boundary, methane diffused to the bottom vertically. By using concentration and isotopic composition of methane and hydrographic parameters for vertical water samples, it is possible to clarify its dynamics such as production and/or consumption in the water column.

Kelley and Jeffrey (2002) observed in the equatorial upwelling region of 10 and 20%

supersaturated methane. Rehder et al. (2002) reported that the enhancement of methane fluxes to the atmosphere in regions of coastal upwelling is likely to occur on a global scale. In this study, the combination of in situ methane production and coastal upwelling result in the property distributions and large methane flux in the eastern North Pacific can be expected.

Tsurushima et al. (1996) reported that methane flux in the East China Sea was somewhat larger than the oceanic usual values. Remarkable supersaturation in coastal regions, including continental shelf zones, has been expected related to biological productivity, advection from nearby sources in shelf sediments, and diffusion and/or advection from local anoxic environments.

ii. CH_4 on-board incubation experiments
ii-a Introduction

Typical methane (CH_4) concentrations in open ocean waters are nanomolar throughout the depth distribution and are maximum in surface mixed layer above the pycnocline. Supersaturation in the mixed layer maximum with respect to the atmosphere have been observed widely (e.g., Lamontagne et al., 1973; Burke et al., 1983). The supersaturations observed in the open ocean indicate the CH_4 production in the surface mixed layer. Bacterial CH_4 production occurs only under strict anoxic condition, so CH_4 supersaturation in the mixed layer is termed the "Ocean Methane Paradox" (Kiene, 1991). Methanogenic bacteria with the potential to produce CH_4 under anoxic conditions were observed in fish intestines and plankton samples (Oremland, 1979), and in sinking particulate matter and zooplankton fecal pellets (Bianchi et al., 1992, Marty, 1993). On the basis of these observations, at present, a mechanism for producing CH_4 in anoxic microenvironment of fecal pellet and releasing CH_4 into the ocean mixed layer is suggested for CH_4 supersaturation in the mixed layer (e.g., Karl and Tilbrook, 1994, Holmes et al., 2000). The fecal pellet microenvironment hypothesis provides a good first-order explanation of the mixed layer CH_4 maximum, but a number of questions remain.

Alternatively, non-biological CH_4 production in seawater via a photochemical pathway has been argued. Wilson et al. (1970) investigated photochemical CH_4 production in seawater and distilled water augmented with natural dissolved organic carbon, but found CH_4 production in only 2 out of 15 experiments. Tilbrook and Karl (1995) observed CH_4 production in irradiation experiments with sea water from the Pacific Ocean and ascribed this CH_4 formation to an as yet unknown, possibly photochemical, production pathway. Bange and Uher (2005) conducted irradiation experiments with marine water to investigate the possibility of photochemical CH_4 formation. They concluded that photochemical formation is negligible in the present ocean, based on their results indicating that CH_4 photoproduction was undetectable under oxic conditions or in the absence of methyl radical precursors.

In this study, we reevaluate the potential for photochemical CH_4 formation by conducting on-board incubation experiments using surface seawater. Recently, CH_4 production under aerobic conditions was found for terrestrial ecosystems (Keppler et al., 2006). This finding is our motivation to reevaluate the potential for photochemical CH_4 formation in surface sea water.

ii-b Materials and methods

Water samples for on-board incubation experiments were collected at the depths of chlorophyll *a* maximum. The samples are divided into three 125 ml glass vials.

Two vials are sterilized with mercury chloride. One vial is stored at dark place until analyses ($Vial_{CH4-dark}$), and the other is irradiated for ~7-10 days and then stored at dark place until analyses ($Vial_{CH4-irradiated}$). Dissolved CH_4 concentrations and its carbon isotopic compositions will be measured by GC/C/IRMS.

2 ml of distilled water saturated with CH_2F_2 is added to the remaining one vial due to deactivate

bacterial CH_4 oxidation. After 7 days incubation, the vial is sterilized with mercury chloride and stored at dark place until analyses ($Vial_{CH4-ox-deactivated}$).

ii-c Expected results

First, the difference in concentration for $Vial_{CH4-dark}$ and $Vial_{CH4-irradiated}$ will be analyzed to determine the potential for photochemical CH_4 formation. If the difference can be recognized, carbon isotopic measurement will be performed to determine the isotopic signature for photochemical CH_4.

Second, the difference in concentration for $Vial_{CH4-dark}$, $Vial_{CH4-irradiated}$ and $Vial_{CH4-ox-deactivated}$ will be analyzed to determine the net bacterial CH_4 production. If the difference can be recognized, carbon isotopic measurement will be performed to determine the isotopic signature for bacterial CH_4.

ii-d References

Alldredge, A. A., Y. Cohen: Can microscale chemical patches persist in the sea? Microelectrode study of marine snow, fecal pellets, Science, 235, 689-691, 1987.

Bange, H. W., U. H. Bartell, S. Rapsomanikis, and M. O. Andreae: Methane in the Baltic and the North seas and a reassessment of the marine emissions of methane, Global Biogeochem. Cycles, 8, 465–480, 1994.

Bange, H.W., and G. Uher: Photochemical production of methane in natural waters: implications for its present and past oceanic source, Chemosphere, 58, 177-183, 2005.

Burke, R.J., Jr., D.F. Reid, J.M. Brooks, and D.M. Lavoie: Upper water column methane geochemistry in the eastern tropical North Pacific, Limnol. Oceanogr., 28, 19–32, 1983.

Cicerone, R. J., and R. S. Oremland: Biogeochemical aspects of atmospheric methane, Global Biogeochem. Cycles, 2, 299–327, 1988.

de Angelis, M. A., and C. Lee: Methane production during zooplankton grazing on marine phytoplankton, Limnol. Oceanogr., 39, 1298-1308, 1994.

Holmes, E., F.J. Sansone, T.M. Rust, and B.N. Popp: Methane production, consumption, and air-sea exchange in the open ocean: An evaluation based on carbon isotopic ratios. Global Biogeochem. Cycles, 14, 1-10, 2000.

IPCC (Intergovernmental Panel on Climate Change), Climate Change 1995, in The Science of Climate Change, edited by J. T. Houghton, L. G. M. Filho, B. A. Callander, N. Harris, A. Kattenberg, and K. Maskell, Cambridge Univ. Press, New York.

Karl, D. M., and B. D. Tilbrook: Production and transport of methane in oceanic particulate organic matter, Nature, 368, 732–734, 1994.

Kelley C. A. and Jeffrey, W. H.: Dissolved methane concentration profiles and air-sea fluxes from 41S to 27N. Global. Biogeochem. Cycle, 16, No.3, 10.1029/2001GB001809, 2002.

Keppler, F., J.T.G. Hamilton, M. Brass, and T. Roeckmann: Methane emissions from terrestrial plants under aerobic conditions, Nature, 439, 187-191, 2006.

Kiene, R.P.: Production and consumption of methane in aquatic systems, In Microbial Production and Consumption of Greenhouse Gases: Methane, Nitrogen Oxide, Halomethanes; Rogeres, J.E., Whitman, W.B., Eds., American Society for Microbiology, Washinfton, DC, 111-146, 1991.

Lamontagne, R.A., J.W. Swinnerton, V.J. Linnenbom, and W.D. Smith: Methane concentration in various marine environment, J. Geophys. Res., 78, 5317–5324, 1973.

Oremland, R.S.: Methanogenlc activity in plankton samples and fish intestines: A mechanisms for*in situ* methanogenesis in oceanic surface water , Limnol. Oceanogr., 24, 1136–1141, 1979.

Oudot, C., P. Jean-Baptiste, E. Fourre, C. Mormiche, M. Guevel, J-F. Ternon, and P. L. Corre: Transatlantic equatorial distribution of nitrous oxide and methane, Deep-Sea Res., Part I, 49,

1175–1193, 2002.

Owens, N. J. P., C. S. Law, R. F. C. Mantoura, P. H. Burkill, and C. A. Llewellyn: Methane flux to the atmosphere from the Arabian Sea, Nature, 354, 293–296, 1991.

Rehder, G., R. W. Collier, K. Heeschen, P. M. Kosro, J. Barth, and E. Suess: Enhanced marine CH4 emissions to the atmosphere off Oregon caused by coastal upwelling, Global Biogeochem. Cycles, 16, 10.1029/2000GB001391, 2002.

Tilbrook, B. D., and D. M. Karl: Methane sources, distributions and sinks from California coastal waters to the oligotrophic North Pacific gyre, Mar. Chem., 49, 51–64, 1995.

Tsurushima, N., S. Watanabe, N. Higashitani, and S. Tsunogai: Methane in the East China Sea water, J. Oceanogr., 52, 221–233, 1996.

Ward, B. B., K. A. Kilpatrick, P. C. Novelli, and M. I. Scranton: Methane oxidation and methane fluxes in the ocean surface layer and deep anoxic waters, Nature, 327, 226–229, 1987.

Watanabe, S., N. Higashitani, N. Tsurushima, and S. Tsunogai: Methane in the western North Pacific, J. Oceanogr., 51, 39–60, 1995.

Wilson, D.F., J.W. Swinnerton, and R.A. Lamontagne: Production of carbon monoxide and gaseous hydrocarbons in seawater: relation to dissolved organic carbon. Science, 168, 1577-1579, 1970.

Yoshida, O., H. Y. Inoue , S. Watanabe, S. Noriki, M. Wakatsuchi: Methane in the western part of the Sea of Okhotsk in 1998-2000, J. Geophys. Res., 109, C09S12, doi:10.1029/2003JC001910, 2004.

(5) Carbonyl sulfide

i. Introduction

Carbonyl sulfide (COS) is the most abundant (about 500 pptv) and most stable (life time is about 16 years) gaseous sulfur species in the background (remote) atmosphere. It is oxidized in the stratosphere to form sulfate aerosols which may influence the radiation budget at the Earth's surface and the stratospheric ozone cycle (Crutzen, 1976). It is emitted from natural sources such as microbial metabolism of sulfur in the ocean and terrestrial environment and anthropogenic sources such as sulfur industry and combustion of fossil fuel and biomass (Chin and Davis, 1993; Watts, 2000; Kettle et al., 2002). Its major sinks are considered to be soil and plant uptake, reaction with OH and OD radials, and photolysis in the stratosphere. However, estimated fluxes of the sources have large uncertainty because they are based on limited observations of COS concentration, and COS budget has not been closed yet. Therefore, isotopic study of COS may provide constraints for relative source strength as well as information on reaction pathways in its formation and destruction processes. Sulfur isotope ratio of COS in the atmosphere or source gasses has not been reported so far, although there is a study on sulfur isotope fractionation in the stratospheric COS which suffers from low analytical precision by balloon-born infrared spectroscopy (Leung et al., 2002).

In this study, we are developing a high-sensitive, high-precision, and rapid analytical system for concentration and sulfur isotope ratios of COS that is applicable to trace COS in environment. Our purpose of this cruise is to collect maritime air samples which contain background COS or COS emitted from nearby oceanic sources for the isotopic analysis.

ii. Materials and methods

Samples were collected in the framework of MR07-04 research expedition on the *R/V Mirai* from July 24 to September 3, 2007.

ii-a COS-concentration and sulfur isotope analysis

Air samples were collected at 9 stations listed in Table 1. At each station, ambient air near the bridge (about 10 m above sea level) was pressurized into a 1 L glass bottle and two stainless-steel canisters at 2-4 atm (absolute pressure) using a sampling device which consists of a diaphragm pump, a back-pressure regulating valve, a desiccant tube packed with $Mg(ClO_4)_2$, and stainless tubes and connectors. Inner surface of the SS canisters are deactivated to prevent COS adsorption or decomposition during sample storage.

iii. Expected results

First, concentration analysis will be performed to determine the sample size and detail procedure for isotopic measurement. Then, stability of COS in the glass bottle and canister will be checked by periodic analysis of concentration using an aliquot of the same sample. Finally, sulfur isotope ratio will be measured by the newly developed analytical system. If succeeded, sulfur isotope ratio of atmospheric COS will be revealed for the first time.

iv. References

Crutzen, P. J.: The possible importance of OCS for the sulfate layer of the stratosphere, Geophys. Res. Lett., 3, 73-76, 1976.

Chin, M., and D. D. Davis: Global sources and sinks of OCS and CS2 and their distributions, Global Biogeochem. Cycles, 7 (2), 321-337, 1993.

Kettle, A. J., U. Kuhn, M. von Hobe, J. Kesselmeier, and M. O. Andreae: Global budget of atmospheric carbonyl sulfide: Temporal and spatial variations of the dominant sources and sinks, J. Geophys. Res., 107 (D22), 4658, 2002.

Leung, F.-Y., A. J. Colussi, and M. R. Hoffmann: Isotopic fractionation of carbonyl sulfide in the atmosphere: Implications for the sources of background stratospheric sulfate aerosol, Geophys. Res. Lett., 29 (10), 1474, 2002.

Watts, S. F.: The mass budgets of carbonyl sulfide, dimethyl sulfide, carbon disulfide and hydrogen sulfide, Atmos. Environ., 34, 761-779, 2000.

(6) Chlorophyll *a*
i. Personnel

Osamu Yoshida[1], Kouhei kawano[2], Tomohiro Miyafukuro[2], Naohiro Yoshida[2], and Yuichi Sonoyama[3]*

[1] Faculty of Environmental Systems, Rakuno Gakuen University

[2] Interdisciplinary Graduate School of Science and Engineering, Tokyo Institute of Technology

[3] Department of Marine Science, MARINE WORKS JAPAN LTD

* Principal Investigator

ii. Objective

Chlorophyll *a* is one of the most convenient indicators of phytoplankton stock, and has been used extensively for the estimation of phytoplankton abundance in various aquatic environments. The object of this study is to investigate the vertical distribution of phytoplankton in various light intensity depth.

iii. Sampling elements

Chlorophyll *a*

iv. Materials and Methods

   Seawater samples were collected 0.5 L at 6 depths from surface to about 200 m with Niskin bottles, except for the Surface water, which was taken by the bucket. The samples were gently filtrated by low vaccum pressuer (<15 cmHg) through Whatman GF/F filter (diameter 25 mm) in the dark room. Phytoplankton pigments were immediately extracted in 7 ml of N,N-dimethylformamide (DMF) after filtration and then, the samples were stored at -20°C under the dark condition to extract chlorophyll a for 24 hours or more. The extracted samples are measured the fluorescence by Turner fluorometer (10-AU-005, TURNER DESIGNS) which was previously calibrated against a pure chlorophyll a (Sigma chemical Co.). We applied the fluorometric "Non-acidification method" (Welschmeyer, 1994)

v. Results
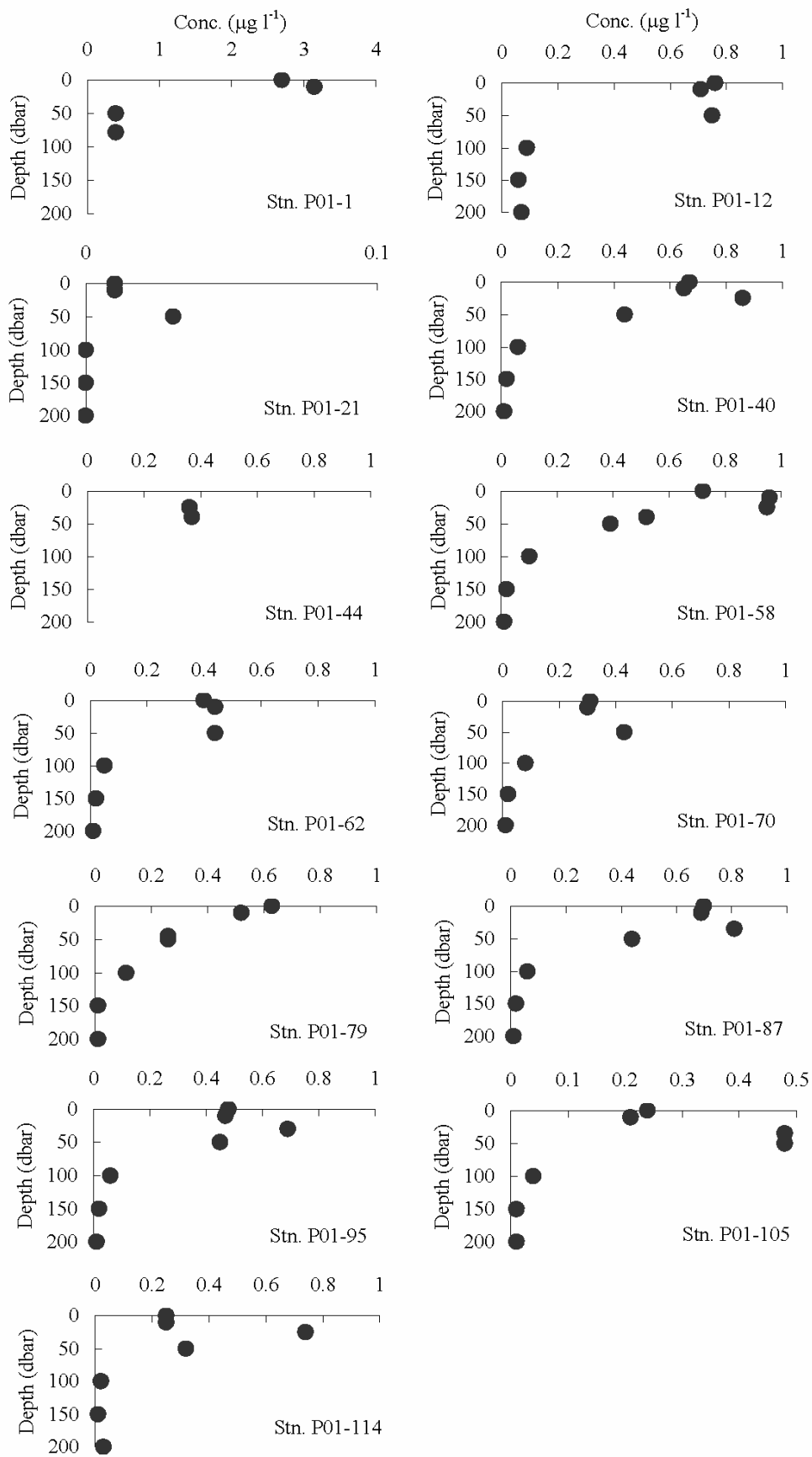
   The results of Chlorophyll a were shown in Figure 1.

Figure 1. The vertical distributions of chlorophyll *a* at MR07-04.

vii. Reference

Welschmeyer, N. A.: Fluorometric analysis of chlrophyll *a* in the presence of chlorophyll *b* and pheopigments. Limno. Oceanogr., 39, 1985-1992, 1994.

3.8 LADCP(Lowered Acoustic Doppler Current Profiler)

(1) Personnel

Shinya Kouketsu (IORGC)

Hiroshi Uchida (IORGC)

(2) Instrument and method

Direct flow measurement from sea surface to the bottom was carried out using a lowered acoustic Doppler current profiler (LADCP). The instrument was the RDI Workhorse Monitor 307.2kHz unit (RD Instruments, USA). Its serial number is 8484. The instrument was attached on the CTD/RMS frame, orientating downward. The CPU firmware version was 16.28.

One ping raw data were recorded. The bin length of 8m. A total of 87 operations were made with the CTD observations in this cruise. Since the pressure resistance of the instrument is 6000m, the instrument was detached on the CTD/RMS frame at St. 11, 12. The performance of the LADCP instrument was good. Profiles were obtained over 100m distance from LADCP in shallow depth and almost 60m in deeper depth.

An inversion method of processing LADCP data in Visbeck (2002) was adopted. GPS navigation data and bottom-track velocities were used in the calculation for constraints. CTD data were used for the sound speed and depth calculation. Shipboard ADCP data are not included in the calculation. Although the echo intensity and correlation are enough large to estimate the velocity in the deep layer, the error velocities are large. This is because the setting of the bin for ensemble average is large in order to calculate with the less computer resource.

(3) Preliminary results

Figures from 3.8.1 to 3.8.3 show the eastward, northward, and error velocity fields. Error velocities estimated by the inversion are large values of 0.05 – 0.5m/s, since the ensemble average bin is set to the large value of 20m in order to calculate the velocity with a note PC. The error velocity is large near the surface may be due to including a lot of outlier data in this calculation.

So we will re-calculate with the proper settings for the inversion method with shipboard ADCP data.

Reference

Visbeck, M. (2002): Deep velocity profiling using Lowered Acoustic Doppler Current Profilers: Bottom track and inverse solutions. *J. Atmos. Oceanic Technol.*, 19, 794-807.
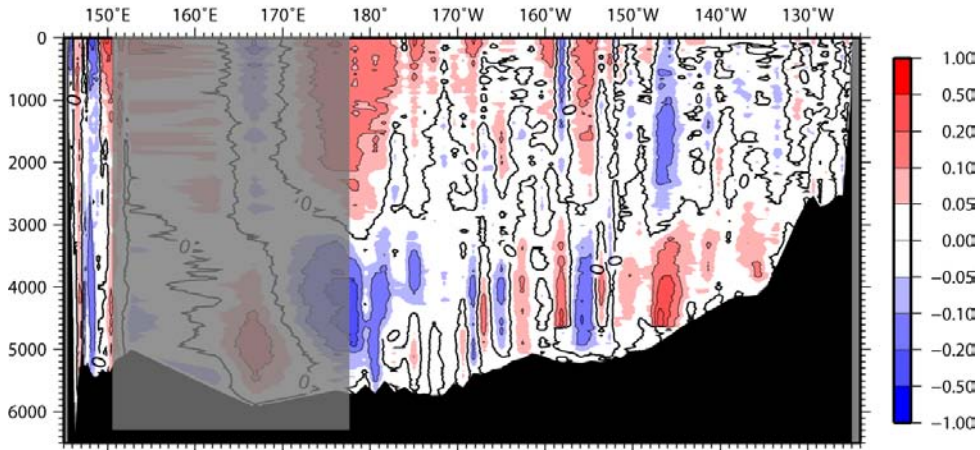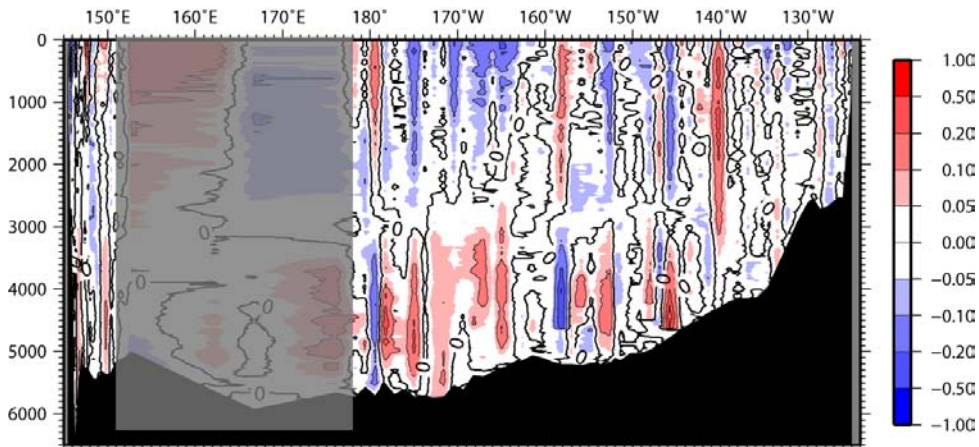
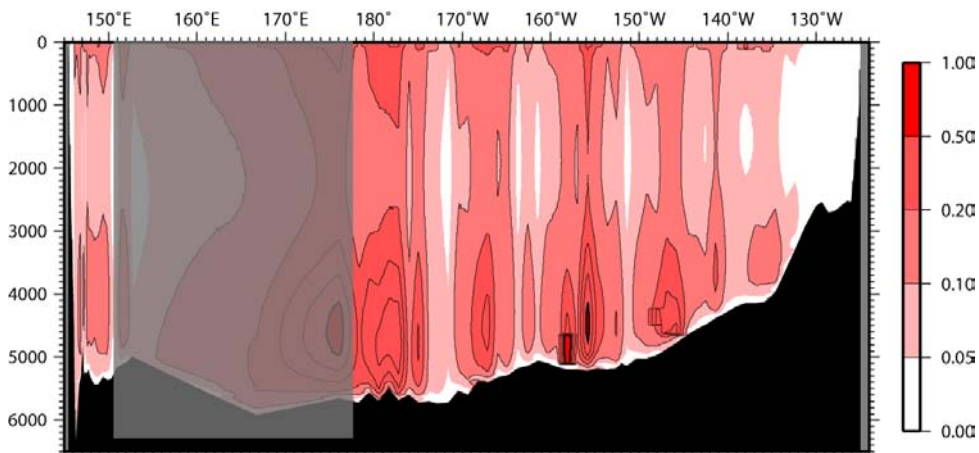Figure 3.8.1 Eastward velocity

Figure 3.8.2 Northward velocity

Figure 3.8.3 Error velocity

3.9 XCTD

September 1, 2007

(1) Personnel

Hiroshi Uchida (JAMSTEC)

Satoshi Okumura (GODI)

Shinya Okumura (GODI)

Ryo Ohyama (GODI)

(2) Objectives

In this cruise, XCTD (eXpendable Conductivity, Temperature and Depth profiler) measurement was carried out to understand upper ocean density structure at CTD stations skipped over.

(3) Instrument and Method

The XCTD used was XCTD-1 (Tsurumi-Seiki Co., Ltd., Yokohama, Kanagawa, Japan) with a MK-100 deck unit (Tsurumi-Seiki Co., Ltd.). Ship's speed was slowed down to 12 knot during the XCTD measurement. The manufacturer's specifications are as follows.

Parameter	Range	Accuracy
Conductivity	$0 \sim 60$ mS cm^{-1}	± 0.03 mS cm^{-1}
Temperature	$-2 \sim 35$ °C	± 0.02 °C
Depth	$0 \sim 1000$ m	

In this cruise, 17 XCTD-1 probes were deployed by using 8-loading automatic launcher (Tsurumi-Seiki Co., Ltd.), except for stations 42, 51, 53, 54, 55, 56, and 57 which were deployed by using hand launcher from the stern of the upper deck.

(4) Data Processing and Quality Control

The followings are the data processing sequence and specifications used in the reduction of XCTD data in this cruise.

1. Data considerably deeper than depth range of the manufacturer's specifications and spikes were manually removed.

2. Missing data by the above editing was linearly interpolated when the data gap was within 15 scans (about 2 m).

3. Temperature and conductivity data were low-pass filtered (running mean with a window of 15 scans).

4. The conductivity data was advanced for 2 scans (about 0.3 m) relative to the temperature data to correct mismatch of response time of the sensors.

5. Pressure was estimated from depth and location (latitude) by calculating backward from a pressure to depth conversion equation (Saunders and Fofonoff, 1976), and salinity was calculated from the pressure, temperature and conductivity data by using the reference conductivity of 42.896 mS cm^{-1} at salinity of 35, temperature of 15 °C (IPTS-68) and pressure of 0 dbar. The reference conductivity value is used in the manufacturer's data processing software.

6. Data was sampled at 1 dbar interval.

7. Salinity bias of the XCTD data was estimated by using tight relationship between temperature and salinity in the deep ocean. Mean salinity at in-situ temperature of 2.75 °C was 34.398 (mean pressure was 993 dbar) for the CTD data of four stations (40, 44, 58, and 60). Difference between XCTD salinity and the mean salinity at temperature of 2.75 °C was considered to be salinity bias of

the XCTD data.

For the XCTD data of station 51, salinity bias could not be estimated because the maximum pressure was too small to estimate. Maximum pressure and the offset correction value to the salinity data with ship intake temperature (SST) and salinity (SSS) are listed below.

Station	Original file name	SST [°C]	SSS [PSU]	Max. pressure [dbar]	Salinity offset [PSU]
41	200708120849.XCT	10.725	32.974	1045	0.009
42	200708121152.XCT	10.580	32.857	1044	0.014
43	200708121449.XCT	10.048	32.835	1044	0.027
45	200708130043.XCT	9.656	32.801	1045	0.032
46	200708130214.XCT	9.676	32.858	1044	0.009
47	200708130358.XCT	9.892	32.858	1044	0.009
48	200708130421.XCT	9.988	32.840	1044	0.024
49	200708130438.XCT	10.116	32.794	1043	0.026
50	200708130548.XCT	10.074	32.782	1044	0.004
51	200708130637.XCT	10.000	32.798	484	-
52	200708130716.XCT	10.100	32.739	1045	0.015
53	200708130834.XCT	10.293	32.755	1045	0.030
54	200708131141.XCT	10.774	32.756	1045	0.023
55	200708131438.XCT	10.788	32.719	1045	0.025
56	200708131734.XCT	10.858	32.735	1045	0.024
57	200708132034.XCT	11.579	32.797	1045	0.009
59	200708140835.XCT	11.560	32.770	1044	0.013

(5) Results

Vertical section of potential temperature and salinity from XCTD is shown in Fig. 3.9.1 combining with CTD data of four stations (40, 44, 58, and 60). Relationship between potential temperature and salinity is also shown in Fig. 3.9.2 with the CTD data.

Reference

Saunders, P. M. and N. P. Fofonoff (1976): Conversion of pressure to depth in the ocean. *Deep-Sea Res.*, **23**, 109-111.
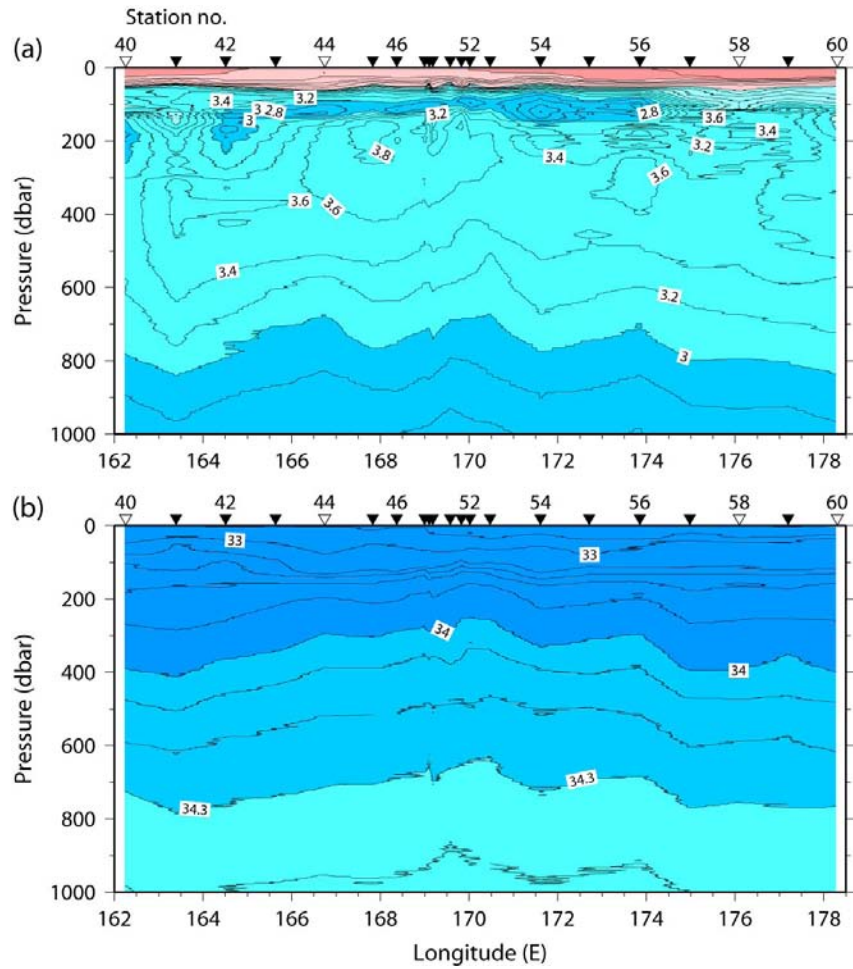
Fig. 3.9.1 Vertical section of (a) potential temperature and (b) salinity. Filled triangles (open triangles) show station locations of XCTD (CTD).
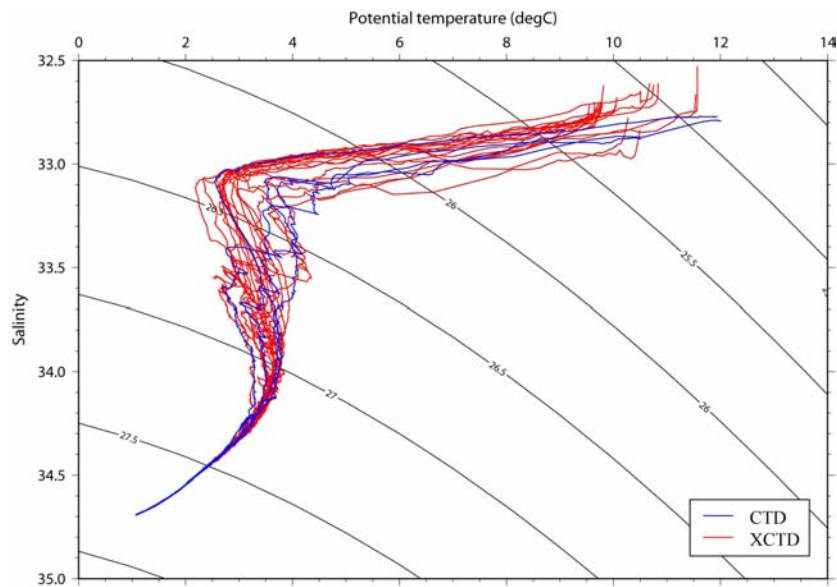

Fig. 3.9.2 Potential temperature plotted against salinity from station P01_40 to 60.

4.1 Argo floats

(1) Personnel

Toshio Suga	(IORGC): Principal Investigator (not on board)
Nobuyuki Shikama	(IORGC): not on board
Kanako Sato	(IORGC): not on board
Mizue Hirano	(IORGC): not on board
Satoshi Ozawa	(MWJ): Technical Staff
Tomoyuki Takamori	(MWJ): Technical Staff
Kenichi Katayama	(MWJ): Technical Staff

(2) Objectives

The objective of deployment is to clarify the structure and temporal/spatial variability of water masses in the North Pacific such as temperature inversions in the subarctic North Pacific.

The profiling floats launched in this cruise measure vertical profiles of temperature and salinity automatically every ten days.   The data from the floats will enable us to understand the phenomenon mentioned above with time/spatial scales much smaller than in previous studies.

(3) Parameters

water temperature, salinity, and pressure

(4) Methods

i. Profiling float deployment

We launched an APEX float manufactured by Webb Research Ltd.   These floats equip an SBE41 CTD sensor manufactured by Sea-Bird Electronics Inc.

The floats usually drift at a depth of 1000 dbar (called the parking depth), diving to a depth of 2000 dbar and rising up to the sea surface by decreasing and increasing their volume and thus changing the buoyancy in ten-day cycles. During the ascent, they measure temperature, salinity, and pressure.   They stay at the sea surface for approximately nine hours, transmitting the CTD data to the land via the ARGOS system, and then return to the parking depth by decreasing volume.   The status of floats and their launches are shown in Table 4.1.1.

Table 4.1.1 Status of floats and their launches

Float

Float Type	APEX floats manufactured by Webb Research Ltd.
CTD sensor	SBE41 manufactured by Sea-Bird Electronics Inc.
Cycle	10 days (approximately 9 hours at the sea surface)
ARGOS transmit interval	30 sec
Target Parking Pressure	1000 dbar
Sampling layers	110 (1950, 1900, 1850, 1800, 1750, 1700, 1650, 1600, 1550, 1500, 1450, 1400, 1350, 1300, 1250, 1200, 1150, 1100, 1050, 1000, 975, 950, 925, 900, 875, 850, 825, 800, 775, 750, 725, 700, 675, 650, 625, 600, 580, 560, 540, 520, 500, 490, 480, 470, 460, 450, 440, 430, 420, 410, 400, 390, 380, 370, 360, 350, 340, 330, 320, 310, 300, 290, 280, 270, 260, 250, 240, 230, 220, 210, 200, 195, 190, 185, 180, 175, 170, 165, 160, 155, 150, 145, 140, 135, 130, 125, 120, 115, 110, 105, 100, 95, 90, 85, 80, 75, 70, 65, 60, 55, 50, 45, 40, 35, 30, 25, 20, 15, 10, 4 dbar)

Launches

Float S/N	ARGOS ID	Date and Time of Reset (UTC)	Date and Time of Launch(UTC)	Location of Launch	CTD St. No.
2811	66102	2007/8/16 23:53	2007/8/17 00:58	46-59.46 [N] 172-41.04[W]	P01-068
2804	66095	2007/8/18 09:48	2007/8/18 12:12	46-59.34 [N] 167-04.38[W]	P01-073
2352	60118	2007/8/22 23:55	2007/8/23 01:32	46-59.69 [N] 151-24.37[W]	P01-087
3050	70495	2007/8/24 01:49	2007/8/24 03:51	46-59.35 [N] 146-55.35[W]	P01-091
3049	70494	2007/8/24 08:13	2007/8/24 10:17	46-58.81 [N] 145-47.72[W]	P01-092

(5) Results

The vertical profiles of sea-water temperature and salinity measured at 46.967°N, 172.771°W, near the location of launch, on August 26th, 2007 are shown in Fig.4.1.1. Potential density can be also calculated from temperature and salinity. The complex structure of temperature in the subsurface layer is obtained in the central subarctic region of the North Pacific the by the Argo floats. The isohaline and isopycnal layer with about 26.2 $kg \cdot m^{-3}$ is found between temperature minimum and maximum in 50-150 dbar.
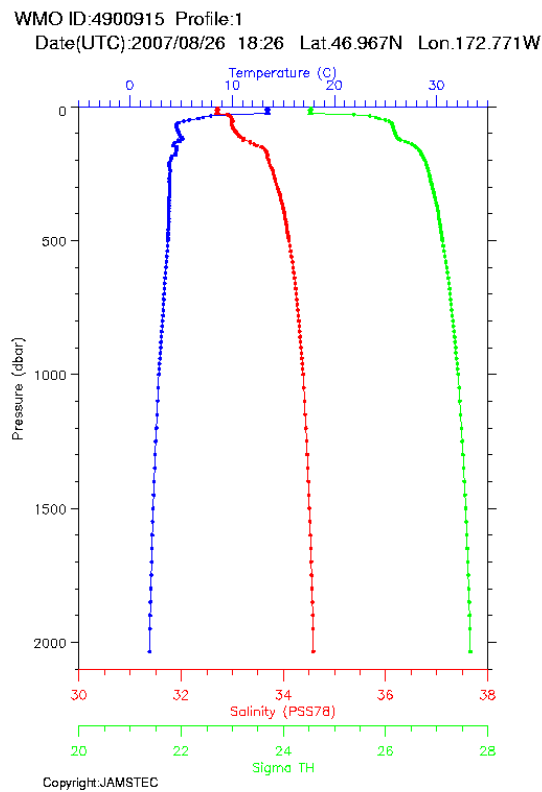

Figure 4.1.1 Vertical profiles of temperature (blue), salinity (red), and potential density (green) measured at 46.967°N, 172.771°W on August 26th, 2007.

(6) Data archive

The real-time data are provided to meteorological organizations, research institutes, and

universities via Global Data Assembly Center (GDAC: http://www.usgodae.org/argo/argo.html, http://www.coriolis.eu.org/) and Global Telecommunication System (GTS), and utilized for analysis and forecasts of sea conditions.